THESIS

TOWARDS UNDERSTANDING THE PROCESSES THAT GOVERN VARIABILITY IN THE SOUTHERN HEMISPHERE

Submitted by

Jonathan D. Woodworth

Department of Atmospheric Science

In partial fulfillment of the requirements

For the Degree of Master of Science

Colorado State University

Fort Collins, Colorado

Summer 2013

Master's Committee:

Advisor: David Thompson

Thomas Birner
Azer Yalin

ABSTRACT

TOWARDS UNDERSTANDING THE PROCESSES THAT GOVERN VARIABILITY IN THE SOUTHERN HEMISPHERE

The climate at extratropical latitudes is strongly a result of the behavior of the zonal mean zonal wind and its inherent variability. This variability is dominated largely by the north-south fluctuation of the midlatitude jet and is identified in the Southern Hemisphere as the Southern Annular Mode (SAM). Recent observations have shown a tendency of the jet to move poleward due to, in part, the forcing associated with stratospheric cooling due to ozone loss and the tropical tropospheric warming from increasing greenhouse gases.

Two dominant processes drive variability in the midlatitude jet: anomalies in the eddy momentum flux (EMF) and the eddy heat flux (EHF). In an attempt to link these processes, this study aims to diagnose a relationship in the observational data via two aspects:

1) To assess the extent to which feedbacks between the EMF and EHF give rise to the annular modes; and
2) To understand, in the context of the atmospheric energy cycle, the dominant patterns of variability of the EMF and EHF fields.

Preliminary results reveal that the variability observed in the extratropical flow may exhibit a slight feedback between these processes. Additionally, it has been found that this variability may be viewed in the context of two distinct structures: (i) those that owe their existence to

conversions between zonal-mean and eddy kinetic energy and (ii) those that owe their existence to conversions between zonal-mean and eddy potential energy.

Past studies have largely focused on the former's impact on the extratropical circulation. However, not much emphasis has been placed on the latter, despite arguably playing an equally important role in driving the variability.

ACKNOWLEDGEMENTS

This thesis would not have been made possible without the help and guidance of my advisor, Dr. David W.J. Thompson. I would also like to thank the members of my committee, Dr. Thomas Birner, Professor of Atmospheric Science at Colorado State University (CSU), and Dr. Azer Yalin, Professor of Mechanical Engineering at Colorado State University (CSU). The support of my research group with the questions and problems encountered over the last two and a half years has been invaluable as well. Additionally, I would like to thank my friends, classmates, and family for their support and perspectives. Lastly, I would like to thank those associated with the NSF Climate Dynamics grant that have made this work possible.

TABLE OF CONTENTS

CHAPTER 1: INTRODUCTION AND BACKGROUND

1.1 - Introduction

Fundamentally, the dynamics that govern the weather and climate on Earth is driven by the temperature gradient between the pole and the equator. When rotation is added into the equations, the laws of physics lead to circulation patterns that influence everything that life experiences, from temperature distribution, winds, precipitation patterns, to the severity and frequency of storms, and a multitude of various other impacts. Of these dynamics, this study examines aspects of the general circulation through the context of the annular modes and the dynamics that are associated with them. It is the processes that govern these annular modes and the resulting variability that provide the motivation of this study.

The dynamical response that this study will focus on is that of the nature of the variability associated with the zonal winds. This variability arises in the form of annular modes that are important in driving weather systems and the resultant climate. This variability of the winds is dominated by the north-south fluctuation of the mid-latitude jet and is driven by two dominant processes. These processes consist of the fluxes of eddy heat and momentum.

While there are many ways to explore these two processes, the work presented in this thesis attempts to further add to the present understanding of how the dynamics that govern the jet stream and resultant storm tracks largely in the context of the Southern Annular Mode (SAM). This will be accomplished in two ways:

1) We will assess the extent to which feedbacks between the fluxes associated with eddy heat and momentum give rise to the annular modes; and
2) We will explore the dominant patterns of variability of these fluxes of eddy heat and momentum in their respective fields.

By looking into these two aspects, insights will be gained in understanding the dynamics as well as raising questions on further areas of research.

1.1.1 – Scope of the Study

In assistance with the study to follow, it is of some benefit to first discuss what the mid-latitude jet is. The mid-latitude jet, also known as the eddy-driven jet, is a region of westerly winds located poleward of the subtropical jet that is associated with the Hadley Cell (Vallis 2006). This jet is barotropic in nature in the sense that the vertical structure is fairly uniform with respect to pressure or height. For reasons that will be discussed later on, the fact that this vertical structure extends to the surface requires that the eddy momentum flux convergence aloft are non-zero to balance the force of friction the surfaces winds experience. The dynamics of why this is the case will be explained in more detail in subsequent sections. With this concept addressed, a discussion concerning the variability of the mid-latitude jet may proceed.

In discussing the leading pattern of variability in the Southern Hemisphere, the commonly ascribed term is the SAM. The SAM can be identified in a variety of fields, including that of sea-level pressure (SLP), zonal mean zonal wind, geopotential height at various levels, as well as angular momentum amongst others (Thompson and Wallace 2000; Hartmann and Lo 1998; IPCC 4th Assessment Chapter 3). This leading mode of variability has been shown to be robust at varying time scales (Baldwin 2001). In terms of SLP, it represents the fluctuation of mass between the polar-regions and the mid-latitudes (Karoly 1990). This change in pressure also manifests itself in a change in the corresponding zonal winds. When looking at the wind fields, this same mode describes the meridional fluctuation of the mid-latitude jet (Karoly 1990; Thompson and Wallace 2000). For the purposes of this study, the diagnostic of the zonal mean zonal winds will be the primary field to analyze these annular modes.

In diagnosing this leading pattern of variability, the emerging pattern is that of a barotropic dipole that has maximum anomalies associated at 40°S and 60°S (Hartmann and Lo 1998; Kidson 1988; Karoly 1990). This structure, as illustrated by Hartmann and Lo (1998), may be seen in Figure 1.1. It has been attributed that the structure and the resultant variability associated with this annular mode is inherent to the internal dynamics of the atmosphere (Limpasuvan and Hartmann 2000). It is this dipole that represents the meridional fluctuation of the mid-latitude jet as mentioned above. The processes that govern this fluctuation are the motivating factor for this study.

As mentioned above, this research will consist of two main components to further understand these processes. The first component will attempt to verify current theory as to how the eddy component of the zonal mean zonal wind projects itself on the zonal wind in observational data and vice versa. The second part of this study will look at the role of the energy cycle as proposed by Lorenz (1955) in how various forcings apply to the dynamical fields associated with the mid-latitude jet. The focus of this study will be on the Southern Hemisphere and the SAM due to the more symmetrical nature as noted by previous work (Kushner et al 2000; Hartmann and Lo 1998; Codron 2007). By focusing on the Southern Hemisphere, the fundamental dynamics will be more easily deduced in analysis. A natural extension of this work would be to apply it to the Northern Hemisphere.

1.2 – Introduction to Dynamical Relations Used for this Study

In this section, a summary of the dynamics associated with the zonal flow will be presented while greater detail will be presented in Chapter 4. This study predominantly looks at the interactions of the zonal wind and how it is related to other dynamical terms.

For the majority of the analysis in this study, the zonal means of a variety of fields are used. By dealing in this zonal context, the effects of asymmetric features, such as the presence of landmasses, are incorporated into the eddy terms. Utilizing this concept then allows one to study the effects of a zonal flow that should be common to all rotating fluids driven by a pressure gradient (Holton 2004). In regards to the zonal mean zonal wind, it may be described as the flow, averaged over all longitude bands, as a singular quantity. The resultant value will give the zonal mean zonal wind as a function of latitude and height. This resultant field lends insight into the overall global general circulation (Holton 2004). However, when looking at this zonal mean flow, it is important to note that in the low levels in the mid-latitudes, the large scale global circulation is inherently unstable where the deviations from this zonal mean flow, termed the eddy component of the flow, drives the resultant circulation (Vallis 2006). In analyzing these zonal mean fields, insights on the global circulation may be obtained.

When performing analysis in this context of using zonal mean fields, it is important to understand how the zonal mean and the resultant eddy component relate. In dealing with the zonal component of a field, one may then define the observed values to be the summation of the zonal mean plus an eddy component. While the zonal mean is field averaged over an entire latitude band, the eddy component is the deviation that the observed field has from this zonal mean. Both components play roles in how the general circulation behaves and understanding the cause of the deviation the field has from the zonal mean is important.

In looking at the zonal mean zonal wind field, the source of the eddy component of the zonal mean flow can, in part, be attributed to baroclinic instability as a result of fundamentally having a varying pressure and density field between the equator and poles. This gradient is termed the basic state for baroclinic instability and is a function of there being a difference of temperature between the poles and the equator. This resulting pressure gradient may be balanced when rotation is introduced. By incorporating rotation, the pressure gradient force can be balanced by the apparent deflection of the wind via the Coriolis force. When these two forces are in balance, it is considered to be in geostrophic balance (Vallis 2006). When disturbances, or eddies, are introduced in the flow, the zonal flow experiences a meridional shift to accommodate the resultant transfer of heat poleward. By looking into how these eddy components in the zonal mean flow interface with the resultant poleward transfer of heat, insight may be gained on how the zonal mean flow behaves. However, before looking at the components that cause the variability, it is important to review the base climatology of the fields that the variability exists in, which leads into the next section.

1.2.1 – Overview of the Zonal Wind Climatology

In this section, a discussion of the climatology of the zonal winds will be provided. As mentioned earlier, the emphasis of this study lies with the zonal wind isolated to that of the Southern Hemisphere. The behavior of the zonal wind is such that at the mid-latitudes, the surface experiences westerlies largely centered about 50 degrees South. There is a similar behavior seen in the Northern Hemisphere as well (Vallis 2006). As seen by Figure 1.2 from Hartmann and Lo (1998), in the Southern Hemisphere, there are two maximums of zonal wind that of the mid-latitude and subtropical jet, located near the tropopause. The tropopause is defined as the pressure level at which the lapse rate changes from decreasing with height to increasing with height due to the presence of ozone (AMS Glossary). As it can be seen, these maximums are found at different latitudes in the annual mean. However, the presence of the sub-tropical jet strongly depends on the season, during which it is strong in the winter and nearly vanished in the summer. These regions of maximum zonal wind are known as jets. The maximum located at 30 degrees is associated with the sub-tropical jet, while the jet located at 50 degrees is known as the mid-latitude jet. The dynamics that govern the formations of these two jets differs.

The formation of these two jets is a result of a differing set of dynamics. While both jets are fundamentally in balance with the temperature field, there are some slight differences. The subtropical jet, the maximum seen at 30 degrees, is largely a result of a strong meridional temperature gradient located at the edge of the Hadley Cell. This jet arises out warm air rising at the equator and while aloft, being acted upon by the Coriolis force resulting in a maximum of westerlies at this edge of the Hadley Cell (Vallis 2006). The mid-latitude jet can be seen to be located at the latitude band where there are also surface westerlies. This jet is more of a result of a barotropic nature in that it is a function of the location of the polar front. Due to this surface flow, it will be shown that this must be balanced by momentum convergence aloft and therefore inherently eddy driven in nature. In other words, this jet is eddy driven by the fact that the westerlies extend from the jet altitude down to the surface. Greater detail to this mechanism will be discussed in Chapter 4 and briefly later in this chapter.

In the analysis used in this study, various approximations of the dynamics may be used. The dynamics that relate this mid-latitude jet to that of eddy momentum convergence is detailed in both the works of Holton (2004) as well as Andrews et al. (1987). However, the former does not take into account for sphericity of the planet in its mathematical relations. However, when comparing the two, this approximation was indistinguishable from the latter's. The relationships that were used for the following work is largely from the relations found in Holton (2004), which are based on the conventional Eulerian mean. This framework of the conventional Eulerian mean will be described in the following section.

1.2.2 – Conventional Eulerian Mean Framework

When looking at the dynamics that govern the general circulation, various approximations may be utilized in order to simplify the diagnosis. For this study, the approximation of the conventional Eulerian mean was used. There are additional frameworks, such as the transformed Eulerian mean (TEM) that may provide further insight and posses some benefits in their application. One such benefit to using the TEM framework is that unlike the conventional Eulerian mean, the TEM allows for isolation of the vertical component of the wind that is balanced by the diabatic heating term. Additionally, instead of looking at equations that have wave forcings separated, the use of TEM allows for all of the zonal wind forcing to be included in the momentum equations. Analysis of the TEM is largely left for additional study.

With regard to the conventional Eulerian mean, this approximation is a method for separating a desired variable into its mean component and its eddy component. What this allows for is to observe how the eddy component can impact the mean component across various fields. When applying this technique to the horizontal momentum equation, the geostrophic balance approximation, the hydrostatic approximation, and the thermodynamic energy equation that are in the log-pressure coordinate system, the following relationships are obtained. For further derivation, please refer to the Holton (2004) text. The key relationship in the following work is that of the horizontal momentum equation as seen in (1.1), though the others play an equally important role in terms of the dynamics.

$$\delta\bar{u}/\delta t - f_0\bar{v} = -\delta(\overline{u'v'})/\delta y + \bar{X} \tag{1.1}$$

$$f\bar{u} = -\delta\bar{\Phi}/\delta y \tag{1.2}$$

$$\delta\Phi/\delta z = H^{-1}RT \tag{1.3}$$

$$\delta\bar{T}/\delta t + N^2 HR^{-1}\bar{w} = -\delta(\overline{v'T'})/\delta y + \bar{J}/c_p \tag{1.4}$$

As the horizontal momentum equation, as given by (1.1), provides much of the insight to the dynamics that govern the variability of the mid-latitude jet, a description of the terms will be provided. In examining this equation, the first term on the LHS is that of the time rate of change of the zonal mean zonal wind. The second term is the Coriolis force acting on the meridional part of the flow. When looking at the RHS of the equation, the first term is the meridional convergence of eddy momentum flux and the second term is the residual forcing, essentially everything else though this term is largely dominated by friction. When looking at this equation, some relationships may be seen.

Some of the relationships observed in this equation provide some insight to the dynamics at hand. The first relation discussed is noting that if the system is in steady state, the time rate of change of the zonal mean zonal wind is zero. With this condition, various balances may be achieved. Above the surface, there is essentially no friction. Thus, at the latitude where the jet resides, the convergence of eddy momentum flux must balance that of the Coriolis term. Similarly, at the surface, there is very little convergence of eddy momentum. This results in a balance between the Coriolis term to that of friction. To have friction acting, there must be surface winds present to act upon. Additional relationships may be seen when observing the column integral of equation (1.1). During this steady state condition where there is no time rate of change associated with the zonal mean zonal wind, the Coriolis term must be zero when integrated over the entire column. If not, there would be a build up of mass at a latitude that would then drive changes in the zonal mean zonal wind. With this constraint, it is observed that the terms on the LHS of (1.1) are zero which leads to the conclusion that in order to have friction or surface winds, there must be a convergence of eddy momentum aloft. This insight to the dynamics will provide the foundation for the analysis done in this study. However, for the sake of completeness, a discussion of the other equations will follow.

Equations (1.2) and (1.3) describe the geostrophic balance and the hydrostatic balance in this Eulerian mean framework. This relation seen in equation (1.2) is the balance of the pressure gradient force as well as the Coriolis force on the resulting wind. Equation (1.3) is that of the hydrostatic approximation. What this relationship describes is that of the vertical component of the pressure gradient force that balances the gravitational force exerted on the air mass (Holton 2004).

The last equation is that of the one associated with the thermodynamic energy equation, as seen by equation (1.4). When looking at the terms associated here, the first term on the LHS is the time rate of change observed in the zonal mean temperature field. The second term on the LHS represents the adiabatic expansion or compression associated with the vertical movement of air parcels. When looking at the RHS of this equation, what is seen is that the first term is that of the meridional convergence of the eddy heat flux while the second term is associated with the diabatic heating that a parcel may experience via latent heating, radiative forcing, or other mechanisms. When applying the same steady state constraint to this equation, that of the zonal temperature not changing in time, it can be seen that the adiabatic warming or cooling of a parcel must balance that of the diabatic heating term plus the effect of eddy heat fluxes. Similar to equation (1.1), the forcing mechanism is that of this meridional convergence of eddy heat flux. How these relationships interact with each other will be explained in a later section.

The above discussion sought to address a brief overview of the components that will be discussed in greater detail in the following chapters relating to this study. Before going into the research conducted in the study, as is presented in Chapters 4 and 5, a concise review of what has been done in past studies will be touched upon next.

1.3 – Literature Review

1.3.1 – Examination of External Forcings of the Mid-Latitude Jet

The above section highlighted how the zonal flow behaves itself in the conventional Eulerian mean framework and the relationships in the dominant equations. Shifting the focus away from the zonal mean zonal wind field to that of its variability gives insight to the behavior of the zonal mean zonal wind fields as a function of time. However, before a discussion on how this study looks at the dynamics associated with the SAM, it is important to do a brief recap on the current state of the problem. As will be briefly described below, understanding the nature of how the mid-latitude jet behaves is still very much in question. The following attempts to summarize current efforts to further gain understanding of the dynamics associated with mid latitude jet.

To present, much work has been done in analyzing how in fact various dynamical fields relate to each other in terms of how the mid-latitude jet has changed in position over time. Recent research looking into how this jet behaves has been looked at through a variety of forcings, both anthropogenic and natural, as well as model simulations with prescribed conditions. Work done by Arblaster and Meehl (2005), Fyfe et al. (1999), Gillett and Thompson (2003), Kushner et al. (2000), Polvani and Kushner (2001), and Yin (2005) have looked into how the dynamics associated with the mid-latitude jet have trended for a poleward propagation of the mid-latitude jet which is analogous to the intensification of the SAM.

One area of focus has been that of looking to external forcings and their effect on the position of the mid-latitude jet. As mentioned above, earlier studies conducted by Fyfe et al. (1999) contribute the poleward shift of the jet to be largely a function of the GHG forcing but not largely associated with that of a connection to the stratosphere. This spurred other studies to look at how various forcings contribute to this poleward jet propagation. For instance, the examination of greenhouse warming, stratospheric cooling, and natural sources such as volcanic and sulfur forcings were looked into by Arblaster and Meehl (2005). What was deduced in that study was that ozone and greenhouse gas (GHG) forcing contributed to most of the observed trends seen in the observations in respect to the poleward shift of the mid-latitude jet. Studies such as Gillett and Thompson (2003) as well Thompson et al. (2011) further look into the role of how the cooling in the stratosphere induces changes in the climate at the mid-latitude surface. Both of these studies illustrate how the dynamical processes linked to the cooling of the stratosphere will impact surface climate. The latter study looks into how the gradual build up of ozone in the Southern Hemisphere as well as increasing GHG is linked to these dominant modes of variability.

This change in the variability also has been looked at from how changing certain parameters in models affect the jets behavior. There has also been work done to see if this same trend of the poleward propagation exhibits itself in basic model simulations and prescribing various heating profiles. Work conducted by Chen et al. (2010) looked at how various heating profiles associated with sea surface temperature gradients affect how the jet moves using an aqua planet model. Other work, explores how the impact on the SAM is initially dependent on where the jet is located and how the dynamics associated with the zonal wind and its respective eddies interact with each other (Simpson et al. 2012). While these efforts are still applicable to help understand the dynamics, there is also been some work to attempt to understand why exactly the variability exists at all.

1.3.2 – Understanding the Modes of Variability

Concurrent with these efforts to understand how the jet will behave to changing profiles of heating or gas concentrations and other variables, many studies have been conducted to observe the fundamental dynamics as to why there is an annular mode present at all. Simple dynamical models have been produced which attempt to simulate the observed annular modes. Work done by Vallis et al. (2004) has been done to simulate the storm tracks and the resultant patterns of variability that are associated with the North Atlantic Oscillation, the analogous pattern of variability in the Northern Hemisphere as the SAM is to the Southern Hemisphere. A simple stochastic stirring of a barotropic model carried out this simulation. This stirring effectively mimics regions of baroclinicity and fluxes momentum into the latitude where the stirring occurs and by the dynamics presented in section 1.2, results in a pattern as observed. In a similar manner, Ring and Plumb (2006) conducted a study to further explore how well these modes of variability arise in a simple model. What was found was that a simple forcing was not adequate to provide the appropriate strength and structure of the modes as seen in observations without the influence of a feedback of the eddy flow back onto the zonal flow. It is this feedback that is the emphasis for the first part of this study.

The effect of this associated feedback has been of interest due to how the jet behaves once it is in a certain location. For clarification, the high index polarity corresponds to a poleward position of the jet while the low index polarity is associated with an equatorward position. Numerous studies have looked at this persistence of the jet to stay in a certain location and have discussed potential feedback mechanisms that allow for the jet to be self-maintaining (Gerber and Vallis 2006; Kidston et al. 2010; Robinson 2005). This eddy-zonal flow feedback then is of particular interest in the pursuit of understanding the basic dynamics that drive the general circulation. Potential feedbacks of the eddy component of the flow onto the zonal mean have been investigated by quite a few studies.

Looking at this feedback process has been examined in the literature. One study, conducted by Hartmann and Lo (1998), looked into the momentum budget of the zonal flow and observed that the zonal flow changes to compensate for the effect of friction that arises and must be balanced by the eddy component of the flow, suggesting a feedback. Further investigation on this feedback and possible mechanism were proposed by numerous studies in both barotropic and baroclinic senses (Hartmann 2000; Robinson 2000). For the purpose of this study, the baroclinic mechanism as proposed by Robinson (2000) will be discussed in greater detail in Chapter 4. With these mechanisms, Lorenz and Hartmann (2001) set out to diagnose the effect of the response of the eddy component of the flow with respect to the anomalies associated with the zonal flow. What was found in their study was that the eddy component of the flow leads changes of the zonal wind. This is expected. However, as seen in Figure 1.3, it is the positive correlation at days 5-20 that suggest that the zonal wind influences the eddy behavior that allows the jet to persist at a certain index. It is this behavior of the wind on the eddies that is looked at in the later chapters of this study.

1.3.3 – Introduction to the Atmospheric Energy Cycle

The second part of this study will look at the processes that dominate the variability seen in the zonal mean zonal wind in the context of the atmospheric energy cycle. Up until this point, much of the analysis in previous studies has looked at how the eddy momentum flux and zonal wind interacts via a variety of scenarios, be it sensitivity to the jet speed, the jet latitude, various temperature profiles, ozone and GHG forcing, etc. However, examining the variability in the context of the atmospheric energy cycle has not seen much attention in the literature.

In examining how these processes relate to the energy cycle, various questions were poised. These questions include how exactly does the energy cycle that drives the atmosphere play into the roles of the variability? What, if any, fields through the propagation down from the various energy reservoirs affect the dynamics that have been seen in previous work? Looking further into how the energy cycle plays a role in various dynamical terms may lead to various ways of thinking how exactly the zonal mean zonal wind interacts with the eddy component.

In an attempt to answer these questions, one first must be introduced to the concept of what the Lorenz Energy Cycle is. This concept first came about via a study conducted by Lorenz (1955). This study essentially set out to detail how the energy is distributed and converted that ultimately impacts the general circulation. In essence, due to hydrostatic balance and the force exerted by gravity, much of the total potential energy (the summation of internal, gravitational potential energy, and kinetic energy) is unable to be realized (Holton 2004). As such, a measure as to what fraction of this total potential energy may be utilized was of interest by Lorenz. This fraction of energy that may be used is termed the available potential energy (APE). Figure 1.4 provides a schematic of this concept.

When examining Figure 1.4, the θ states represent differing potential temperatures that are associated with different air masses. When looking at the left hand side of Figure 1.4, what is seen is higher θ air will rise while colder θ air will sink until it has reached static stability as seen by the right hand side of the figure. It is this redistribution of mass that is realized as the available potential energy that then drives the general circulation (Randall 2010). With this concept, how does one quantify the amount of APE that is able to be realized?

1.3.3.1 – Calculating APE

Calculating the available potential energy can be done a variety of ways. In all instances, these formulations seek to quantify the available energy that may convert to various kinetic processes. While there are many different formulations as to how this quantity may be expressed (Lorenz 1955; Holton 2004; Vallis 2006; Winters and Young 2009; Boer 1989; Smith 1968; Randall 2010), the expression given by Randall (2010) will be shown here.

$$A = \frac{a^2}{2}\int_{-\pi/2}^{\pi/2}\int_{0}^{2\pi}\int_{0}^{p_s}\frac{\bar{T}}{(\Gamma_d - \Gamma)}\left(\frac{T'}{\bar{\bar{T}}}\right)^2 \cos\varphi\, dp\, d\lambda\, d\varphi \qquad (1.5)$$

When observing this equation, it is seen that the available potential energy is an intrinsic characteristic of the entire atmosphere (Lorenz 1955). This expression is essentially a way of adiabatically redistributing the mass present in the atmosphere. Being able to quantify this APE has lead to studies to further understand its importance.

As alluded to, studies have been conducted to examine the nature of this available potential energy in a variety of ways. One such study (Winter and Young 2009) looked at how the budget of available potential energy is applied in terms of horizontal convention in regards to buoyancy. What was found was that there are a few ways in which the reservoir associated with the available potential energy may be drawn from that is then associated with conversions to kinetic and internal energy in the atmosphere. Additionally, there has been work (Pauluis 2006) that looks into the potential sources and sinks of this quantity in the essence of a moist atmosphere, where water in the atmosphere may be used as a metric to determining the available potential energy. What these studies show is that there is a fundamental importance in understanding how available potential energy is understood in its role of maintaining the general circulation. This maintenance of the general circulation requires that the reservoir of available potential energy be drawn upon and converted to kinetic energy. It is the processes that generate kinetic energy that are of interest.

This kinetic energy must be continually generated to offset the losses of friction that, in turn, increase the internal energy in the atmosphere. This generation of kinetic energy requires that the atmosphere act as a heat engine in the sense that available potential energy must be continually added for the kinetic energy conversions to be drawn upon (Pauluis 2006). This source of available potential energy can be inferred from Equation 1.5. In summary where there is substantial heating, such as the tropics, there is a generation of potential energy. This generation of energy must be balanced by a corresponding loss through a sink. The associated energy sink is due to the radiative imbalance found within the troposphere (Pauluis 2006). Once this source of available potential energy is generated, it then undergoes various conversions to other energy reservoirs, such as that of kinetic energy, which then influences the general circulation. It is these conversions between energy states from this initial generation of available potential energy that is described by the Lorenz energy cycle. A brief description of this cycle follows.

1.3.3.2 – The Lorenz Energy Cycle

This generation of APE is largely a result of the difference in solar insolation between the tropics and the poles. A qualitative perspective of this energy cycle is given in Holton (2004). In summary, the process is as follows: Initially, APE is generated as a result of the enhanced tropical diabatic heating as well as radiative cooling associated with the polar regions. With this reservoir of APE, eddies associated with the poleward transport of heat are generated at the surface in the attempt to smooth out this equator to pole temperature gradient. In doing so, this process converts this APE to that of eddy potential energy. At the same time this poleward flux of heat is also being transformed into eddy kinetic energy through the rising motion associated with the flux of eddy heat and momentum (as will be described in Chapter 4). This reservoir of eddy kinetic energy may then feed into the zonal mean kinetic energy via pumping momentum into the jet (associated with the zonal mean kinetic energy) by the flux of eddy momentum. Dissipation as a result of surface friction presents itself in both the eddy and zonal reservoirs of kinetic energy. To complete the cycle, there is a component that relates the zonal mean potential energy to that of the zonal kinetic energy. This conversion is what is seen with large-scale meridional circulation, such as that given by the Hadley Circulation (Randall 2010). Figure 1.5 shows a schematic of these processes and how they interact with one another.

A schematic showing how these various forcing mechanisms are related is seen in Figure 1.5. As it can be seen, the GE and GZ terms represent the generation of the available potential energy terms for the zonal and eddy kinetic energy reservoirs. After this generation, there are multitudes of ways in which this energy may be converted as well as drawn upon. The two dominant processes that govern the leading pattern of variability represent the conversion terms. The process of the flux of eddy heat is given by the conversion terms CA and CE, whereas the process associated with the flux of eddy momentum is represented by the conversion term CK. A more detailed discussion of these processes is found in Chapter 5.

Due to these conversion terms being at various stages of the energy cycle, the available potential energy may then ultimately be viewed in the context of the zonal mean as well as eddy components of the flow. How these fields interact with each other and how the energy is diffusive is dependent on various forcing mechanisms associated with the eddy fluxes of momentum and heat. Examining how the various processes within the energy cycle affect the variability of the zonal mean zonal winds (SAM) is the purpose of the second half of this study as they are associated with distinct structures.

It can be stated that the processes that govern the general circulation, and the resulting variability, may be viewed in two distinct structures. These structures are associated with different energy reservoirs. As mentioned, the process between zonal mean available potential energy/eddy potential energy to that of the eddy kinetic energy is associated with the poleward flux of heat. It is therefore expected that the leading mode of variability in the eddy kinetic energy should largely explain the variance within this poleward flux of heat. This variance however, is different from that associated with the leading mode of variability of the zonal winds, or SAM. As much past literature has shown, the SAM explains a large fraction of the variance within the field associated with that of the eddy flux of momentum, or the conversion between the eddy and zonal kinetic energies. These two distinct structures, associated with either one of these forcings, are both important in understanding how the general circulation is maintained. The analysis performed in Chapter 5 attempts to further dissect these two structures.

1.4 – Outline and Objective of Study

This chapter sought to provide an introduction to the work that this study will encompass. In addition, a brief literature review discussing the nature of the problem has been provided. The methodologies and data used for this study will be presented in the following chapter. Chapter 3 will then touch upon the base climatology of various dynamical fields that will set the stage to discussing the variability associated with select fields in Chapters 4 and 5.

Chapter 4 represents the findings in accordance to that of the first goal of this study. This chapter was motivated by the results obtained by Lorenz and Hartmann (2001), with the baroclinic mechanism proposed by (Robinson 2000). The goal of Chapter 4 is to diagnose this feedback in the observational data as it pertains to the mechanism proposed and to see if the observations reflect current theory. The driving idea behind this work is to explore what exactly precedes the eddy momentum flux that in turn influences the zonal mean zonal wind.

In Chapter 5, the focus will be largely centered on the findings in Chapter 4 in terms of the forcing mechanisms of the eddy fluxes of heat and momentum. What this chapter seeks to explore is largely how these fields relate to each other and how they project onto various other dynamical fields. During the analysis of these forcings, it will be looked at how the two forcing mechanisms relate to the energy cycle proposed by Lorenz. This will be covered in more detail in Chapter 5, but may shed light on how the current thinking may be enhanced when viewing from this new framework.

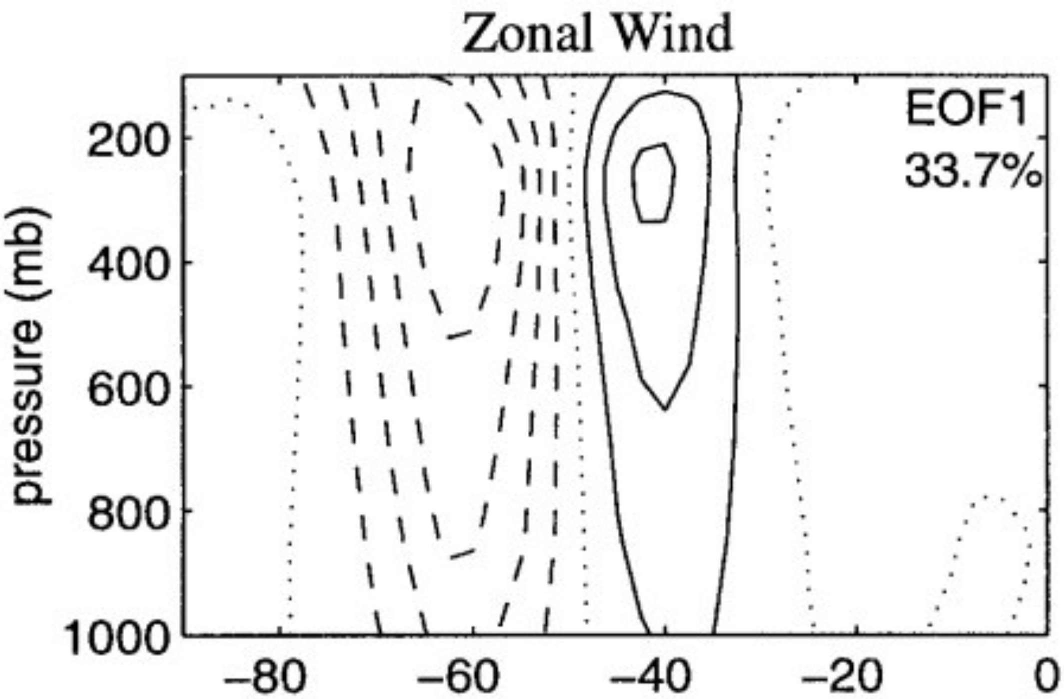

Figure 1.1 Leading EOF of the zonal mean zonal wind from Hartmann and Lo (1998). Explained variance is given in percent. Dashed contours are negative, the zero contour is dotted.

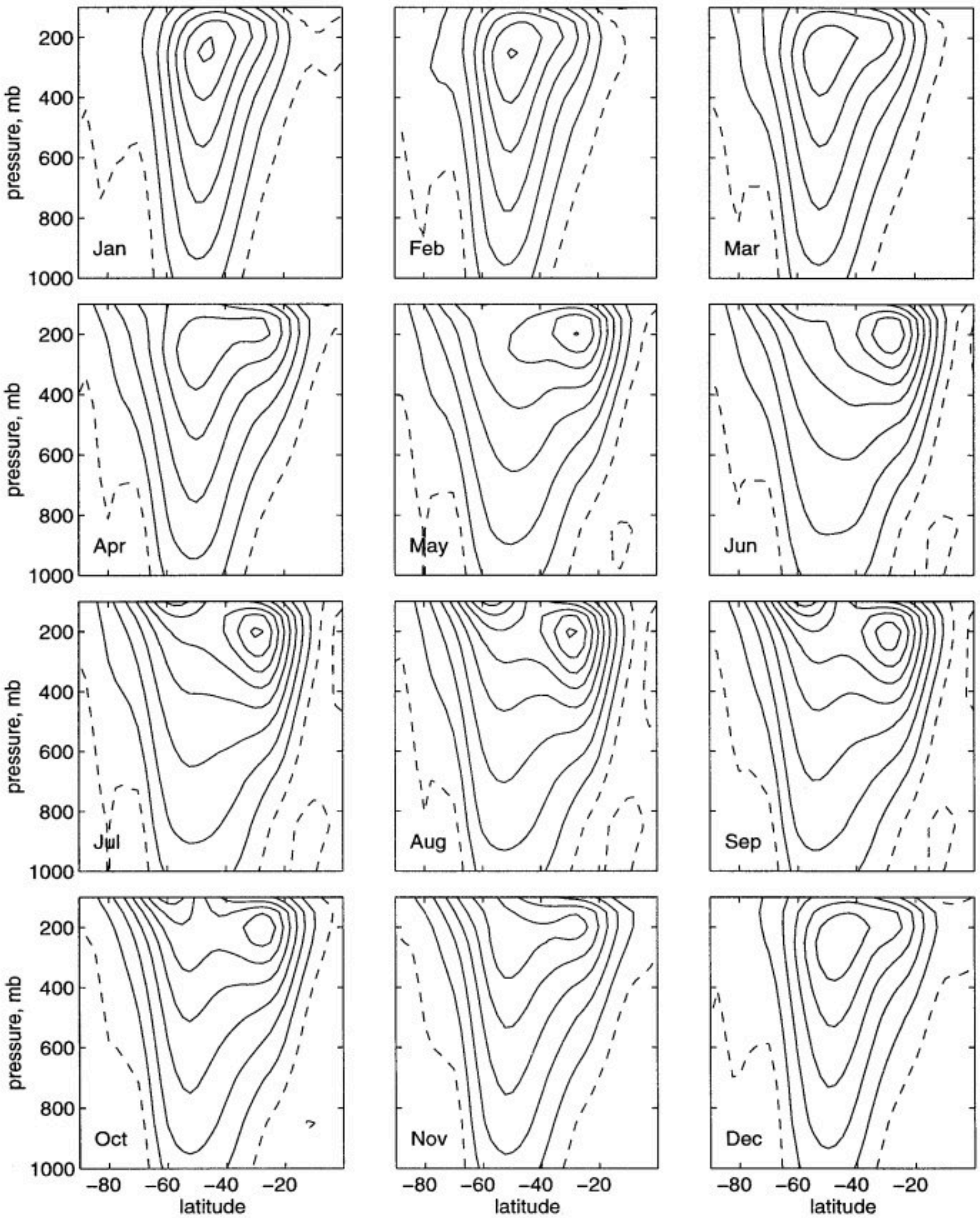

Figure 1.2 Monthly mean zonally averaged zonal wind in the Southern Hemisphere for the period 1985–94. Contour interval is 5m/s. The zero and negative contours are dashed. From Hartmann and Lo (1998).

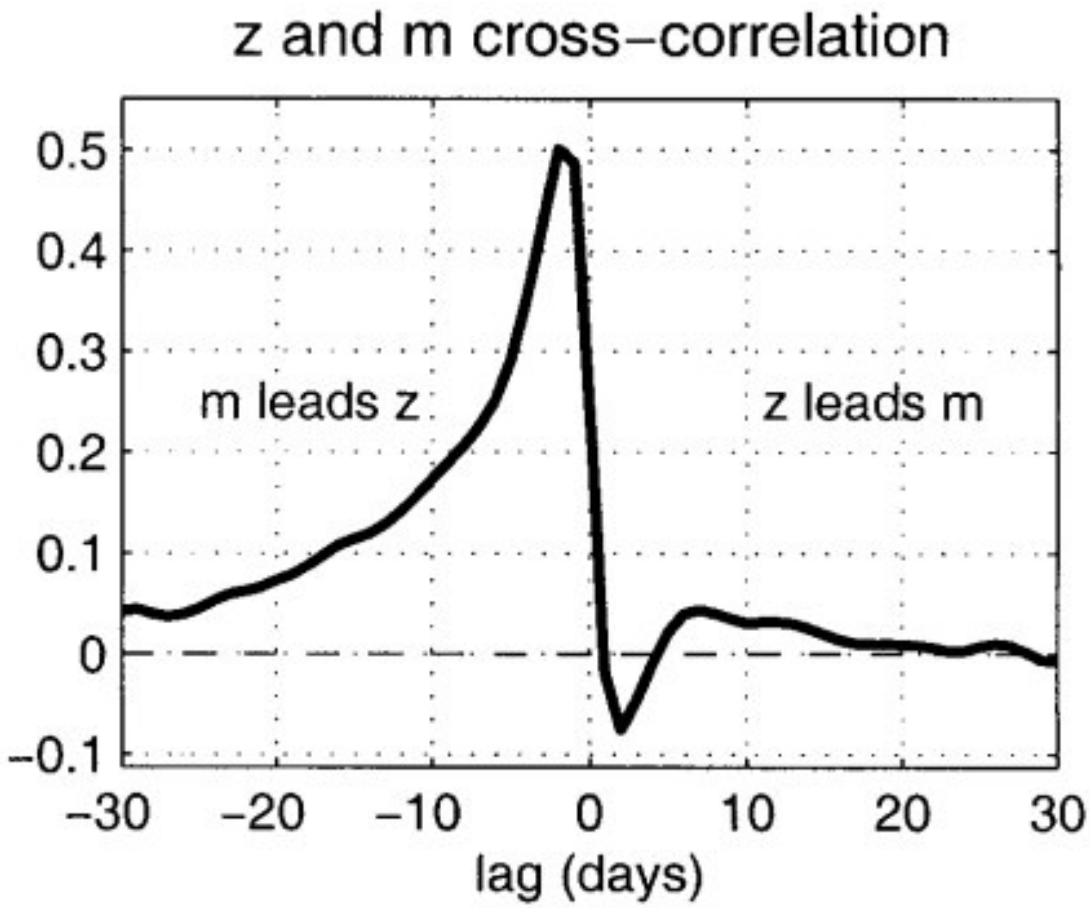

Figure 1.3 Cross-correlation between M and Z. "M" is the eddy forcing of the flow and "Z" is the leading index of the zonal mean zonal wind. Figure from Lorenz and Hartmann (2001).

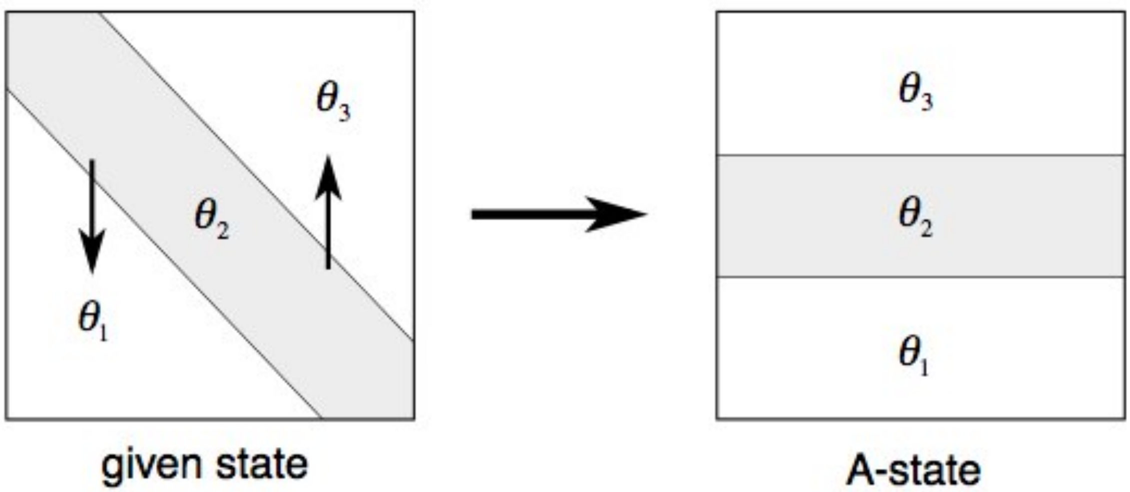

Figure 1.4 Illustration of the release of Available Potential Energy. Figure taken from Randall 2010. The redistributing of the theta states to equilibrium represents the Available Potential Energy that can be realized in the atmosphere.

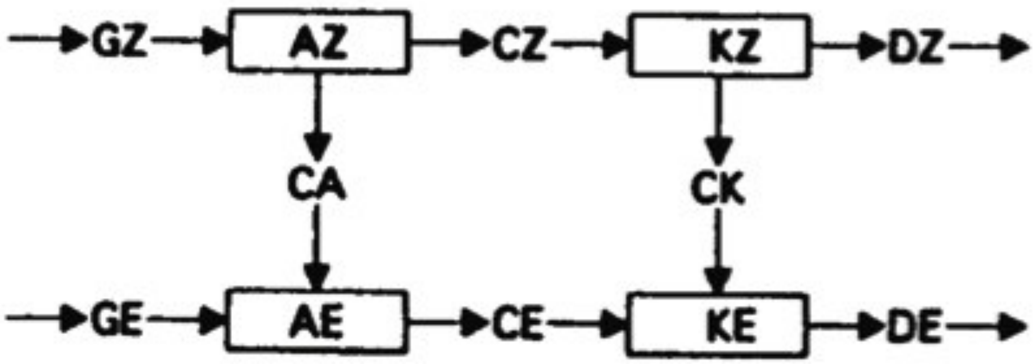

Figure 1.5 Schematic of the Energy Cycle taken from Randall 2010. GZ is the generation of available zonal potential energy. AZ is the zonal mean available potential energy. KZ is the zonal mean kinetic energy. AE is the eddy available potential energy. KE is the eddy kinetic energy. GE is the generation of eddy available potential energy. DZ and DE are the dissipation of zonal and kinetic energy. CZ,CA,CK,CE are the conversion terms.

CHAPTER 2: DATA AND METHODOLOGY

2.1 Observational Data

The data that was utilized for analysis in support of this thesis was that of the sub-daily reanalysis data of the zonal and meridional wind, and that of temperature produced by the European Centre for Medium-Range Weather Forecasts (ECMWF). The resolution of the data used was that of the ERA-Interim that provides a grid of 1.5° by 1.5° latitude/longitude with a time span consisting from January 1, 1979 to December 31, 2011. This time span was chosen as a result of satellite observations being largely available from 1979 onwards and that the Era-Interim data set went as far back as 1979 at the time of this writing (Kalnay et al. 1996; Uppala et al. 2008). Furthermore, for each field, 15 pressure levels (1000, 900, 850, 800, 700, 600, 500, 400, 300, 250, 200, 150, 100, 70, and 50mb) were used. Due to the more zonally symmetric nature of the Southern Hemisphere (SH), for this study, only the SH latitudes were analyzed.

The ECMWF dataset is a reanalysis product that utilizes both observational and model outputs in a method known as data assimilation. The advantage of using a reanalysis product, such as ERA-Interim, is that the process of data assimilation allows fields to be calculated for all grid points using a interpolation like fit. This process subsequently lends itself to being used to study various climatological fields and processes (Wang et al. 2000). However, a caveat when using products such as this are that due to the span of the data used, all measurements may not have been recorded in the same fashion and as a result, provide a limitation to the utility of the reanalysis (Trenberth et al. 2001). However, in the case of the ERA-Interim, the quality of the re-analysis product has shown to be fairly consistent with observations well into the stratosphere via satellite measurements (Uppala et al. 2008).

There are benefits to using the ERA-Interim over that of the ERA-40 product. The main changes from the previous package, that being the ERA-40 is that the data assimilation accounts for, amongst many changes, 12 hour 4D-Var, T255 horizontal resolution, new humidity analysis, correction of satellite bias in radiance data, and others (Uppala et al. 2008). This improvement in the reanalysis scheme has been shown to being more in agreement over time with that of observations. This is supported by the fact that since 1979, the data collected via satellite has led to better quality data that can be used as inputs for these re-analysis packages (Kodera 2004; Kalnay et al. 1996). Figure 2.1 from Uppla et al. (2008) illustrates the improvement of these reanalysis packages. What is seen in the figure is that after 1978, there is a substantial improvement in the fit of the data due to improvements in the data collection via satellite soundings (Kodera 2004; Uppla et al. 2008). It is also seen that the fit of the data increases greater over time due to the improvements in how the reanalysis are conducted, especially in the Southern Hemisphere. With this in mind, climatological studies using data from the re-analysis packages are becoming more refined, but it is important to know the source of the data being used in the study and hence why it was mentioned.

2.1.1 Field Derivation

To conduct the analysis for this study, a range of variables needed to be examined from the ERA-Interim dataset. From this data set, the fields of temperature (T), zonal wind (u), and meridional wind (v) are extracted and used to derive various dynamical fields. All variables were initially downloaded at sub-daily resolution, being at 0, 6, 12, and 18 hour points during a day. The motivation for the use of sub-daily data was that fields, such as eddy fluxes of heat and momentum, is best calculated at the finest time resolution possible as a result of their inherently short life cycle. From this, daily as well as monthly means of fields were calculated depending on the field in question.

With the data obtained, various aspects of the dynamical fields could then be analyzed. The following chapters make use of these various dynamical fields in differing aspects. Chapter 3 looks at the base climatology, whereas chapter 4 and chapter 5 examine the anomalous fields in different contexts. For this study, the variables of zonal wind, eddy momentum flux, eddy heat flux, eddy kinetic energy, temperature, as well as the meridional temperature gradient were used. Depending on the analysis at hand, these fields were calculated at a specified pressure level and subsequently plotted. In order to plot these variables analyzed for this study, it should be noted how these fields were calculated.

The formulation of these fields involved the use of a single variable or a product of variables that were then manipulated. While the singular fields of zonal winds and temperature are rather straightforward, the formulation of the flux fields and the gradient fields will be explained. To calculate the fluxes of eddy heat and momentum, the process was as follows: At the sub daily level of the data, for each field, the zonal mean was subtracted from the data. This results in departure fields which are hereby designated as u', v', and T'. With these departure fields calculated, the eddy flux variables could be calculated as the multiplication of the u' and v' terms to get $u'v'$ as well as the v' and T' terms to get $v'T'$. With these fields, the daily average was then found. Subsequently, with the daily averaged fields, the zonal mean was then calculated (if needed) resulting in a field that was then a function of latitude, pressure level, and day. A similar process was followed to calculate the eddy kinetic energy (EKE), which is defined as:

$$\mathrm{EKE} = 0.5*[(u')^2 + (v')^2]$$

Where the brackets denotes zonal mean of the quantity. Taking the derivative of the desired field in a discretized manner over the appropriate index also created gradients of desired fields.

In all analysis outside of looking at the climatology, the seasonal cycle was removed. The seasonal cycle, as defined by Straus (1983), is defined as the average for each day of the year over a multi-year time span. Thus, to remove the seasonal cycle from the data, the daily average for each day was removed from the specified grid point in the data set. In the event monthly data was utilized, it was derived from the daily mean anomalous fields. By using these anomalous fields, various statistical methods could be used to further understand the dynamics in question.

2.2 Data Analysis

This study has two aspects that are the focus for analysis. The first component, as alluded to in the previous chapter and discussed in greater detail in Chapter 4, explores how the baroclinic mechanism put forth by Robinson (2000) is evidenced in the observational data. The second part of this study, discussed in Chapter 5, then explores the relationship of the forcings associated with the eddy fluxes of heat and momentum in the context of the atmospheric energy cycle.

For both aspects of this study, preparation of the data had to be conducted. Since this study is focused in the Southern Hemisphere, the data first had to be truncated to correspond to the Southern Hemisphere latitudes. In the process of manipulating the data fields, various checks along the way were conducted to see if the results matched those as seen in various past studies seen in literature. These checks then gave confidence in extending the analysis to that of looking at the variability of the dynamical fields in question.

To explore the variability in the data, and how the fields relate to one another, statistical tools such as EOF analysis, filtering, linear regressions, as well as correlations are used in a variety of ways to illustrate the relationships between the various dynamical fields. A further description, as well as how the fields were derived will be presented in the following sub-sections.

2.2.1 Diagnostics

The dynamical fields analyzed in this study are outlined in Holton (2004) as well as Andrews et al. (1987) and are represented by the equations (1.1) to (1.4) in the previous chapter. As mentioned earlier, the equations and resulting variables used for this study are those found within the conventional Eulerian Mean framework. The primary equation analyzed in this study comes about from the horizontal momentum equation, (1.1) restated below as equation (2.1).

$$\delta\bar{u}/\delta t - f_0\bar{v} = -\delta(\overline{u'v'})/\delta y + \bar{X} \tag{2.1}$$

To obtain the fields in the above equations, the data for zonal wind, meridional wind, and temperature were manipulated as described above.

To check that the fields were being derived correctly, all terms in equation (2.1) were calculated and plotted to see if the approximations held (not shown here). As may be expected, the time rate of change of the zonal mean zonal wind (first term) is balanced fairly well by the vorticity term (second term), and the convergence of eddy momentum flux (third term). Due to this balance, there is confidence in how the fields were generated and thus, the methods outlined above will be carried out for further analysis. The various statistical methods used throughout this study are explained below.

2.2.2 Linear Regression

One of the statistical tools used in this analysis is that of linear regression. This sort of analysis attempts to model a relationship between a variable and its dependent variables. The resulting model of the data is of the form:

$$\hat{y} = a_1 x + a_0 \tag{2.2}$$

In this equation, $\hat{y}$ represents an estimate of what the observed y would be assuming there is a linear relationship between the dependent variables, given by x. In other words, it is assumed that x is known with precision, and $\hat{y}$ is estimated on these known values of x. For the purposes of this study, the variables a_1 and a_0 represent the coefficients (slope and y-intercept respectively) that are fitted in accordance with the method of least squares. This method seeks to minimize the square of error at each data point. For this method, the error is defined as the following.

$$Q = \sum_{i=1}^{N} \left(\hat{y}_i - y_i\right)^2 = \sum_{i=1}^{N} \left(a_1 \cdot x_i + a_0 - y_i\right)^2 \tag{2.3}$$

To find the coefficients of a_1 and a_0, two equations must be solved, as there are two unknown variables. Setting the derivative of Q with respect to a_1 equal to zero for one equation and setting the derivative of Q with respect to a_0 to zero for the other equation gives the two required relationships. When solving for both a_1 and a_0, the following equations are obtained:

$$a_1 = \frac{\overline{x'y'}}{\overline{x'^2}} \tag{2.4}$$

$$a_0 = \overline{y} - a_1 \cdot \overline{x} \tag{2.5}$$

Where the numerator of a_1 is the covariance between x' and y' and the denominator is the variance of x. This term, a_1, is the regression coefficient (slope) of the line of best fit. The variable, a_0, is the y-intercept. The regression coefficient is useful as it gives a physical interpretation of the strength of the relation between the variables in question. However, there is a downside associated with regression. Although it gives insight about the strength of the relation, it does not yield any information about how close the dependent variables hold to the line of best fit. For this, another statistical tool is needed, that of correlation.

2.2.3 Correlation

The correlation coefficient is another useful statistical measure of a data set. As opposed to linear regression, the correlation coefficient does not provide any sort of physical meaning relating to the data. What it does provide is a sense of how well the data created by the *x* and *y* variables fits the line of best fit. The closer the data fits around the line of best fit, the higher the correlation and vice versa. In more precise terms, the correlation coefficient is a measure of the fraction of variance explained by the fit.

To calculate the correlation, the following relation is used.

$$r = \frac{\overline{x'y'}}{\sigma_x \sigma_y} \tag{2.6}$$

What is seen in the above equation, is that the numerator is the same as that is found for the linear regression coefficient (Equation 2.4), being the covariance between *x'* and *y'* while the denominator is the product of the standard deviations of *x* and *y*. The range for *r* has values that are between -1 to 1, with -1 representing values of *x* and *y* that are exactly anti-correlated with one another and a positive 1 when the *x* and *y* variables are exactly correlated to each other. When the correlation is 0, the variables *x* and *y* are uncorrelated.

Some relations can be seen from this correlation coefficient. Using a little bit of algebra, one can rewrite the regression coefficient as the product between the correlation coefficient and the ratio of the standard deviation of *y* to the standard deviation of *x*. Key observations with the correlation coefficient is that it only works for a linear relationship and that any correlation does not reveal a cause or effect type relationship. Additionally, for this thesis, the usage of lead-lag correlations is also used in which the respective variables are lagged with respect to the other and then correlated. This is done, as correlation on its own will not reveal quadrature relationships.

2.2.4 Empirical Orthogonal Function (EOF) Analysis

2.2.4.1 – Description of Fields Selected and Associated Caveats

A major part of this study makes use of EOF and principal component analysis. Essentially, what this statistical tool accomplishes is finding the patterns in the data that explain the greatest fraction of variance within that field. For this study, the EOFs and their corresponding principal component time series were calculated for various fields in question, including the fields of zonal wind, eddy momentum fluxes, eddy heat fluxes, and eddy kinetic energy. As was mentioned in the literature review section in Chapter 1, these PC's and their corresponding EOFs can be created and checked against previous literature for consistency. This check against the literature gave confidence in pursuing further analysis with these leading PCs.

Chapters 4 and 5 examine the leading PCs of different fields. Chapter 4 relates the dynamical fields to that of the SAM. The SAM is defined in this study as the leading PC of the 300mb zonal wind field. This is consistent with other literature (Barnes & Hartmann 2010; Hartmann & Lo 1998; Lorenz & Hartmann 2001; Kushner et al. 2001 and many others). As mentioned in other sections, the SAM may also be defined by using various other fields, such as the leading PC in sea level pressure (SLP) in the Southern Hemisphere (Thompson and Wallace 2000). Chapter 5, meanwhile, focuses on the leading PCs that are associated with the eddy fluxes of heat and momentum and how they then relate to each other. However, in both of these analyses, there are some caveats to the formulation of these leading PCs.

One caveat for this formulation of leading PCs lies in what latitude bands were utilized for the fields in question. For this analysis, in calculating the leading PC of the zonal mean zonal wind at 300mb, the latitude range of 20°S to 90°S was used for all fields except that of the eddy flux of heat. This latitude was chosen to focus on the variability outside that associated with the tropics. This logic was also applied to the PCs associated with that of the eddy momentum fluxes and eddy kinetic energy. However, for the eddy heat fluxes, the latitude range was set to encompass solely the range of 20°S to 70°S. The reason for this discrepancy from the other fields is that the eddy heat fluxes are calculated at the 850mb level as opposed to 300mb for the other dynamical fields. This allows for the variability of the eddy heat fluxes to disregard the impacts created from interaction with the surface due to the Antarctic continent. With these PCs calculated, the spatial EOFs were then regressed upon the raw Southern Hemisphere data for the respective field for the entire latitude bands (0°-90°S).

A second caveat for the formulation of the leading PCs is that of which time average was used for various parts of the analysis. In addition to the daily fields, the monthly EOFs were calculated by taking the monthly means of the daily PCs. To conduct the EOF analysis, the raw data had to be conditioned in a manner that was described as in section 2.1.1. With these anomalous fields, the desired range for the latitudes as described above was isolated. Thus, the resulting size of the arrays in which the daily EOF was performed was initially on a matrix A consisting of M = 12053 days by N = 48 (35) latitude points. The 48 refers to fields that utilized 20°-90°S and the

35 refers to fields that utilized 20°-70°S. The monthly leading PCs were then the monthly average of the daily PCs.

2.2.4.2 – EOF Analysis Description

With EOF analysis, what is desired is to find a single 1xN state vector that explains the largest fraction of all the variance in your matrix, A. For each data matrix A, a weighting of the square root of the cosine of the respective latitude was applied. The purpose of this weighting is to account for the convergence of the meridians. The weighting consisting of the square root of the cosine is such since the covariance matrix, which is defined as $A^T A$, is a product of the grid point time series.

Once these weighted fields were obtained, the techniques of singular value decomposition (SVD) were applied. This technique manipulates the specified data matrix A such that it outputs U, S, and V matrices that fit the following relation.

$$A = USV^T \tag{2.7}$$

Where U has dimensions of MxM, S has dimensions of MxN, and V^T has dimensions of NxN. From these matrices, what is found is that the columns associated with U are the PC time series for A and the columns in V are the corresponding EOFs of A. Additionally, the diagonal elements in S are associated with the singular values of A (square root of the eigenvalues shared by AA^T and $A^T A$). Once these PCs are found, they are then standardized to have the mean be zero and the standard deviation to be one. The resulting EOFs are then found by regressing the specified PC on the unweighted anomalous data of the specified field over the entire latitude band of the Southern Hemisphere (0°-90°S).

These resulting plots of the EOFs will be discussed further in the upcoming sections, namely those in Chapter 4.

2.2.5 Filtering

In parts of this study, filtering of the data was applied to explore how various frequencies within the data set contributed to the trends seen in the analysis. For the filtered time series the data used was of the same format as described in section 2.1. All formulation of the various fields are identical to that previously mentioned.

Filtering allows for the separation of various components that contribute to the signal found in the dynamical field. Due to some of the findings in the past literature (Lorenz and Hartman 2001), both low pass and high pass filtering was applied to various dynamical fields. The basis for looking at various frequencies in select dynamical fields is that low frequency response, or the "redness", of the signal is a common, intrinsic characteristic of the variability found within the eddy fields that may be independent of the zonal mean zonal wind. By looking at various frequencies of the forcing fields, such as eddies on the zonal wind and vice versa as the first part of this study explores, one could make a case for a feedback that is dependent on both of the fields in question (Lorenz and Hartman 2001).

There are many types of filtering algorithms that may be used. In this study, the Butterworth filter was applied to obtain both the low pass frequency as well as the high pass frequency found within the data. The frequency cutoff was set at 10 days to isolate the eddy component that exceeds that amount, termed synoptic, and less, termed the residual (Lorenz and Hartman 2001). The cross product frequencies were not looked at in this study. The Butterworth filter is a recursive filter in the sense that the filtered output depends on both the previous values of unfiltered and filtered data. The general format of this type of filter is given by equation 2.8, where the first term is the weighting function applied to the unfiltered time series and the second term is the weighting function applied to previous values of the filtered time series.

$$g(t) = \sum_{i=0}^{J} [b(i+1)\cdot(ft - i\cdot dt)] + \sum_{j=1}^{k} (a(j)\cdot g(t - j\cdot dt)) \tag{2.8}$$

In regards to the Butterworth filter, the associated response is that of the following:

$$\left|R^2(w)\right| = \frac{1}{1 + \left(\frac{w}{w_c}\right)^{2N}} \tag{2.9}$$

Where w_c is the cutoff frequency and N+1 is the number of weights utilized. A thing to note is that the higher the N, the sharper the cut-off and the more closely it resembles a perfect boxcar response.

The above describes the data, the methods of data formulation, as well as how the data is manipulated via a variety of statistical tools. All analysis done in the following chapters utilizes these methods described above to attempt to answer the two aspects of the study. With these tools, the results and discussion of the analysis follows.

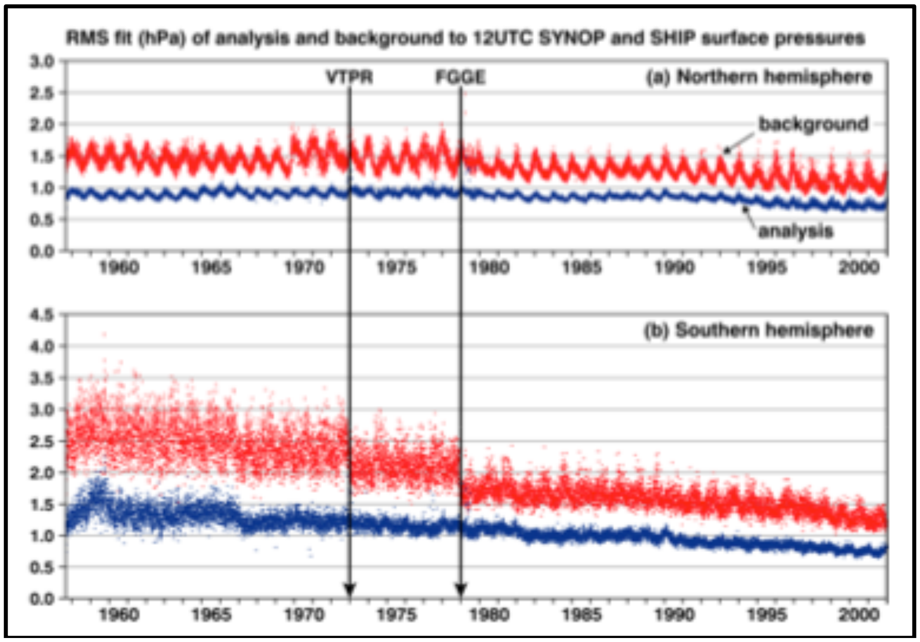

Figure 2.1 From Uppala et. al (2008). Daily Values of the root-mean-square background (red) and analysis (blue) fits to 12UTC SYNOP and SHIP measurements of surface pressure (hPa) over the extratropical northern and southern hemispheres.

CHAPTER 3: OBSERVATIONS OF THE SOUTHERN HEMISPHERE CLIMATOLOGY

The objective of this chapter is to provide a physical overview and discussion of the climatology of various dynamical fields. In knowing the climatology, one can explore how variability about that climatology plays a role in influencing future climate. The motivating factor for this examination of the climatology is that in knowing this base state, the associated variability will largely be centered on it. This variability will lead to changes that affect the resulting precipitation patterns, temperature fields and other climatological aspects that influence life on this planet (Holton 2004; Hudson 2012; Kaspi and Schneider 2011). This chapter will discuss the base state of the dynamical fields that affect the SAM through the Robinson baroclinic mechanism as presented in Chapter 1. With this climatology established, the following chapters discuss aspects regarding the variability.

To examine this climatology, the methods outlined in Chapter 2 are used. The climatology of the zonal wind, eddy fluxes of heat, eddy fluxes of momentum, eddy kinetic energy, and that of the meridional temperature gradient are obtained and discussed. Via the use of these methods, the climatologies are presented in both a zonally varying sense as well as in the zonal mean. Additionally, the climatology as a function of pressure level is also touched upon for specified fields. The following subsections will discuss each dynamical field and how it interfaces with the others.

3.1 – Zonal Wind Climatology

3.1.1 – Zonal Varying Field

The zonal mean zonal wind is the first field in which the climatology will be examined. Figure 3.1 is a panel that presents the zonally varying wind field in the zonal mean, and the respective eddy fields, for the 300mb and 850mb levels. The motivation for looking at these two levels was such that the jet and the resulting factors that influence its behavior tend to be observed at the 300mb level. Additionally, as mentioned in Chapter 1 and more in Chapter 4, this variability aloft then induces changes seen at the surface, which is represented at the 850mb level. Additionally, in each row of the panel, the annual, winter, and summer means are shown. For reference, the annual mean is defined as the time mean of the field without regard to season and is merely the mean of all days of record in the data. The winter mean is defined as the time mean isolated to days that fall within the months of June, July, and August as is convention in the Southern Hemisphere. Similarly, the summer mean is defined as the time mean of all days that fall within the time of December, January, and February. For all plots in this figure, red regions correspond to that of regions of westerly winds whereas the blue regions are associated with easterly winds.

As the SAM manifests itself in the fluctuation of the zonal mean zonal wind aloft, the first aspect of the climatology will focus on that of the 300mb pressure level. When observing the 300mb zonal wind field in Figure 3.1, it can be seen that the winter component tends to dominate that of the annual mean. This is what is expected, as during the winter season, the temperature gradient between the equator and the pole is much larger than it is during the summer season (Holton 2004). When looking at the top panel of Figure 3.1, both the subtropical jet and the mid-latitude, or eddy-driven, jet can be distinguished. In the climatology, the subtropical jet is more prevalent during the winter and spans the longitudes of 90°W to about 60°E between latitudes of approximately 20°-30°S. However, when contrasting the winter season to that of the summer season, it is seen that this subtropical jet nearly vanishes. In a similar fashion, the mid latitude jet exhibits a tendency of being relatively constant throughout the year. This mid-latitude jet has the greatest zonal winds between longitudes of 30°W to about 90°E centered largely upon the latitude band of 50°S. This pattern of zonal wind climatology is consistent with past studies (Hoskins and Hodges 2004; Codron 2007; Barnes and Hartmann 2010; Lorenz and Hartmann 2001). Additional insight may be found when looking at the corresponding eddy field.

In addition to looking at the climatological mean of the zonal winds, the associated eddy fields of the 300mb pressure level may also be observed in the second panel of Figure 3.1. The eddy fields, as discussed about in Chapter 2, are defined as the deviations from the zonal mean. Upon observation, similar to the full field, the winter season in the Southern Hemisphere tends to dominate the overall pattern seen in the annual mean. When examining the top two panels, it is seen that the regions where the deviations are the most significant are in the same locations to first order as where the climatological winds are. This goes in line with the previous statement that the majority of where the changes occur, in terms of the jet variability, resides to where the jet is initially located. The climatology of the 300mb level winds has an influence on the location of the 850mb level climatology.

Due to the linkages between the 300mb and 850mb winds via the baroclinic mechanism proposed in Chapter 1, the climatology of the zonal wind at the 850mb level was examined as well. The 850mb zonal mean zonal wind climatology is presented in the third panel of Figure 3.1. As with the 300mb plots, the red shading corresponds to that of associated westerly winds and the blue for easterly winds. Both the summer and winter seasons have similar structure that well represents the annual mean. As will be explained in Chapter 4, the structure is a ring like pattern that is largely confined to the latitudes of 40°-60°S with the strongest winds being located in the Indian Ocean sector.

Like what was done with the 300mb level, the resulting eddy field of the 850mb wind is shown in the bottom panel of Figure 3.1. When looking at the annual mean, there appears to two regions of positive eddy values in the corresponding latitudes to where the climatology lies, being 40°-60°S. One such region is in the Indian Ocean sector, which is largely attributed from the winter season. The other large area of positive eddy values is that in the Atlantic sector that is attributed to the summer season. An observation of sharp contrasts in the zonal wind at 850mb may be seen at the Antarctic continent, as well as on the western sides of the South America and Africa. This is largely a result of the topography intersecting this pressure level.

Another way to diagnose the climatology is to examine how the zonal mean fields behave at all levels. This will give insights to the variability as in this study, the variability requires the use of zonal mean fields and the resulting PCs from these zonal mean fields. The following discussion looks at what the base climatology of the zonal mean zonal winds is and the main features found within.

3.1.2 - Zonal Mean Field

This section discusses the climatology of the zonal mean zonal winds. While the climatology of the zonal varying plots can give insight into regions where the jets have the highest intensity, one can also gain insight into looking at the zonal mean fields. Observing the zonal mean fields is useful as diagnostics, such as the conventional Eulerian mean framework, use the zonal mean parameters to gather insight on the dynamics of the general circulation (Holton 2004). This approach is used more extensively in later parts of this study.

Figure 3.2 shows the zonal mean of the full zonal wind field at 300mb. As with the convention used in the previous figures in this chapter, the annual, winter, and summer means are plotted. The last panel in this figure shows an overlay of the three means. What can be seen is that there is an equatorward shift in the latitude of the zonal wind maximum, corresponding to approximately 28°S in the winter from about 50°S in the summer. This corresponds to the subtropical jet location that largely manifests itself in the winter season but becomes non-existent in the summer. Interestingly, both the annual and summer means result in a maximum zonal wind at around 50°S. This is due to the fact that the mid-latitude jet is present year round as opposed to the subtropical jet. As with prior discussion, the 850mb winds are discussed next.

Figure 3.3 shows the same plot as Figure 3.2 except that it is in regards to that of the zonal mean zonal wind at 850mb. What is seen is that the region of maximum surface winds, for annual, summer and winter means, is in the same latitude where the mid latitude jet exists as seen by the maximum zonal winds in Figure 3.2. This goes in line with present theory (Holton 2004;

Hartmann and Lo 1998; Robinson 2000), where to have surface winds, momentum fluxes must be present.

That the 300mb and 850mb winds are largest at the same latitude is a result of the nature of the dynamics associated with the mid-latitude jet. The linkage between these levels of the zonal mean zonal wind can be more clearly seen in Figure 3.4. In this figure, the zonal mean zonal wind is shown as a function of pressure level and latitude. As the figure illustrates, the associated westerlies of the jet stream aloft extend throughout the troposphere to the surface. As the previous figures have alluded to, the presence of the subtropical jet is most pronounced in the winter season and is not there in the summer. In all the means, it is seen that the westerlies extend from the eddy driven jet to the surface at a latitude of about 50°S. This is a signature of the jet being eddy driven as opposed to the subtropical jet where no such surface westerlies are present at the same latitude. The dynamics that drive this is explained in Chapter 4.

3.2 – Eddy Fluxes of Momentum

3.2.1 – Zonal Varying Field

The nature of why the mid-latitude (eddy-driven) jet extends throughout the troposphere is due to the fluxes of eddy momentum. As a result, examining the climatology of the eddy fluxes of momentum is of interest. The flux of eddy momentum is defined as the product of the eddy components of the meridional (v) and zonal (u) wind fields. Similar to the previous section, the zonally varying and zonal mean at 300mb, as well as the zonal mean as a function of height will be discussed.

Figure 3.5 shows the zonal varying map of the eddy momentum flux at the 300mb level for the annual, winter, and summer means. For these figures, the blue shading represents a poleward flux and the red is an equatorward flux. Examining this figure shows that the winter mean dominates the amplitude when compared to the summer, and the annual mean by extension. The latitude where the maximum poleward eddy momentum flux occurs lies at around the same amplitude as where the subtropical jet resides during the winter season. When compared to that of Figure 3.1, it is seen that the zonal range of the eddy momentum fluxes tends to be a bit varied in relation to that of the maximum zonal winds associated with the subtropical jet. In contrast to the summer mean, it is seen that the regions of maximum eddy momentum flux are roughly at the same longitudes as that of the winter season but shifted slightly more poleward. The regions seen in the summer mean are associated with the mid latitude jet since as mentioned in the previous section, in the summer, the mid-latitude jet dominates the zonal wind climatology. When looking at the summer means in both Figure 3.1 and 3.5, it is seen that the regions of the maximum respective values (which holds primarily for the 850mb level of the wind and not necessarily other levels) reside at the same longitude bands, which is to be expected as the mid latitude jet is eddy driven and where the highest winds are located should be co-located with the regions of highest eddy momentum flux. Similar to the zonal mean zonal wind field, the zonal mean of the eddy momentum flux will be examined.

3.2.2 – Zonal Mean Field

As with the zonal wind fields, looking at the zonal mean can lead to further insight. Figure 3.6 shows a plot of the eddy momentum flux at 300mb for annual, winter, and summer. For each season, it is seen that the eddy fluxes are equatorward (positive values) of 55°S poleward and poleward (negative values) equatorward of 55°S. Another observation is that the amplitude of the eddy momentum fluxes is greatest in the winter season for both the poleward and equatorward components.

The eddy momentum flux can be seen with respect to height in Figure 3.4. As illustrated, the region of largest poleward flux is centered about the latitude of ~35° S at a pressure level of 300mb. There is also a region of equatorward flux, as seen in Figure 3.4 and Figure 3.5 that is centered about 70°S at 300mb as well. As with theory, these fluxes are located aloft and their associated winds do not reach the surface, as evidenced by Figure 3.4.

3.3 - Eddy Fluxes of Heat

3.3.1 – Zonal Varying Field

As mentioned in previous sections, the eddy heat flux is the product between the eddy fields of the meridional component of the wind, v, and that of the temperature, T. As per the theory outlined in previous works and in Holton (2004), this transport of eddy heat flux will be near the surface. For this reason, the 850mb pressure surface was selected.

Figure 3.7 illustrates the zonal varying climatology associated with that of the eddy heat flux at 850mb. When looking at Figure 3.7, it is seen that like the momentum flux, the winter season experiences the greatest amplitudes. The reason for this is largely due to the stark contrast in temperatures between the pole and the equator during winter. This temperature contrast increases the baroclinicity in the Southern Hemisphere and thus results in the largest transport of heat. In this figure, it is seen that the largest values of poleward eddy heat flux tend to be at very poleward latitudes. The sign convention, as with the eddy momentum flux, is that negative values represent a poleward transport and positive values represent an equatorward transport of heat. Due to the topography interfering with the 850mb pressure level, the regions intersecting the Antarctic continent should be taken with some skepticism. Due to the dynamical balances outlined in previous chapters as well as what is explained in Chapter 4, the regions of highest eddy heat flux should be poleward of the regions of maximum eddy momentum flux as well as roughly co-located in terms of the westerly zonal winds at 850mb. When comparing Figures 3.1, 3.5, and 3.7, it is seen that this is indeed the case.

3.3.2 – Zonal Mean Field

Figure 3.8 shows the zonal mean field associated with the eddy heat flux. Due to the topographic concerns, only latitudes equatorward of 70°S have been presented. It is observed that a poleward eddy heat flux is evident over the Southern Hemisphere latitudes, as seen by the negative values. Winter, as has been the theme across other fields, exhibits the greatest amplitudes. When comparing the summer and winter seasons, it can be seen that there is a relative maximum at 50°S and 60°S respectively. When looking at the annual mean, it can be seen that the relative maximum poleward transport of eddy heat flux is approximately 20° poleward of the maximum poleward eddy momentum flux. This is consistent with the dynamics associated with the conventional Eulerian mean framework.

Figure 3.4, shows the eddy heat flux as a function of pressure. As was mentioned previously, it is expected that the maximum values should occur at pressure levels near the surface. When looking at Figure 3.4, it is seen that the largest values do lie in the lower troposphere, at pressure levels of 700-1000mb. However, it is interesting to note that this poleward flux of heat extends into the stratosphere over a fairly broad latitude range. These forcings caused by the eddy fluxes of heat and momentum will be explored further in later chapters.

3.4 – Meridional Temperature Gradient

3.4.1 – Zonal Varying Field

The meridional temperature gradient is another field that the climatology will be looked at. This field is defined as the gradient of the temperature field with respect to latitude. Knowing this quantity is of interest as it is a measure of the baroclinicity in a region. Using the past work conducted by Eady (1949), it can be stated that high baroclinicity is associated with a strong meridional temperature gradient. As will be mentioned in subsequent chapters, knowing the regions of where baroclinicity is high is important, as these are the regions in which baroclinic waves are generated.

Figure 3.9 shows the climatology of the 850mb zonal varying eddy heat flux. Aside from the interfaces the 850mb level has with the continents, the regions of maximum poleward heat gradient tend to lie in the same latitude region as that of the eddy heat flux. This is as expected as the regions of largest baroclinicity will tend to be where the eddy heat flux is at a maximum.

3.4.2 – Zonal Mean Field

Figure 3.10 shows the zonal mean of the meridional temperature gradient. To first order, these plots are quite similar to that of those presented in Figure 3.8. To a large degree, across the annual and both season means, the degree of baroclinicity seems to stay relatively constant at around the -1K/1.5 degree of latitude. While the climatology of this field is presented here, this measure of baroclinicity, as well as the other discussed fields will be revisited in subsequent chapters to further gain insight on the associated dynamics.

This chapter sought out to briefly describe the climatology across a multiple of various fields that will be the subject of analysis in future chapters. Taking a look at the climatologies can give insight on how these various dynamical fields interact with one another. In the following chapter, it is this discussion of a baroclinic mechanism that relates these fields together.

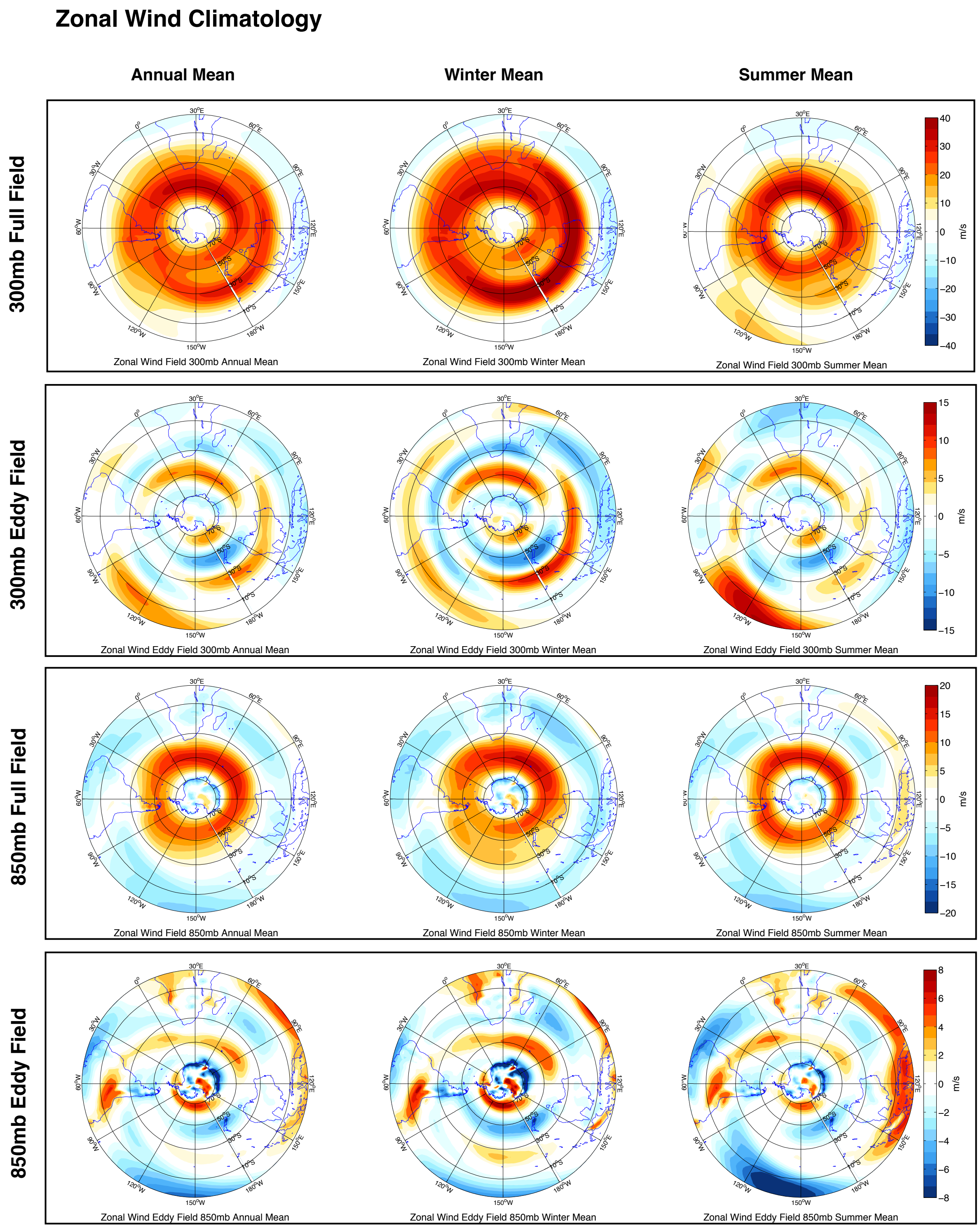

Figure 3.1 Climatological mean of the zonal wind as a function of latitude and longitude for 300mb and 850mb and their respective eddy fields.

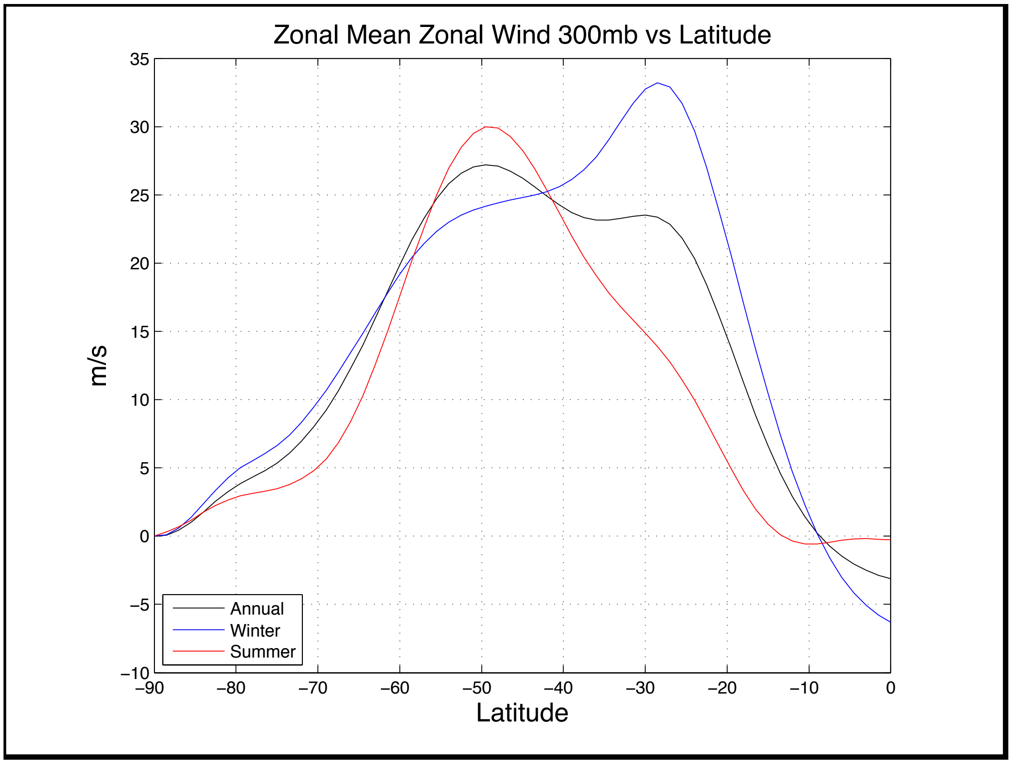

Figure 3.2 Climatological mean of zonal mean zonal wind as a function of latitude for 300mb for annual, winter, and summer means.

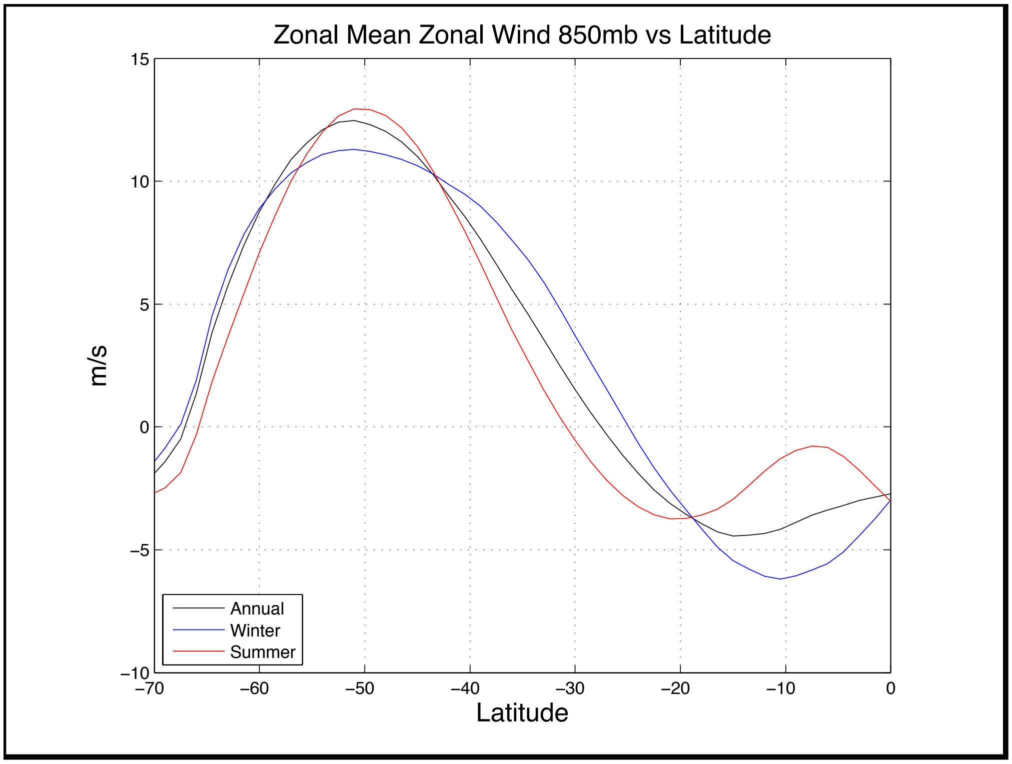

Figure 3.3 Climatological mean of zonal mean zonal wind as a function of latitude for 850mb for annual, winter, and summer means.

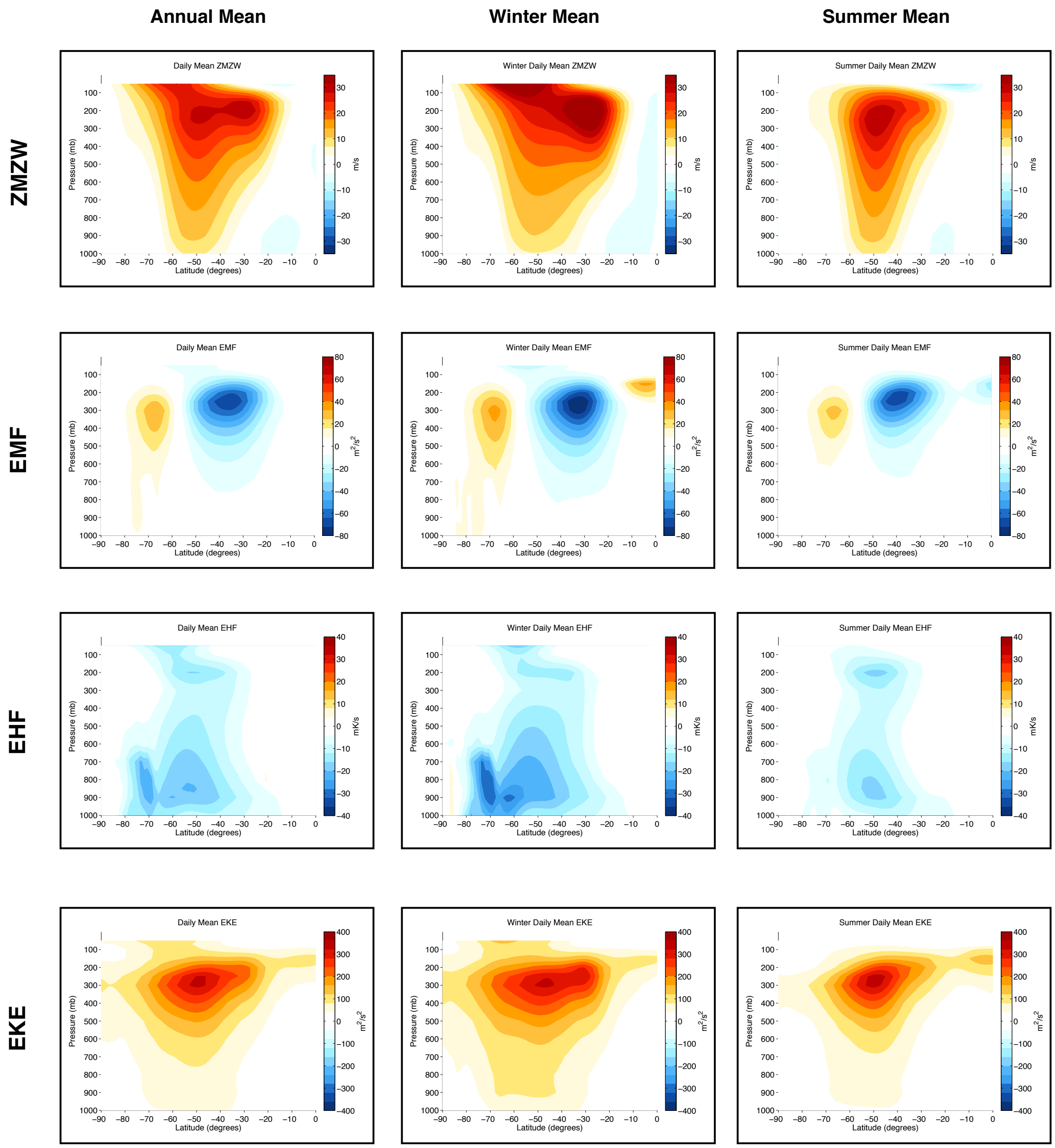

Figure 3.4 Climatological mean of zonal wind, eddy momentum flux, eddy heat flux, and eddy kinetic energy as a function of latitude and pressure level.

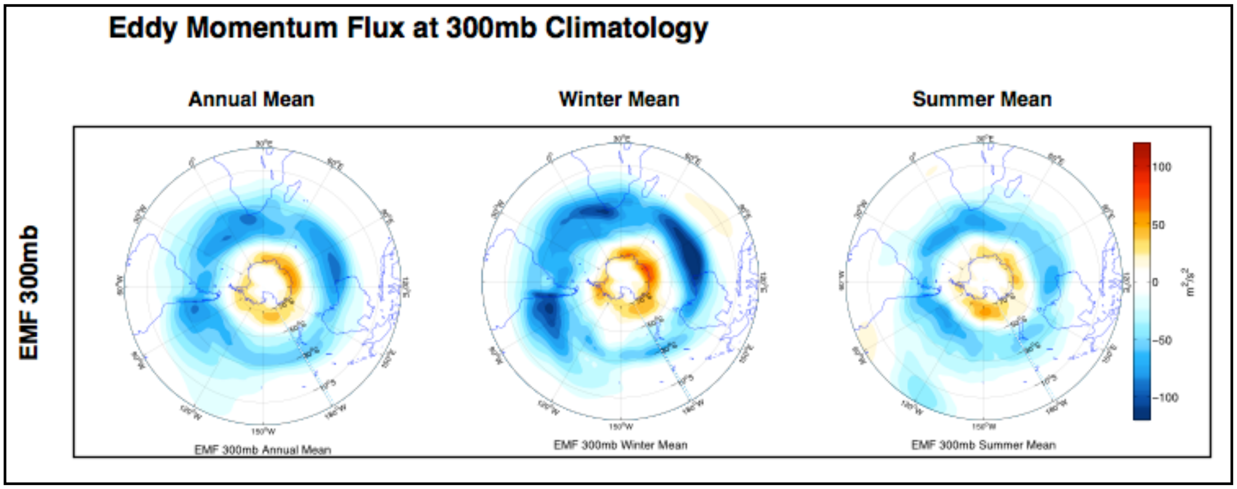

Figure 3.5 Climatological mean of eddy momentum flux as a function of latitude and longitude at 300mb.

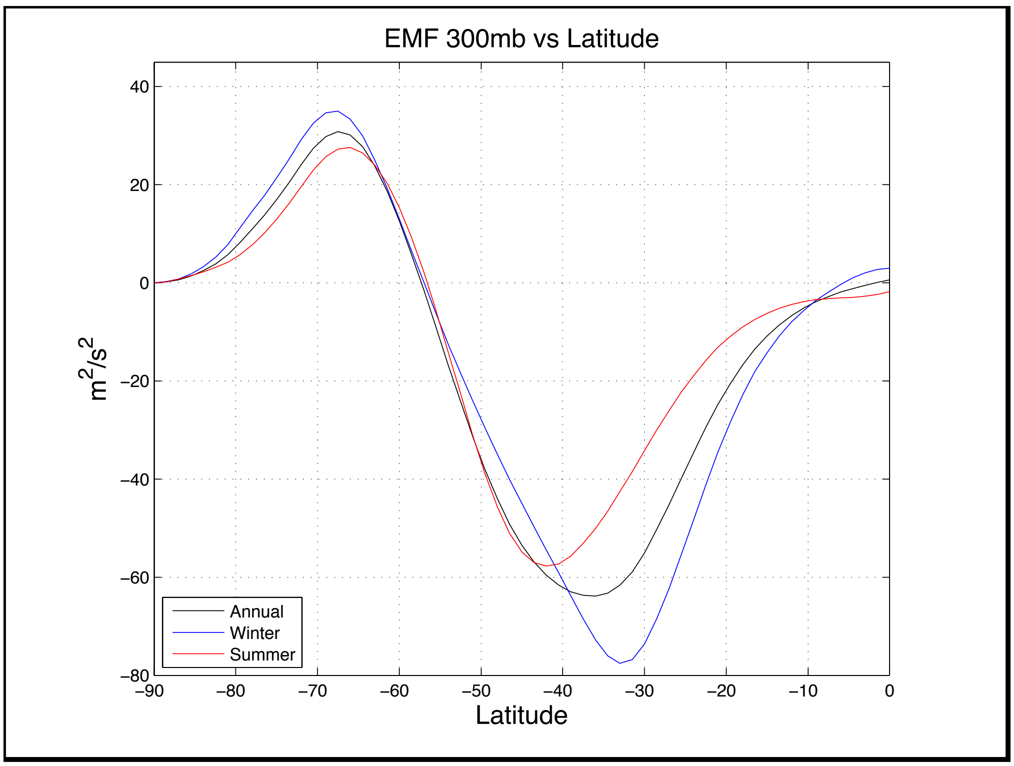

Figure 3.6 Climatological mean of the zonal mean eddy momentum flux as a function of latitude at 300mb for annual, winter, and summer means.

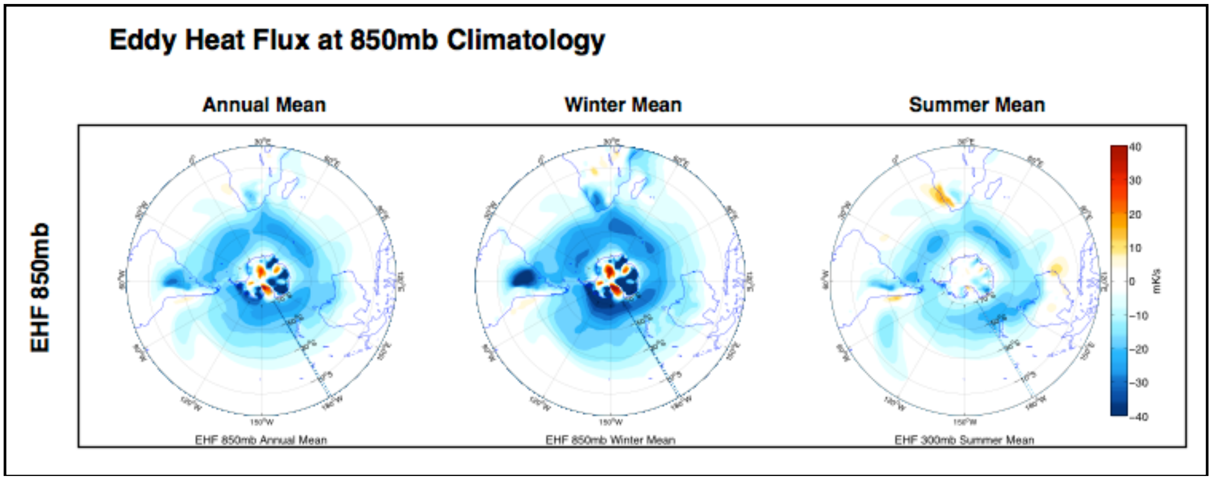

Figure 3.7 Climatological mean of eddy heat flux as a function of latitude and longitude at 850mb.

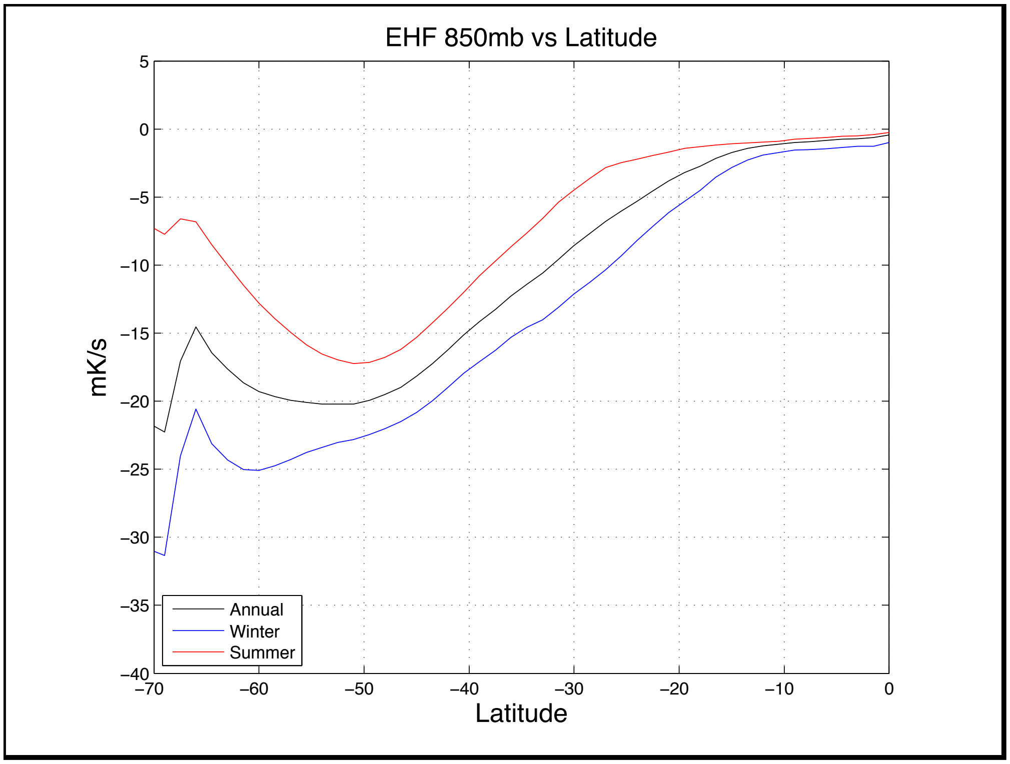

Figure 3.8 Climatological mean of the zonal mean eddy heat flux as a function of latitude at 850mb for annual, winter, and summer means.

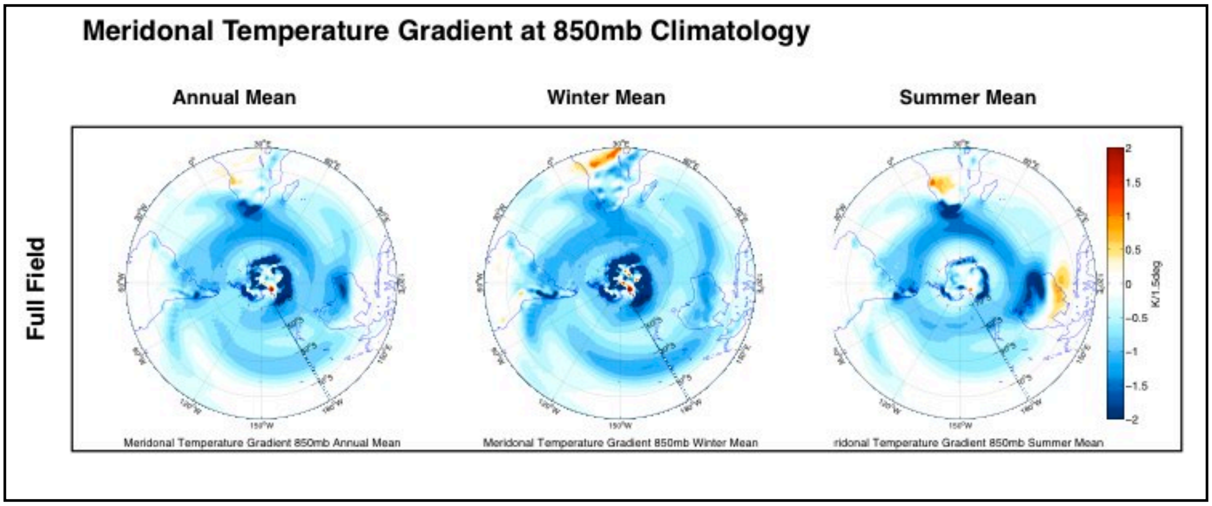

Figure 3.9 Climatological mean of meridional temperature gradient as a function of latitude and longitude at 850mb.

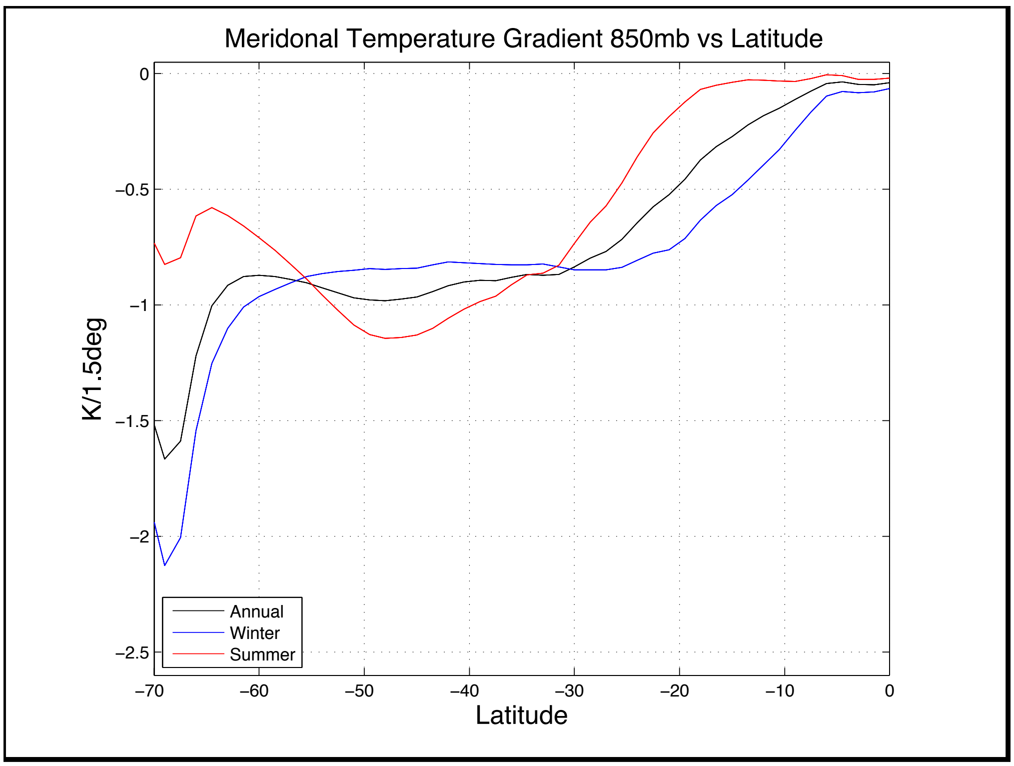

Figure 3.10 Climatological mean of the zonal mean meridional temperature gradient as a function of latitude at 850mb for annual, winter, and summer means.

CHAPTER 4: EXAMINING THE PHYSICAL NATURE OF THE ANNULAR FEEDBACKS

The first component of this study is to examine current theory pertaining to how the eddy flux of heat relates to that of the eddy flux of momentum. As mentioned in Chapter 1, there have been many studies that have looked into the behavior of the dynamics associated with that of the mid-latitude jet. What has been observed is that the interactions between the zonal and eddy components of the circulation are such that there is a tendency for the jet to want to stay in a position once moved. It is this behavior between the eddy and zonal components of the flow that has led to many studies on a possible feedback mechanism (Gerber and Vallis 2007; Kidston et al. 2010; Robinson 2006). To understand the feedback mechanism, the variability of the zonal mean zonal wind first needs to be explained.

4.1 – A Look at the Variability of Various Dynamical Fields

Before discussing the nature of the feedback mechanism, it is important to first understand the nature of the variability associated with the zonal mean zonal wind. As described in Chapter 1, the leading pattern of variability in the Southern Hemisphere may be identified through a multitude of fields and has been termed the Southern Annular Mode (SAM). However, the zonal mean zonal wind is used as the diagnostic field in this study. When looking at the SAM through the context of the zonal mean zonal wind, the leading patterns represent differing behaviors.

The leading patterns of variability associated with the zonal mean zonal wind represent behavioral tendencies in the jet. It is documented that the leading EOF is the variability of the jet in terms of latitude, whereas the second EOF is largely associated with the pulsation of the set (Lorenz and Hartmann 2001). For the purpose of this study, the leading EOF of this field, the SAM, as well as those associated with other dynamical fields will be where most of the analysis is conducted. To obtain the leading patterns of variability, the data and methods as described in Chapter 2 were utilized.

By performing an empirical orthogonal function (EOF) analysis on the daily zonal mean zonal wind at 300mb, what is found is that the variability presents itself as a barotropic dipole that has maximum anomalies at 40°S and 60°S (Hartmann and Lo 1998; Kidson 1988; Karoly 1990). The leading EOF accounts for over 37% of the variance explained and that the second leading EOF is shown to explain about 21% of the variance. The resulting structure may be seen in Figure 4.1. This structure is in agreement to that performed in past literature, such as Figure 1.1, taken from Hartmann and Lo (1998) and Figure 4.2 taken from Lorenz and Hartmann (2001). A similar agreement is seen with the second EOF. Here, it is seen that there is a tri-pole with minima centered on 70°S and 30°S with a large maxima at 50°S. However, there are some differences in the amplitude as well as the variance explained. This is largely a result of how the EOFs were calculated in the sense of the domain utilized as well as the time period. These factors lead to the slight differences between the patterns, but for the most part, are consistent with the literature. To examine how the fluxes of eddy heat and momentum affect the SAM, their variability also needs to be examined.

As with the zonal mean zonal wind, additional leading patterns of other dynamical fields may be observed. Figure 4.3 shows the leading patterns of variability that are associated with that of the eddy momentum flux at daily resolution. What is seen here is that the leading pattern of variability is a pulse with a maxima centered just equatorward of 50°S. This structure accounts for close to 50% of all variance within this field. When looking at the second leading pattern of variability, what is seen is that there exists a dipole with relative minima and maxima at 55°S and 35°S and explains for ~23% of the variance.

Similarly, this same analysis can be performed on the eddy flux of heat. Like the leading mode of the eddy flux of momentum, the leading pattern of variability of the eddy flux of heat is a pulse at 55°S and explains 33% of the variance. The second EOF of this field is also a dipole with minima and maxima at 70°S and 42°S and explains 21% of the variance. These patterns may be observed in Figure 4.4. When comparing the variability of these two forcings, some observations may be seen. In examining the leading patterns of variability between the eddy fluxes of momentum, and that of the eddy flux of heat it is seen that leading EOFs (both 1 and 2) of the eddy momentum flux have their greatest magnitudes equatorwards of the respective centers of action associated with the eddy flux of heat. The reason as to why this is will be detailed in later sections.

The last dynamical field at which the variability of which was explored is that of the eddy kinetic energy, as was defined in Chapter 2. Akin to the fluxes of heat and momentum, the leading EOF of EKE is represented by a monopole just equatorward of 50°S and explains 34% of the variance. Similarly, the second EOF of EKE is a dipole with maxima and minima at 65°S and 35°S respectively. The resulting structures may be seen in Figure 4.5. When compared to the leading

EOFs of the flux of eddy momentum, it is seen that the regions of peak magnitude align fairly well with each other, for reasons that will be discussed later.

4.1.1 – An Examination as to How the Fields Relate to One Another

With the variability of the above fields examined, past studies have looked into how these fields affect the SAM. To this effect, an analysis of the SAM was conducted in more detail in the Hartmann and Lo (1998) study. In their study, what they had found was that when looking at the TEM framework, interesting insights could be obtained by performing a momentum analysis amongst the various dynamical fields. In doing so, they were able to show how the changes in the zonal winds were impacted, and in what relative magnitude, to the fluxes of eddy heat and momentum. It was found that changes in these fluxes supported changes of the zonal flow in response to surface drag that is associated with the variability. This finding supports the notion of a potential feedback that exists between the zonal mean flow and that of eddy component. This result led to a future study (Lorenz and Hartmann in 2001) to quantify the nature of this feedback.

In the Lorenz and Hartmann (2001) study, the findings of Hartmann and Lo (1998) were extended. In this study, it was found that the forcing term associated with the flux of eddy momentum, defined as the projection of the SAM onto the first term on the right hand side in equation 1.1, leads the zonal wind when a lag cross-correlation plot is created. This behavior is expected as the zonal mean wind responds to the forcing due to the flux of eddy momentum. However, the question regarding a feedback is whether or not these eddy momentum fluxes respond to changes in the zonal wind. The findings in this study appear to state that this may be the case. Revisiting Figure 1.3 from Chapter 1, it is observed at positive lag there is a positive correlation from day 5 onwards. This region of positive correlation is what Lorenz and Hartman (2001) attribute to the evidence of a positive feedback. With this evidence of a proposed feedback, many studies were conducted to further examine the nature of the SAM.

With this leading mode in the Southern Hemisphere, much work has been attempted to try and understand the nature associated with this variability. Past efforts have made use of various models in attempts to understand the dynamics (Chen et al. 2010; Vallis et al 2003; Ring and Plumb 2006). Additional efforts have explored how the eddy and zonal components of the flow interact with each other through a variety of approaches (Gerber and Vallis 2007; Barnes et al. 2010; Barnes and Hartmann 2010; Lorenz and Hartmann 2001). From these works, and others, many feedback mechanisms have been identified to explain this behavior seen with the SAM. The proposed mechanisms have been nicely summarized by a study conducted by Kidston et al. (2010) as well as introduced in a study by Hartmann (2000). For the purpose of this study, a baroclinic mechanism put forth by Robinson (2000) will be the focus of this study . A brief summary of this mechanism is presented.

Of these feedbacks presented and discussed in the literature, the Robinson (2000) feedback mechanism was also examined. This feedback mechanism, baroclinic in nature, involves processes that result in the eddy component of the flow adjusting to the zonal wind anomalies in a manner that the initial baroclinicity is positively reinforced. Robinson (2000) explains how such a mechanism would work and other studies (Blanco-Fuentes and Zurita-Gotor 2011) support this feedback mechanism as proposed by Robinson (2000). As a result, it is this baroclinic mechanism that will be the focus of the first part of this study

4.2 – Description of the Robinson (2000) Mechanism

4.2.1 Response of the Circulation to Fluxes of Heat and Momentum

Before one can discuss the feedback that was proposed by Robinson (2000), it is important to go through how the circulation that drives this feedback will behave. As this study is looking at the forcings associated with the eddy flux of heat and momentum in the conventional Eulerian mean framework, each forcing will be looked at individually. This description of the circulation is mathematically related via the equations that were introduced in section 1.2.2.

4.2.2 – Response Due to Eddy Flux of Momentum

The first forcing that will be discussed is that of the flux of eddy momentum. To aide in the discussion of this forcing, as well as that of the eddy flux of heat, Figure 4.6 will be utilized. Figure 4.6 illustrates how the various dynamical fields interact with one another via the Robinson (2000) feedback mechanism. When looking at the schematic, a poleward transport of eddy momentum flux creates a region of divergence on the equatorward side and a convergence in the poleward side. A divergence of momentum flux is denoted as a positive quantity as the gradient of momentum flux is increasing and vice versa. With this gradient the response of the circulation may be deduced from the governing equations presented in section 1.2.2.

When examining the equations in section 1.2.2 as well as the schematic in Figure 4.6, various insights may be observed. Noting that aloft and at steady state, this divergence of eddy momentum flux must be balanced solely by that of the Coriolis term due to the absence of friction. Diagnosing each term with respect to sign, it can be shown that in this region of eddy momentum flux divergence, there is a poleward-induced circulation. Similar reasoning will show that in the region of eddy momentum flux convergence, there is an associated equatorward flow. Due to conservation of mass, where these two branches of circulation meet results in a downward flow that is associated with adiabatic warming. Similarly, upon reaching the surface, this downward branch will flow in a meridional manner to complete the circulation of the cells as shown via Figure 4.6. Note that at the surface, the meridional branches of the circulation must be balanced by friction as seen in equation (1.1). As mentioned in section 1.2.2, this friction, and thus surface winds, is only possible as a result of there being eddy momentum fluxes aloft. It is of note that the response to this forcing enhances the equator to pole temperature gradient. The response due to the forcing of the eddy flux of heat is different and will be discussed next.

4.2.3 – Response Due to Eddy Flux of Heat

In a similar manner, the response to eddy heat flux may be examined through the context of the same governing equations. Initially, with a poleward flux of heat, there are associated poleward surface winds. This poleward flux of heat is effectively acting against the response caused by the flux of eddy momentum by reacting to mitigate the temperature gradient between the equator and pole. This poleward flow of air results in a convergence of eddy heat flux polewards of where the initial baroclinicity originated. As a result, this convergence must be accompanied by a vertical rise in circulation. Similarly, a downward branch of circulation accompanies the divergence region equatorward of the region of initial baroclinicity. Upon reaching the tropopause and due to conservation of mass, the circulation branches aloft will then travel equatorwards, which completes the circulation. The circulation response to that of the eddy heat flux further intensifies the flux of momentum at this source latitude. This behavior suggests that there is a relationship of the eddy flux of heat to that of the eddy momentum flux.

As an aside, the above discussion was viewed in the context of the conventional Eulerian mean framework. However, one may also examine the response through the Transformed Eulerian Mean (TEM) framework. In the TEM framework, the poleward flux of heat is analogous to vertically propagating waves. As these waves travel vertically, a portion of them will break upon reaching the tropopause. Those that do not break will be diverted and travel meridionally. In traveling meridionally, these waves will flux momentum into the jet. This interaction between the fluxes of heat and momentum illustrates how a feedback may exist. The next section will discuss how this feedback, in the context presented by Figure 4.6, manifests itself in the observational data.

4.3 - Proposed Feedback Loop

The baroclinic mechanism put forth by Robinson (2000) consists of a few steps. The mechanism is one that emphasizes the role of baroclinic eddies, namely that associated with the eddy flux of heat that are generated at the surface. The proposed feedback is as follows: Initially, these baroclinic eddies are generated in a region where there is anomalous zonal wind. These baroclinic eddies then propagate meridionally away from this source region, and upon doing so, flux momentum into this source latitude. This flux of momentum into the latitude where the baroclinic eddies were generated drives a circulation that enhances the surface westerlies or zonal wind anomalies that started the process initially. What he found was that this proposed feedback, in which the eddy component of the flow interacts and influences the zonal flow which then influences the eddy component of the flow, is a result of surface drag. As described in section 1.2, it was shown that in the presence of eddy momentum fluxes aloft, there must be surface winds to accompany it and with surface winds, there is friction. This may be seen visually in Figure 4.6.

Figure 4.6 summarizes this process in a visual manner. In this figure, imagine that the region of greatest baroclinicity lies between points (2) and (3). In this region, the baroclinicity acts to generate anomalous baroclinic wave activity that is associated with vertically propagating wave activity and a poleward flux of heat. These vertically propagating waves, as a result of the baroclinic activity in the mid latitudes, travel until they reach the tropopause. Upon reaching the tropopause, a portion of these waves break and a portion are able to propagate and travel meridionally. This meridional travel of the wave activity fluxes momentum into (1) and is the region of eddy momentum flux convergence. This eddy momentum flux convergence then drives a residual circulation as governed by equation (1.1). This resulting change in the meridional circulation drives adiabatic temperature changes at points (2) and (3) which reinforce the temperature gradient and the resultant baroclinicity. It is this sequence of events that this first part of the study seeks to find in the observational data.

4.4 – Diagnosing the Feedback

To diagnose this feedback loop in the observational data, the dynamical fields that are listed in equations (1.1) and (1.4) from Chapter 1 are examined. These fields are then analyzed using the methods as outlined in Chapter 2.

One of the statistical tools that are utilized to diagnose this is that of lag-regression plots. This type of plot is useful as it essentially allows one to see how various dynamical fields relate to each other as a function of time. For the purpose of this study, the dynamical fields involved in the proposed feedback were all regressed upon the leading PC of the zonal mean zonal wind. In other words, these fields were regressed upon the SAM and should give insight as to how these fields relate in terms of magnitude of their respective signature as well as time relation to that of the leading pattern of variability in the Southern Hemisphere.

Figure 4.7 illustrates how the various fields behave when regressed upon the SAM as a function of time. When looking at these observations, it can be seen that a sequence of events may be seen that seem to agree with the baroclinic mechanism that was proposed by Robinson (2000). Walking through this figure, evidence of a feedback may be seen.

The sequence of events begins with the upper left plot of Figure 4.7. Here, the eddy momentum flux field has been lag-regressed upon the SAM. Consistent with the findings in Lorenz and Hartmann (2001), this eddy forcing precedes the changes in the zonal wind as evidenced by the large amplitudes at negative lags. What is seen in this figure is that this forcing of eddy flux of momentum gradually intensifies from beyond 20 days before the jet shifts position and maximizes a few days before the zonal mean zonal wind responds. When referring back to the before mentioned schematic, this region of eddy flux of momentum is given by point (1). Following this peak of eddy momentum flux forcing, the zonal mean zonal wind at 300mb, the meridional temperature gradient, and the surface wind response should shortly follow.

The response of the zonal wind is seen in the top right panel of Figure 4.7. Consistent with mechanism proposed, the forcing given by the eddy flux of momentum results in the zonal mean zonal wind field responding largely a few days after the occurrence of the peak flux of eddy momentum. The response of the zonal mean zonal winds is given by a strong dipole that represents the meridional shift of the zonal wind. This is consistent with the schematic provided in Figure 4.7. It is this signature in the wind field that represents the leading mode of variability of the wind in the Southern Hemisphere, or SAM (Thompson and Wallace 2000). With this change in the jet, a change in baroclinicity is expected if there is to be a feedback.

The middle row, left column of Figure 4.7 illustrates the change of baroclinicity seen at the surface when regressed upon the SAM. Alongside the response seen with the midlatitude jet, the resulting circulation is such that there is adiabatic heating associated with the descending branch and adiabatic cooling with the ascending branch. This change occurs seemingly simultaneously with the changes in the jet, as evidenced by the corresponding lags where the peak amplitudes reside. This is consistent with the explanation given to how the circulation responds to eddy momentum fluxes in section 4.2. The lag regression plot of the meridional temperature field gradient taken at 850mb illustrates this increase in baroclinicity. This plot illustrates that in response to the initial eddy momentum forcing, that the temperature gradient between the pole and equator is increasing, as shown by point (2) in the schematic (Figure 4.6). As this figure illustrates, the change in this field occurs at the same lag as that experienced by the zonal mean zonal wind aloft at lag day 0. This is expected due to the circulation cell that develops.

The zonal mean surface winds should also respond to that of the flux of eddy momentum. The corresponding lag-regression may be seen in the second row, right column of Figure 4.7. As expected with the mechanism, the changes of the surface winds happen simultaneously to each other but after that of the initial eddy momentum forcing. A similar dipole pattern is seen as that of the SAM response aloft but of lesser magnitude. This decrease in wind speed relative to the 300mb winds is largely a response to that of friction. With this change in surface winds and baroclinicity, it should be expected that a poleward flux of heat would follow suit.

In the left column of the bottom row of Figure 4.7, the eddy heat flux field is lag-regressed upon the SAM. In order to complete the loop, these heat fluxes should induce further generation of eddy momentum fluxes. This regression of the heat fluxes on the SAM seems to suggest that this loop is complete. However, before describing this evidence, some observations will be noted. When looking at the plot, there is a poleward heat flux at positive lags consistent with the changes in the meridional temperature gradient. This poleward heat flux is represented by the predominant negative values at 70°S at lag values of 3-10 days. However, upon observing the plot, equatorward fluxes of heat at shorter positive lags are seen. This difference between positive and equatorward fluxes of heat was found to be largely a result of different frequencies of the eddy flux of heat. The high frequency component, being less than 10 days, of the eddy heat flux is responsible for the poleward component while the low frequency, being greater than 10 days, component is responsible for the equatorward flux. The methods of filtering were discussed in section 2.2.6. This breakdown of the eddy heat flux into various frequency components may be seen in Figure 4.8. However, as mentioned earlier, this plot suggests that a feedback is present.

Evidence of this feedback is seen when one focuses on the poleward component of the eddy heat flux. It is observed that there is a maximum poleward component that regresses strongest on the SAM at lag of 4-6 days after the changes in the zonal mean zonal wind are observed at a latitude poleward of the eddy momentum flux. This is consistent with the schematic as shown in Figure 4.6. If there were to be a feedback, it would require a poleward flux of heat at relatively long positive lag that would result in further poleward fluxes of eddy momentum. This feedback seems to present itself. When looking back at the first lag-regression plot in Figure 4.7, there is a slight notion of poleward eddy momentum flux at 5-10 days. This eddy momentum flux occurs past that of the eddy heat flux at lag 4-6 days, which infers that there may be in fact, observational evidence of such a feedback that was described by Robinson (2000).

Another field that is of interest is looking at the eddy kinetic energy (EKE) when it too, is lag-regressed upon the SAM. This plot may be seen in the third row, right column of Figure 4.7. What is seen is that the EKE experiences increases at the same latitude as the jet where westerlies are enhanced and decreases where the jet is seeing an increased easterly component (decreased westerly component). These changes in EKE are occurring largely at positive lags after the changes in the zonal winds have occurred. How the EKE relates to the SAM and the forcings of eddy heat and momentum will be explored in greater detail and this result serves as a prelude for the upcoming chapter and next component of this study.

To further diagnose the relation of the eddy heat flux to that of the eddy momentum flux, averaging techniques, as well as regressing on the eddy heat flux field was done. To see if the eddy momentum flux is related to the eddy heat flux, the region associated with a poleward transport of heat was averaged between latitudes 50°S to 75°S. The response of the eddy momentum flux to that of the averaged index of the eddy heat flux may be seen in Figure 4.9. What this figure shows is that there is a poleward eddy momentum flux that occurs before the poleward heat flux. However, the positive values of eddy momentum flux at slight positive lags suggest that after a poleward flux of heat, there is an equatorward flux of eddy momentum that goes against this potential feedback between these fields.

The aim of this chapter was to see if the feedback mechanism proposed by Robinson (2000) was present in the observational data set. From the figures presented, there does seem to be evidence that such a feedback exists. The following chapter now seeks to isolate these forcings of eddy heat and momentum and look at them through the context of the atmospheric energy cycle to attempt to gain further insight into how these fields interact with each other. By analyzing these two forcing mechanisms on their own, it will be of interest to see how connected they are. Techniques such as correlations between the various leading PC's of these fields as well as how the general circulation responds to these forcings explicitly will be examined and discussed in the next chapter.

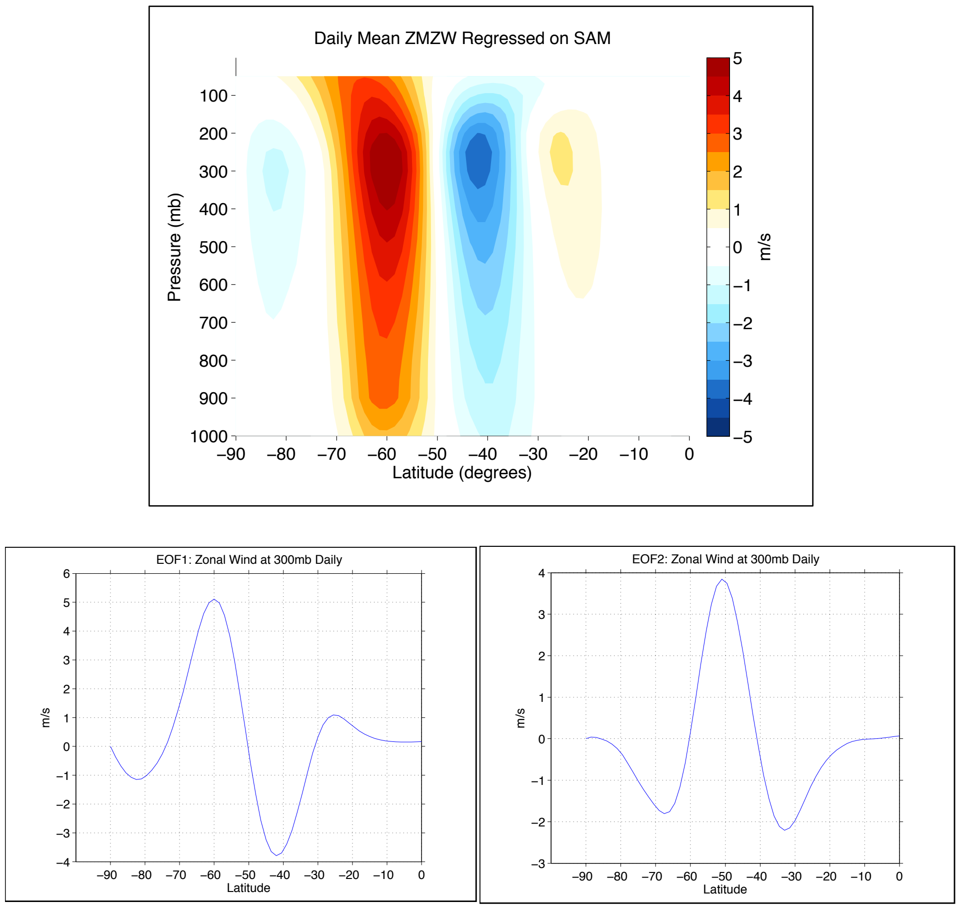

Figure 4.1 Leading EOFs of the zonal mean zonal wind at 300mb based on daily mean data. Top shows ZMZW at all levels regressed upon SAM. Bottom shows the SAM (left) and EOF2 (right). EOF1 explains 37.26% of the variance and EOF 2 explains 20.84% of the variance.

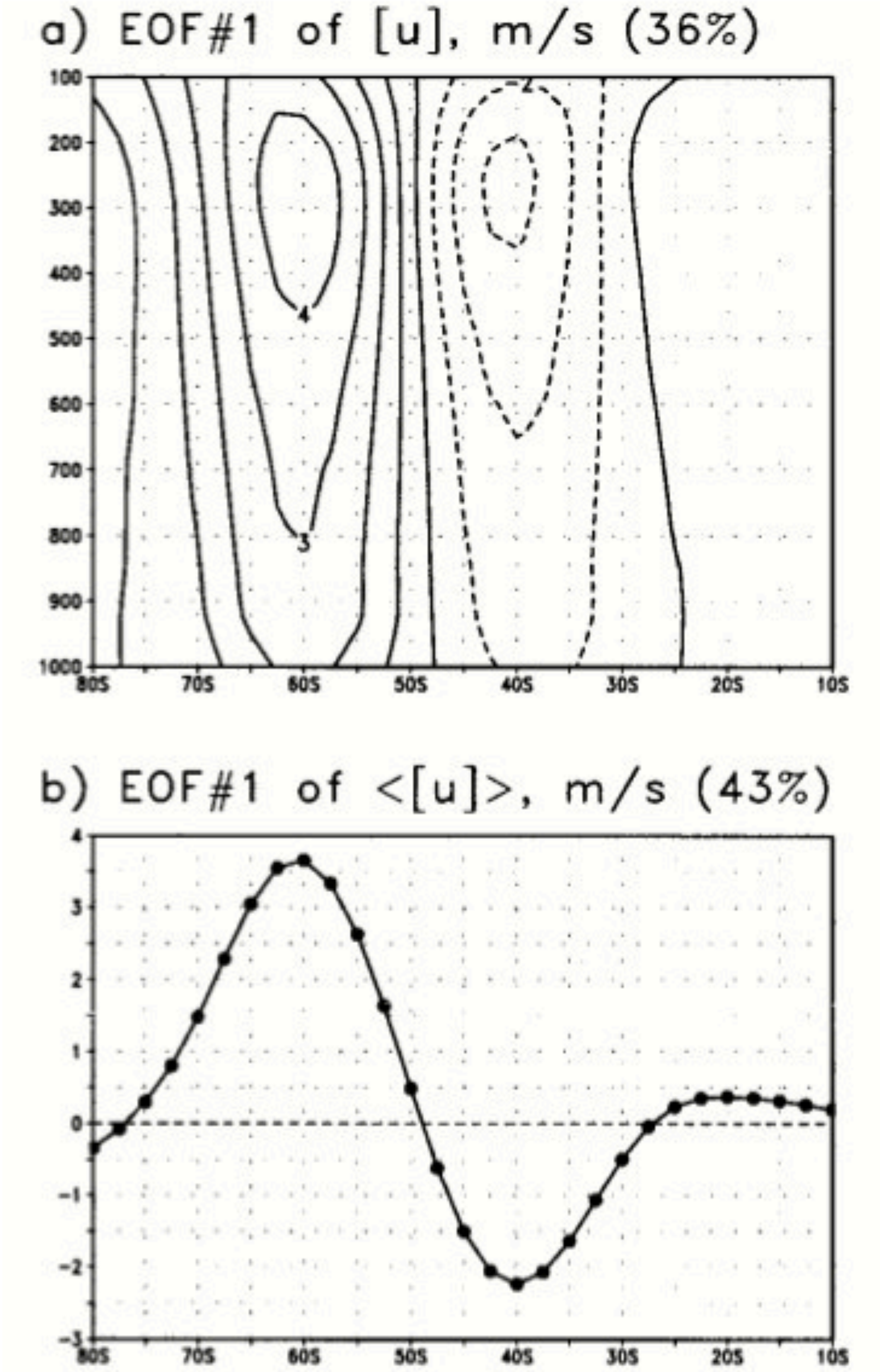

Figure 4.2 From Lorenz and Hartmann (2001). The top panel shows EOF1 of the zonal mean zonal wind. The bottom panel shows EOF1 of the vertical and zonal mean zonal wind. The percent variance explained is given at the top-right corner of the plot.

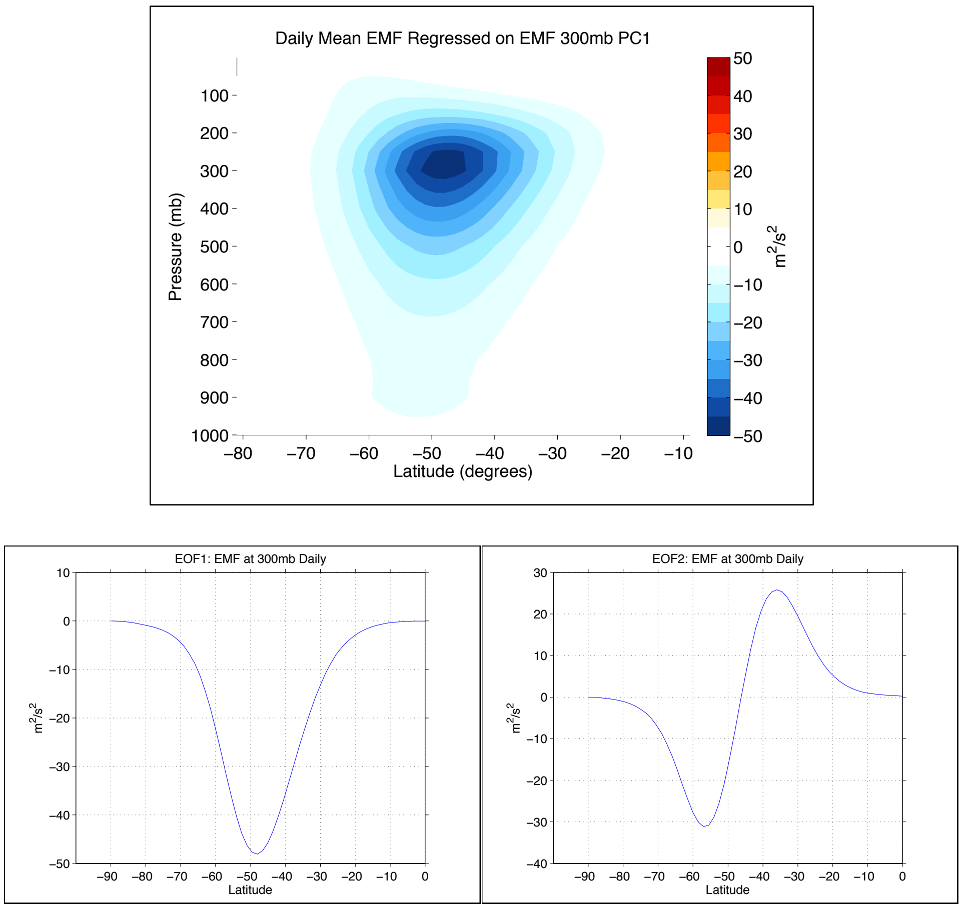

Figure 4.3 Leading EOFs of the zonal mean eddy momentum flux at 300mb based on daily mean data. Top shows EMF at all levels regressed upon EMF 300mb PC1. Bottom shows EOF1 (left) and EOF2 (right). EOF1 explains 49.52% of the variance and EOF 2 explains 22.91% of the variance.

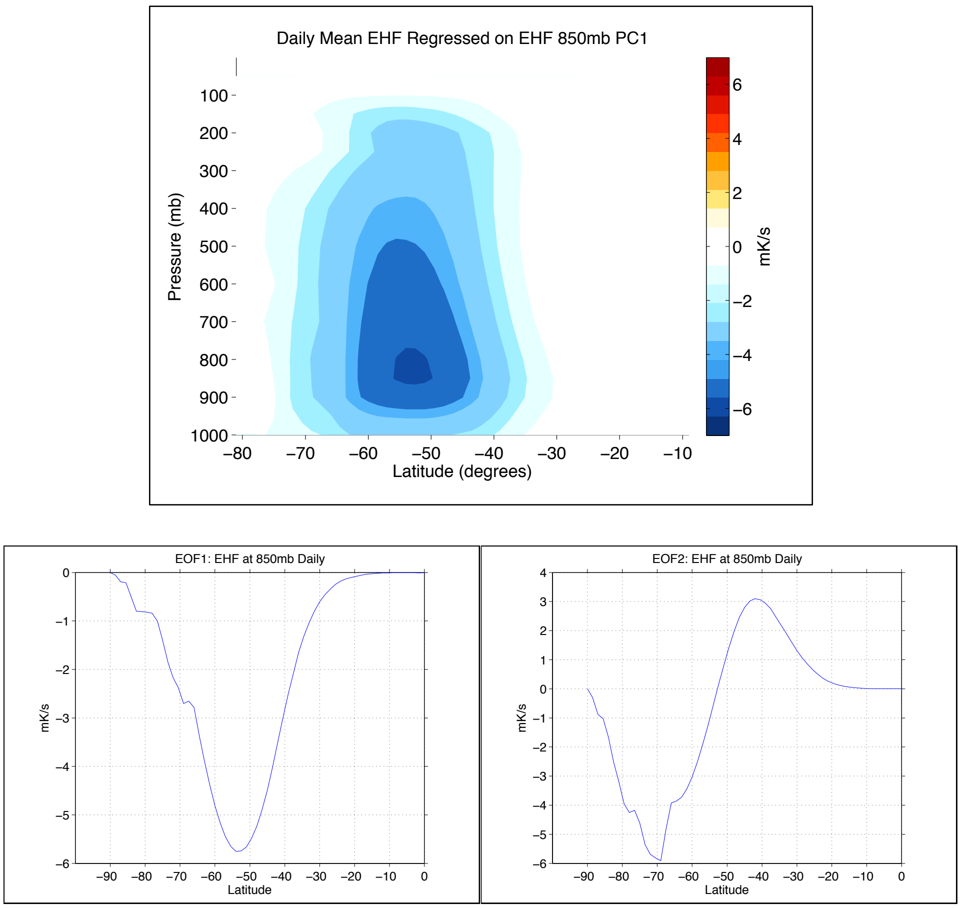

Figure 4.4 Leading EOFs of the zonal mean eddy heat flux at 850mb based on daily mean data. Top shows EHF at all levels regressed upon EHF 850mb PC1. Bottom shows EOF1 (left) and EOF2 (right). EOF1 explains 32.68% of the variance and EOF 2 explains 21.15% of the variance.

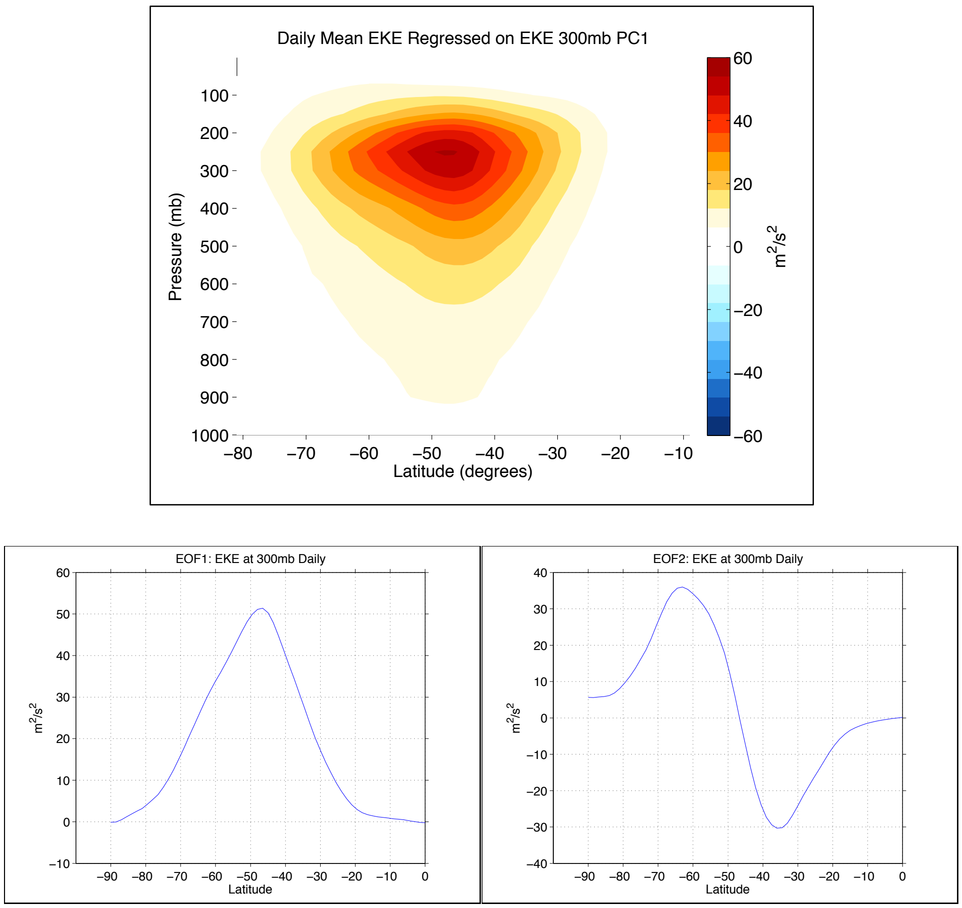

Figure 4.5 Leading EOFs of the zonal mean eddy kinetic energy at 300mb based on daily mean data. Top shows EKE at all levels regressed upon EKE 300mb PC1. Bottom shows EOF1 (left) and EOF2 (right). EOF1 explains 34.42% of the variance and EOF 2 explains 18.63% of the variance.

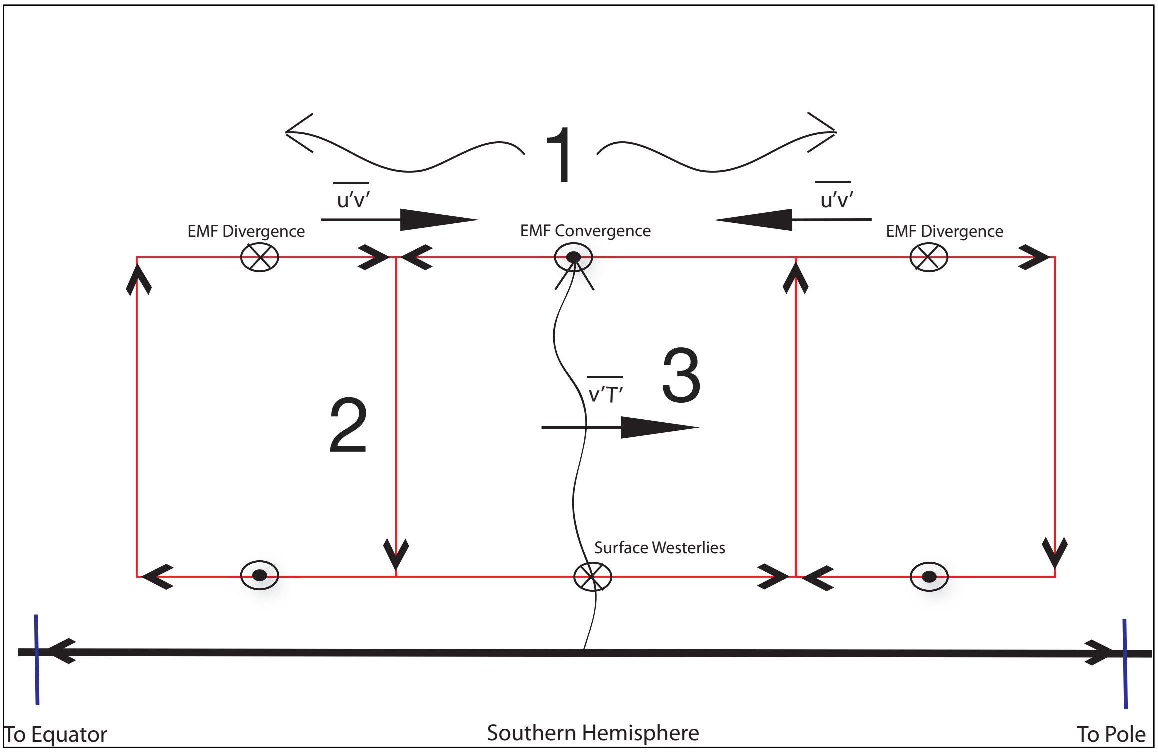

Figure 4.6 Schematic of the Robinson (2000) mechanism. Schematic shows the circulation response to that of the eddy momentum flux (EMF) and to that of the eddy heat flux.

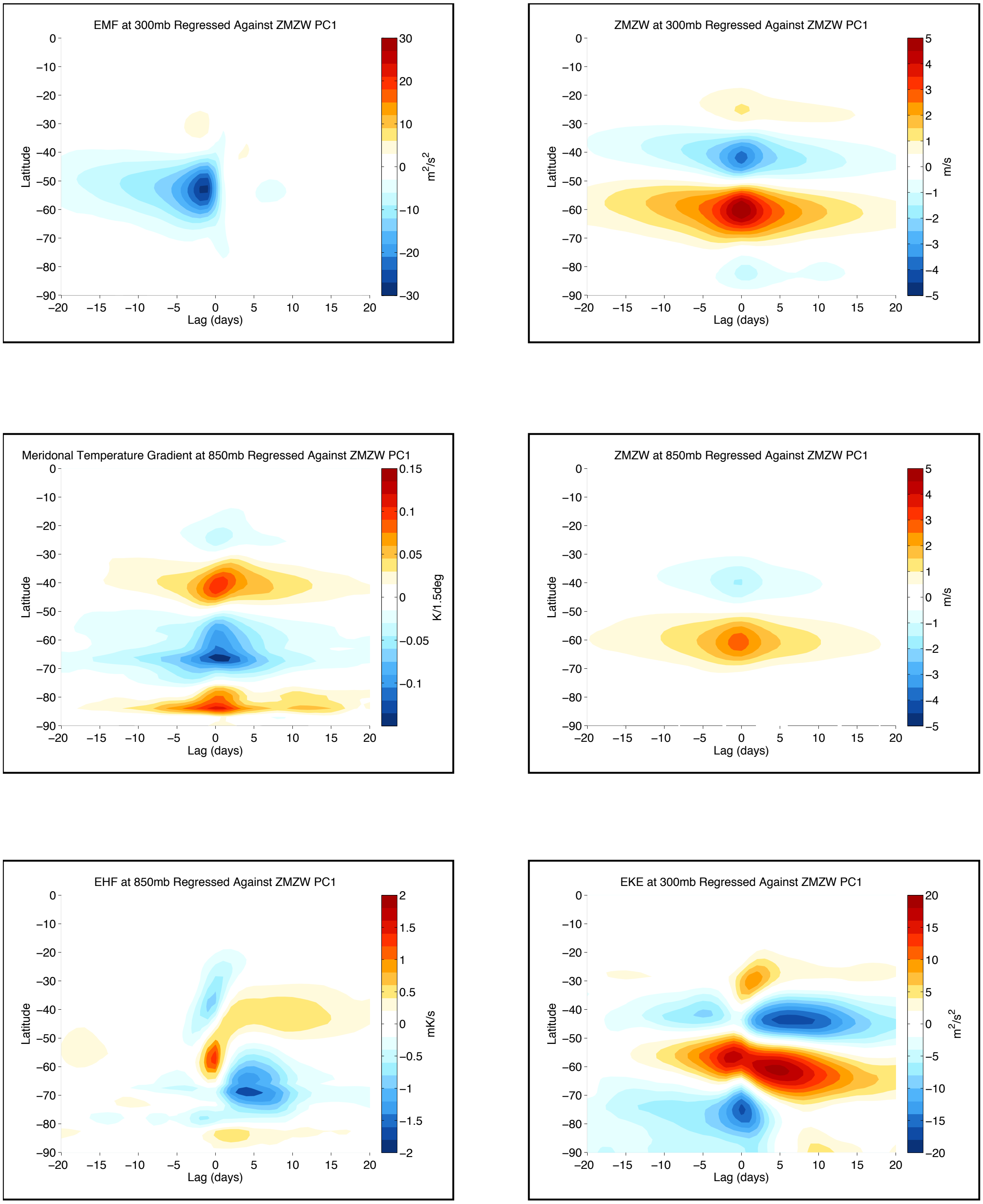

Figure 4.7 Dynamical fields regressed upon the SAM. Column 1: (Top- eddy momentum flux; Middle- meridional temperature gradient; Bottom- eddy heat flux). Column 2: (Top- zmzw at 300mb; Middle- zmzw at 850mb; Bottom- eddy kinetic energy)

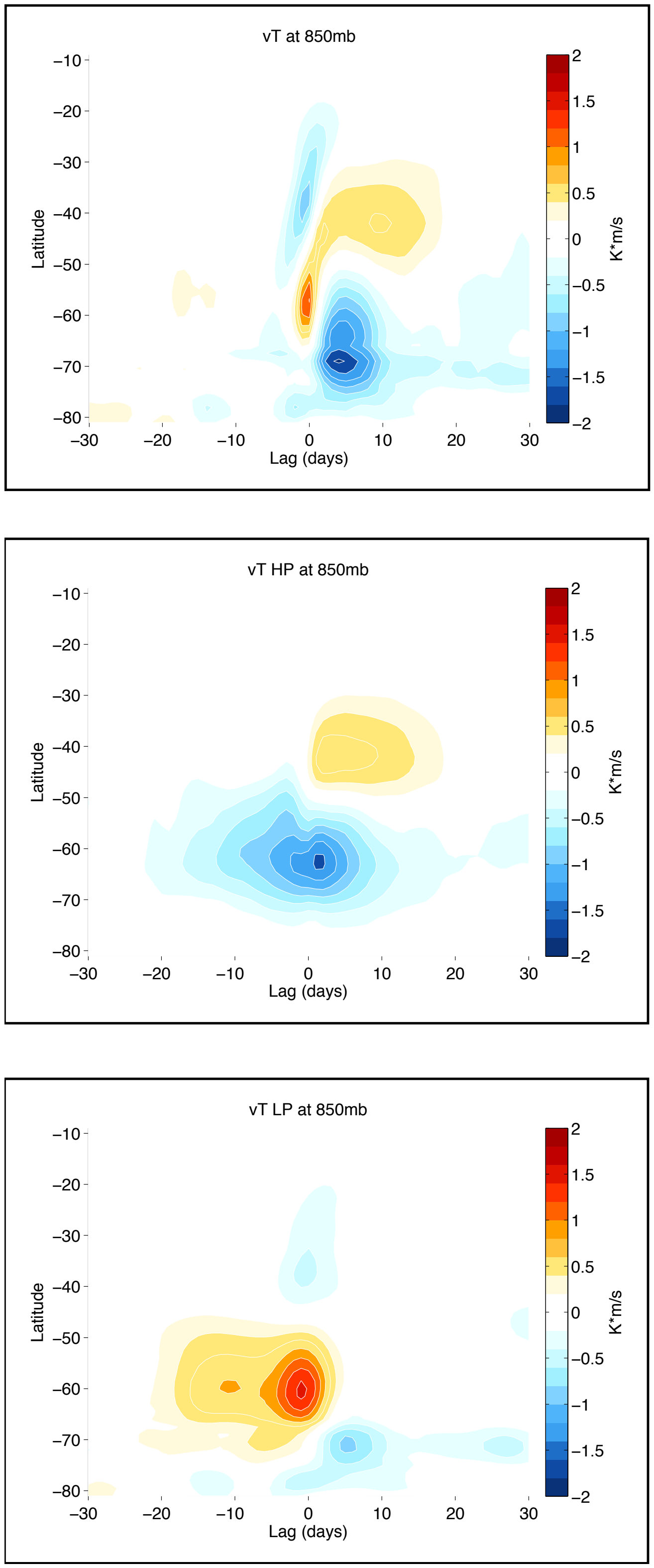

Figure 4.8 Eddy heat flux regressed upon the SAM. Top panel is full field, middle panel is for wave fluxes with frequencies less than 10 days; the bottom is for greater than 10 days.

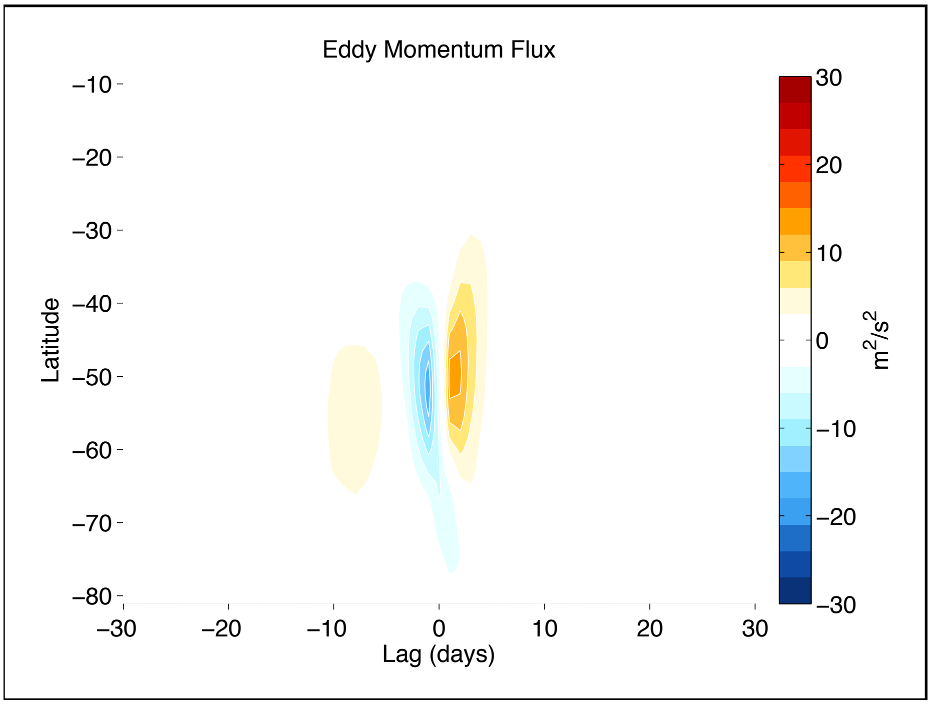

Figure 4.9 Eddy Momentum Flux regressed upon the eddy heat flux averaged between latitudes 50°-75°S.

CHAPTER 5 – EXPLORING THE LEADING EOFS OF THE FLUXES OF EDDY HEAT AND MOMENTUM

Chapter 4 examined how the proposed baroclinic feedback mechanism proposed by Robinson (2000) manifested itself in the observational data. This chapter will extend on those findings and will further examine the eddy fluxes of heat and momentum. The examination of these forcings will be looked at through the context of the atmospheric energy cycle. Exploring the fluxes of eddy heat and momentum in this context will shed new insight on the understanding of the variability associated with the zonal mean zonal flow in the Southern Hemisphere.

As discussed in Chapter 1, both of these forcings provide an equally important role in driving the general circulation. However, when looking at the energetics associated with the atmosphere, these two forcing terms draw upon distinct energy reservoirs. It follows that further insight to the dynamics of the general circulation may be uncovered by examining the leading patterns of variability of these reservoirs and how they impact the circulation.

5.1 – Analysis and Diagnosis

To look at these distinct structures associated with the energy cycle, various dynamical fields were manipulated. Similar to Chapter 4, these fields were then regressed upon the leading indices of the forcings that represent these structures. Regressions, correlations, as well as lead-lag regressions for both zonal mean and zonally varying fields are included in the below mentioned results in a manner described in Chapter 2. The data used for the following analysis is also that as described in Chapter 2. From these methods, the following results are presented.

5.2 – Results

In this section, the leading patterns of variability associated with the eddy fluxes of heat and momentum are investigated as per the methods mentioned above. These two fluxes are the dominant conversion terms between energy reservoirs and represent distinct structures when looking at the zonal mean zonal wind field and how the dynamics interact with that of the eddies. By examining the variability associated with these two forcing terms, the impacts on the general circulation via each may be examined.

To examine the variability, the leading PC of the eddy flux of momentum at 300mb as well as that of the leading PC of the eddy heat flux at 850mb are used as indices. These indices are then used to examine other dynamical fields to their relation to the energy cycle. As mentioned in Chapter 2, the time series used to construct these indexes are based off of the daily averaged data from sub-daily increments. For the flux of eddy momentum, the leading index encompasses the latitude bands from 20°S to 90°S. As mentioned previously, this latitude range was chosen to emphasize the variability that is centered outside of the tropics. For the leading index of the flux of eddy heat, the latitude range used was from 20°S to 70°S. The reason for this is a result of not having land interference at the 850mb level with this poleward flux of heat. By using this latitude range, this surface interference is avoided. For all regressions, the full latitude band for the Southern Hemisphere is regressed on these indices. What will be seen is that the latter time series corresponds to that associated with the SAM while the former time series corresponds to that of the energy reservoir associated with the eddy kinetic energy. First however, will be an examination as to how these forcings impact the general circulation. This is done by utilizing the concept of the mass stream function and will be discussed next.

5.2.1 – Mass Stream Function

In Figures 5.1 and 5.2, various anomalous fields in the daily mean are shown regressed upon the leading index of the eddy flux of heat in the first column, and the eddy flux of momentum in the second column. These regressions will show how much of the selected field's anomalies are represented by that of these respective indices. For each column, the associated stream function has also been regressed upon these indices. This is shown by the dashed and solid contours on the plots. A discussion of this stream function and the dynamical fields follow.

The first part of the discussion will be that in regards to how the stream function responds to these leading PC indices. The stream function shown in these figures is that of the meridional overturning mass transport. These are useful in that this stream function can describe how the circulation of the atmosphere behaves in the zonally averaged sense. While there are different expressions given as to how to calculate this stream function (Doos and Nilsson 2011; Hantel 1974; Vallis 2006; Holton 2004), only the expression used in the first two references will be used as it takes into account mass, which is conserved. This expression, as seen in equation 5.1, gives the stream function as a function of pressure and shows the circulation in the Eulerian mean framework.

$$\psi(y,p) = \frac{1}{t_1 - t_0} \cdot \int_{t_0}^{t_1} \int \int_0^p \frac{v(x,y,p',t)}{g}\, dp'\, dx\, dt \qquad 5.1$$

With this value for the mass stream function calculated, the accompanying regressions against these two leading indices of eddy flux of heat and momentum are shown. When looking at Figure 5.1 and 5.2, the solid contours are representative of positive values (clockwise), whereas the negative values (counter-clockwise) are shown by the dashed contours. The units, as shown in the figure captions, are of kg/s. Examining the resultant patterns isolate how the circulation responds to these forcings.

Figures 5.1 and 5.2 illustrate the anomalous stream function regressed upon the leading indices of the fluxes of eddy heat and momentum. It is seen that there is a tri-pole associated with that of the eddy flux of heat and a dipole pattern with the eddy flux of momentum. Additionally, the mass stream function when regressed upon the standardized leading PC of the eddy flux of heat is approximately four times lesser in magnitude (2e8 vs. 8e8 kg/s) than when regressed upon the standardized leading PC of the eddy flux of momentum. For the positive branch associated with the stream function, the greatest values both tend to be located near the 500mb pressure level. However, when regressed against the eddy flux of momentum, this region of maximum magnitude in the stream function is shifted slightly poleward when compared to that when regressed upon that of the eddy heat flux. The same observation for the zero mass stream function value is also present. Looking at the equatorward cell, it is seen that the maximum magnitude of the circulation is shifted a few hundred millibars up when regressed upon the eddy heat flux when compared to that of the eddy momentum flux (400mb vs. 600mb). With these observations stated, the differences in the behavior of these forcings may be touched upon.

Comparing the latitudes in which these anomalous mass circulations develop can lead to some insight in the behavior induced by these two separate forcings. When looking at how the circulation responds to the various forcings, it is seen that they act largely with each other across the latitudes associated with the Southern Hemisphere. However, some latitudes see somewhat competing effects when regressed on these leading indices of the forcings. In the lower troposphere, the ascending branch in response to the eddy heat flux is approximately between 45°S-65°S, while the descending is largely between 25°S-45°S. When looking at the same mass flow stream function when regressed upon the eddy momentum flux, it is seen that this ascending region is associated with the latitudes of 55°S-85°S whereas the descending branch is between latitudes 25°S-55°S. As it can be seen, at some latitudes (55°S-65°S), the ascending branches are collocated but at other latitudes (45°S-55°S), the stream functions have opposite signs to each other. Further insights as why this may be the case will be explored via the investigation of other dynamical fields, as will be discussed next.

5.2.2 – Various Gradient Fields Regressed on the Leading Indices of the Forcing Terms

The previous section looked at the anomalous mass circulation stream function regressed upon the eddy fluxes of heat and momentum. This section will attempt to further diagnose why the stream function behaves as it does by looking at other dynamical fields. The fields that will be looked at in this section are those incorporate a gradient, being Du/Dt, DT/Dt, and DT/Dy, or the time rate of change of the zonal wind, the time rate of change of the zonal temperature, and the meridional gradient of temperature respectively. These fields have been regressed on both forcings and are shown in the shaded contours in Figure 5.1 alongside the accompanying anomalous mass stream functions. The first field that will be discussed is that of the time rate of change of the zonal mean zonal wind.

5.2.2.1 – Time Rate of Change of Zonal Mean Zonal Wind

Recalling from Chapter 1, the time rate of change of the zonal mean zonal wind is one of the dynamical terms present in the horizontal momentum equations that govern the zonal flow. From Figure 4.6 of Chapter 4 and the resulting discussion, a thermally indirect cell (rising air poleward and sinking air equatorward) is introduced in response to the poleward flux of heat. It is seen that equatorward of the ascending branch, there are corresponding surface westerlies. Additionally, when observing Figure 5.1.a, it is seen that this response is seen in the observations between latitudes 45°S-65°S. A similar reasoning is responsible for the easterly zonal mean zonal winds that are observed in the upper troposphere. Likewise, this forcing of eddy heat flux causes easterly components of the winds at the surface poleward of the ascending branch of the indirect cell as well as equatorward of the descending branch. This response in the zonal wind is what is expected via the mechanism proposed in previous chapters. With this behavior of the time rate of zonal mean zonal winds discussed in response to the flux of eddy heat, it is of interest to examine how it responds to that of the flux of eddy momentum.

Similar to that of the time rate of change of the zonal wind response via the eddy flux of heat, the response associated with the eddy flux of momentum is approximately the same. The thermally indirect zonal circulation sees a westerly anomalous component of the zonal wind present equatorward of the ascending branch as well as a easterly anomalous component equatorward of the descending branch. However, compared to that associated with the eddy flux of heat, the zonal wind response is equivalently barotropic in the sense it is uniform with respect to pressure level. This response is very similar to that of the Figure 4.7 (b) as well as the leading EOF of the daily mean zonal wind shown in Figure 4.1 in that it manifests itself as a dipole structure with enhanced westerlies around 60°S and easterlies at 40°S. This further illustrates how the conversion term, being the flux of eddy momentum is largely responsible for the variance seen in the zonal wind, aka the SAM. When comparing this response to that seen against the eddy flux of heat, it is seen that the accompanying structure is different, especially in regards to varying pressure level.

5.2.2.2 – Time Rate of Change of Temperature

The next field that will be looked at is that of the time rate of change with respect to temperature. As with the convention used for the field discussed above, the response due to the eddy flux of heat will be discussed first and then followed by that of the response associated with the flux of eddy momentum. These responses may be seen via Figure 5.1 (c) and (d) respectively.

What is seen is that when regressed upon the leading index of the eddy heat flux in Figure 5.1 (c), there is a substantial region of warming throughout the entire troposphere. This warming is coincident with the ascending branch as it represents a poleward flux of heat. As expected, there is a slight cooling at equatorward latitudes corresponding to the descending branch of the circulation caused by the eddy flux of heat. This cooling represents the removal of heat from the tropics poleward. Next, the response of the time rate of change of temperature as a result of the flux of eddy momentum will be discussed.

When compared to that regressed upon the eddy flux of momentum, it is seen that the response at poleward latitudes is that of a cooling effect and not warming as was seen with the flux of eddy heat. This contrast leads one to believe that the heating associated with the eddy flux of heat is down gradient while that associated with the flux of eddy momentum is counter-gradient. Being down-gradient, this response to the eddy heat flux is such that it is effectively acting to wipe out the equator to pole temperature gradient whereas the response associated with the eddy momentum flux is in such a way that the baroclinicity is increased due to increasing the initial temperature gradient. This would seem to indicate support of a feedback in which the circulation, largely that in response to the flux of eddy momentum is acting to maintain itself.

5.2.2.3 – Meridional Gradient of Temperature

Similar to the plots shown in Figure 5.1 (c) and (d), those shown in (e) and (f) are those of the meridional temperature gradient regressed upon the leading indices of heat and momentum. What is seen in (e) is that with the ascending branch associated with the response to the eddy heat flux, there are positive values of DT/Dy along the surface as a result of the poleward heat flux. This goes in line with the air rising as a result of the convergence of the eddy heat flux. This is evidenced by the large positive values centered upon the rising branch of the anomalous mass circulation. This region of warming is accompanied by a region of cooling as the air descends on the equatorward side of the cell. How does this compare to the response from the eddy flux of momentum?

In contrast to this, the response to the eddy flux of momentum is such that there is a region of heating (~45°S) that is associated with the descending branch of the circulation due to adiabatic processes. Similarly, there is adiabatic cooling on associated with the ascending branch of this cell. This contrast shows that the responses due to that of the eddy flux of heat and momentum oppose each other. In one sense the response from the eddy heat flux acts to smooth the temperature gradient, while the response due to the momentum flux acts to strengthen it even more so.

In the next section, seeing how these conversion terms regress upon each other as well as the energy reservoir of eddy kinetic energy in which there is a direct linkage (as seen in Figure 5.2) between these forcings will be examined.

5.2.3 – Eddy Flux of Heat/Momentum and Eddy Kinetic Energy Terms

Figure 5.2 shows the eddy fluxes of heat and momentum as well as that of the eddy kinetic energy regressed upon the leading indices of the eddy fluxes of heat and momentum. The regressions are akin to those seen in Figure 5.1. In examining panel (a), it is seen that the eddy momentum flux response to the eddy heat flux has a varied structure. Positive values (where positive is that of a northward flux) are observed to largely occur on the poleward branch of the thermally indirect cell at around 300mb. This location of positive eddy flux of momentum is consistent with that seen with the schematic of the Robinson (2000) mechanism in Figure 4.7 of Chapter 4. When observing that schematic, recall that there is an equatorward flux of eddy momentum located south of the poleward flux of heat as well as a poleward flux of eddy momentum located north of the region associated with the poleward heat flux. This behavior is what is seen in both panels (a) and (c). Panel (c) is the eddy flux of heat regressed against the leading index of the 850mb eddy flux of heat. By construction, the region where the poleward heat flux is greatest is at 850mb. The location of this region of maximum poleward heat flux is equatorward of the ascending branch of the thermally indirect cell, consistent with Figure 4.7. How these two fields respond to the flux of eddy momentum is seen in panels (b) and (d).

The responses of how the two forcings respond to that of the flux of eddy momentum is seen in panels (b) and (d) of Figure 5.2. Panel (b) is the flux of eddy momentum regressed upon itself at the 300mb level. By construction, the largest signature is at 300mb. When comparing this region of poleward momentum flux to that of the Robinson 2000 mechanism schematic (Figure 4.7), as well as to panels (a) and (c), it is seen that the expected behavior in terms of where these dynamical features act in relation to each other is observed. However, in panel (d), which is the eddy heat flux regressed on the eddy flux of momentum at 300mb index, there is a strong signature of a poleward flux of heat in the upper troposphere as well as a slight equatorward flux of heat extending throughout the mid to lower troposphere at the latitude associated with the largest heat flux, as seen by panel (c). However, just equatorward of this region of northward heat flux, a region of slight poleward heat flux is experienced. Instead of focusing on the conversion terms, it is of note to see how the energy reservoir of eddy kinetic energy responds.

The next field that will be looked at is that of the eddy kinetic energy. As mention in previous sections, the eddy kinetic energy is a reservoir that is in part supplied from the conversion of zonal-mean available potential energy via the poleward transport of heat. The premise of this analysis is that the energy reservoir of eddy kinetic energy should have a similar structure to that of what is seen with the eddy flux of heat. As seen in panel (e), the signature of the eddy kinetic energy is a monopole isolated to a region in the upper troposphere. This signature is very similar to that which is associated to that of the first EOF of the EKE as was seen in Figure 4.5. When observing how this eddy kinetic energy is influenced by that of the leading pc of the flux of eddy momentum at 300mb as seen in Figure 5.2 panel (e), the associated structure is much weaker in magnitude and is presented as a weak dipole. This suggests that associated structures associated with the fluxes of eddy heat and momentum are different in how they interact with the energy cycle.

These results give insight in a variety of measures. In the first instance, how the forcings of heat and momentum interact with each other from both a dynamical response as well as the associated response in relation to the zonal mean circulation lends support to the mechanism as proposed by Robinson (2000). Another measure is that when looking at these dynamical fields, there are distinctly different structures that are associated with the eddy fluxes of heat and momentum, depending on which forcing the field is regressed upon. As has been mentioned, the SAM may be explained by that of the leading mode of variability associated with the flux of eddy momentum. However, the results in this section shows that this flux of eddy momentum does not explain the same structures as seen in other dynamical fields, as evidenced in the difference of the regression plots as seen in Figure 5.2. Additionally, it can be seen that when observing the leading EOF of the eddy heat flux as seen by Figure 4.4, the same pattern is present when the eddy kinetic energy is regressed upon this leading PC of the eddy heat flux, lending evidence that the structure of these two fields is the same. This is not the case when the eddy kinetic energy is regressed upon the eddy momentum flux, which is what is responsible for the structure associated with the SAM.

The next section will further look at the responses of various dynamical fields in response to these forcings but with a lag component as well.

5.2.4 – Lag-Regressions In Response to the Fluxes of Eddy Heat and Momentum

In this section, the analysis performed is similar to that conducted in Chapter 4. By performing lag-regressions, a comparison of how various dynamical fields relate to these two forcings as a function of time may be examined.

Brief descriptions of the figures that examine the lag regressions are as follows. Figure 5.3 shows plots of lag regressions of the flux of eddy momentum at 300mb, flux of eddy heat at 850mb, and the zonal mean zonal wind at 300mb regressed upon the leading PCs of the flux of eddy heat at 850mb (left) and the flux of eddy momentum at 300mb (right). Figure 5.4 shows the zonal mean temperature at 850mb, the eddy kinetic energy at 300mb, and the meridional temperature gradient at 850mb regressed on these two indices. Lastly, Figure 5.5 shows how the convergence of eddy momentum flux responds to these indices. A discussion of the findings via these figures is the topic for the following discussion.

5.2.4.1 – Response to Eddy Flux of Heat

The response due to the eddy flux of heat, as shown in the left column of Figure 5.3 will be discussed first. In examining the response of the various fields to that of the eddy heat flux, what is seen is a sequence of events that one would expect as outlined by the processes mentioned in Chapter 4. Panel (c), by construction, is the leading EOF of the eddy heat flux. With this poleward flux of heat, there is a subsequent shift in the anomalous winds in which there is an easterly component centered upon 55°S and a slight westerly component poleward of 70°S as seen in panel (e). Shortly following this change in the wind, it is seen that there is a poleward flux of eddy momentum a few days later, as seen in panel (c). This sequence is consistent with the findings in Chapter 4, when these fields were regressed upon the SAM. However, observing that the zonal wind does not possess much of a signal when regressed upon the heat flux is in line with previous conclusions that the structures associated with the eddy heat flux and the eddy momentum flux are different. As will be seen when discussing the response to the flux of eddy momentum, this difference in response in the winds will substantiate this difference. However, the response of other fields in response to the flux of eddy heat is discussed next.

Figure 5.4 shows the response of temperature, EKE, and the meridional temperature gradient to the flux of eddy heat. With this eddy heat flux, it follows that the temperature field will respond. When looking at panel (a) of Figure 5.4, it is seen that in the regions where the poleward flux of heat is occurring (panel (c) of Figure 5.3), there is an increase in surface temperature at poleward latitudes at positive lag as would be expected. Similarly, where this heat flux originated from, there is a decrease in temperature. The meridional gradient of this change in temperature is seen in panel (e) of Figure 5.4 and is consistent with panel (a). As stated in previous chapters, with this flux of heat, there is vertical wave activity that feeds into the eddy kinetic energy reservoir. As expected, at slight positive lag from that of the poleward heat flux, there is in increase seen in EKE at the same latitudes. As described in the Lorenz energy cycle, from this EKE reservoir, the conversion term that is associated with the eddy flux of momentum is present to convert this EKE to that of the zonal mean kinetic energy that is associated with the jet. As such, what would be expected is for the poleward flux of eddy momentum to lag slightly behind the generation of EKE. When observing panel (a) of Figure 5.3 to that of panel (c) of Figure 5.4 that is indeed what is the case when regressed upon the eddy flux of heat. Figure 5.5 panel (a) shows the corresponding meridional gradient of this eddy momentum flux and is consistent with that of the panel (a) of Figure 5.3.

5.2.4.2 – Response to Eddy Flux of Momentum

This next section will now look at these fields through the response associated with that of the eddy flux of momentum. This examination will utilize the same set of figures as the response discussed to that of the flux of eddy heat.

Similar to the response of the eddy heat flux, there does seem evidence that there is a poleward flux of heat that shortly precedes that of the eddy momentum flux when looking at panels (b) and (d) of Figure 5.3. The associated convergence of eddy momentum flux may be seen in panel (b) of Figure 5.5. This flux of eddy momentum then drives large changes in the zonal mean zonal wind as seen by panel (f). This response of the zonal wind is much greater to that seen with that due to the eddy heat flux, suggesting that the accompanying structures are different. With this change in the zonal winds, a thermally indirect cell develops via the mechanisms explained in prior sections. This thermally indirect cell is then accompanied by a surface flux of heat, as seen by the region in panel (d) at lags 5-10. However, unlike the response to the eddy flux of heat, the temperature responds such that there is significant cooling, especially at higher latitudes, as seen by panel (b) of Figure 5.4. This is due to the fact that the circulation response to that of the eddy momentum flux is such that even without a poleward flux of heat, a thermally indirect cell is generated. Thus, the ascending branch associated with this cell experiences cooling via adiabatic process and adiabatic warming due to compression on the descending branch. This cooling and warming is seen in panel (b) of Figure 5.4 and is consistent with the circulation response to that of the flux of eddy momentum. The corresponding meridional temperature gradient is seen in panel (f) of Figure 5.4. Another observation is that the EKE response to this flux of eddy momentum is quite different than that seen with the eddy heat flux. This difference in response illustrates how the leading PCs associated with these two forcings are quite different.

These structures associated with the two forcings are quite different as evidenced by the responses seen by the zonal mean zonal wind and that of the EKE to these forcings. When observing how the EKE responds to the flux of eddy momentum as seen in panel (d) of Figure 5.4 it is seen that there is relatively weak dipole like signal compared to the strong pulse as seen in response to the eddy heat flux (panel c of Figure 5.4). Meanwhile, as mentioned earlier, the zonal mean zonal wind strongly responds to the leading PC associated with the flux of eddy momentum (panel f of Figure 5.3) but does not project nearly as well with the eddy flux of heat (panel e of Figure 5.3).

In summary, this section explored how various fields behaved when regressed upon the leading indices of the eddy fluxes of heat and momentum. What was found is that the associated responses, as was discussed in Chapter 4, is supported in terms of the mechanism provided. However, the accompanying structures associated with the eddy kinetic energy and the eddy flux of heat, has been shown to vary compared to that of the zonal mean zonal wind and the flux of eddy momentum. It is proposed that further analysis should be conducted to explore why this may be the case as both of these forcings have implications in how the general circulation responds. The next section will further look at these leading indexes of the eddy forcing of heat and momentum by examining the correlations between various fields and indices.

5.2.5 – An Examination of the Correlations Between the Leading Indexes of Various Fields.

Table 5.1 looks at the correlations between the leading two PCs of the zonal wind at 300mb, eddy momentum flux at 300mb, the eddy heat flux at 850mb, and the eddy kinetic energy at 300mb in both daily (top) and monthly (bottom) means. Theoretically, the correlations between the leading two PCs of the same fields are zero as a result of their orthogonallity. Correlations give a measure of how well the two PC time series are to each other. The higher the correlation, the greater the relationship is between the two fields and vice versa. A discussion of the findings of Table 5.1 is provided below.

At first glance, the correlations in Table 5.1 between these indexes are not that high. What is seen is that the conversion terms (that associated with the eddy fluxes of heat and momentum) are correlated relatively high (in comparison) to their respective energy reservoirs as illustrated by Figure 1.5. As mentioned in previous sections, the differences between the structures associated with these forcings are evident in the correlations. While not shown in Table 5.1, the daily correlation between the leadings PCs of the zonal kinetic energy and that of the zonal mean zonal wind is |0.975|. This high correlation is expected as the zonal mean zonal wind derives its energy from this zonal kinetic energy reservoir. Meanwhile, the correlation between the leading PC of the eddy flux of momentum and that of the zonal wind is ~|0.27| for daily and ~|0.56| for the monthly mean. Similarly, relative high levels of correlation are found between the leading PC of the EKE and the eddy heat flux, being ~|0.47| for daily, and ~|0.34| for monthly. It is interesting to note that both of the leading PCs associated with the eddy heat flux are relatively highly correlated with the leading PC of the EKE. When comparing the correlations of the EKE, ZMZW, eddy flux of heat, and eddy flux of momentum, it is seen that the correlations between the eddy flux of heat and EKE are approximately twice that of the correlations between the EKE and flux of eddy momentum. A similar statement may be made concerning the relationship between the correlations between the ZMZW and the flux of eddy momentum vs. the eddy flux of heat. These correlation values lend a numerical basis for a difference in the structures between these two fields. With this cross-correlation analysis performed, the next step is to examine how each PC time series behaves when auto-correlated.

Figure 5.6 shows how the autocorrelations of the ZMZW, eddy flux of momentum, and the eddy flux of heat as a function of lag. The autocorrelation is a correlation of a time series with itself at various lags and is, by definition, 1 at lag 0. The lag is a shift of the time series with respect to itself by the specified number of days (lag). The resultant correlation is what is plotted. The following gives a discussion on the findings as a result of performing this auto-correlation analysis.

Figure 5.6 is composed of 4 panels, with the left column being that of the autocorrelation of the daily indices of the leading two PCs and the right column being of the monthly indices of the leading two PCs. When observing the daily indices, what is seen is that both fluxes of eddy heat and momentum reach a correlation of 0 at about 4 days. Meanwhile, the zonal mean zonal wind persists to maintain a positive correlation well out to a few weeks and beyond. The reason for this is that the forcings associated with that of the eddy fluxes of heat and momentum influence the behavior of the zonal mean zonal wind and slowly decays with time. The forcings provided by these two fluxes are impulse-like in nature due to the sharp drop offs in correlation. This behavior is seen in both the first and second PCs of these fields. However, when now looking at the right column of Figure 5.6, what is seen is that these lag correlations have no memory in when the monthly average is used. The response that the zonal mean zonal wind has to the various forcings is limited to an impulse-like behavior.

The correlations between the various fields have shown that the conversion terms associated with their respective energy reservoirs tend to be relatively highly correlated but do not exhibit much correlation to each other when analyzed. Additionally, in the daily mean context, both forcings of eddy heat and momentum are impulse like in behavior but the lag-correlation with respect to that of the zonal mean zonal wind has some memory as a result to responding to these forcings. However all analysis thus far, including the formation of the PCs of these forcing terms, has relied on the zonal mean quantities for the respective fields. Looking at how these fields relate in a zonal varying manner will be touched upon briefly in the next section in the pursuit of gaining a bit more understanding.

5.2.6 – A Brief Examination of the Two Forcing Terms in the Zonally Varying Case

As with regression plots of section 5.4.4, Figure 5.7 will show the regressions of these forcing fields in relation to each other using monthly mean data. However, this figure does so in the zonally varying case at the levels in which the leading PC time series for each forcing term was calculated as opposed to the zonal mean quantities used in section 5.4.4.

Figure 5.7 is laid out in the following manner. The left column shows how the various fluxes of eddy momentum (a) and heat (c) regress upon the leading PC of eddy heat flux. Note that the panels (b) and (c) are effectively the EOFs as were seen in Chapter 4 but in the monthly index. Panel (b) effectively shows a region of strong poleward eddy momentum flux largely centered on the 50°S latitude band. A similar observation may be seen in panel (c), where there are predominant poleward heat fluxes centered just poleward of 50°S. The large positive values seen at the pole in panel (c) and (d) is largely a result of the interference of the Antarctic continent with the 850mb level and results in the strong values seen there. Panel (a) meanwhile shows a tendency for an equatorward flux of eddy momentum in response to the eddy heat flux, in opposition to that of the response via the eddy flux of momentum as seen in (b). This opposite response is also seen in the eddy heat flux field in response to these two forcings (c) and (d). This suggests that the structures associated with these two forcings are inherently different in how they explain the general circulation.

A further look into the nature associated with this eddy heat flux and its robustness will be the topic in the next section.

5.2.7 – The Robustness of the Structure Associated with the Eddy Heat Flux

As seen in previous sections, the accompanying structures that govern the various circulations are different when analyzed through that of the eddy heat flux, and that of the eddy momentum flux. As has been seen, the structures that accompany the variance associated with the zonal mean zonal wind manifests itself in the corresponding dynamical field of eddy momentum flux. However, this same structure does not accompany that associated with the eddy heat flux. Instead, it has been shown that when looked through the energy cycle that the zonal kinetic energy field, associated with the zonal mean zonal wind, is fairly well correlated to that of the eddy momentum flux but not to the eddy heat flux. However, the eddy heat flux has been shown to be more highly correlated to the eddy kinetic energy reservoir and not to the reservoir of zonal kinetic energy. Both of these reservoirs are important to understanding the nature of the general circulation. However, this analysis has only looked at one level of the eddy heat flux. This section attempts to highlight that the findings found thus far are not unique to a certain level, but is in fact robust and inherent to the nature of the eddy heat flux.

Figure 5.8 shows the eddy heat flux field at 850mb from 0°S to 70°S regressed upon the leading PCs of the eddy heat flux from 20°S to 70°S at various pressure levels. Each panel in Figure 5.8 shows various pressure levels of these resulting regressions. When observing these panels, it is seen that at the lower levels, panel (c), that the resulting regressions have essentially the exact same shape and representation of a poleward flux of heat. As the pressure level decreases, such as in panel (b), what is seen is that the shape remains the same but the magnitude as well as the latitude at which the maximum poleward flux of heat occurs is shifted equatorwards and lessens in magnitude. This change may be in part due to the differences between the signal of the eddy heat flux found at the 850mb and that of the lower levels. While these regressions are consistent amongst the levels compared to the 850mb eddy heat flux, does the pattern of variability at each level remain consistent with the other?

Instead of looking how the eddy heat flux at 850mb regresses upon various leading PCs of the eddy heat flux at various levels, it is of note to look at the EOF of each level of eddy heat flux. As with Figure 5.8, each panel in Figure 5.9 shows various pressure levels of the eddy heat flux and their respective EOF. What is seen in these panels is that in regions of similar pressure levels, such as that in panel (c), the EOFs are remarkably similar to each other in structure. In fact, the latitude in which the greatest heat flux occurs roughly stays in the same region across all pressure levels associated with the troposphere. There is some poleward migration of the maximum eddy heat flux associated with pressure levels in the stratosphere, as seen in panel (a). This similarity in variability of the eddy heat flux at various levels lends support that the findings in this chapter are robust and should support further study into this line of inquiry.

In summary, the structures associated with the eddy heat flux and that of the eddy momentum flux are quite different when various dynamical fields are regressed upon them. This has lead to wanting to explore in greater detail how the eddy heat flux, as well as the accompanying energy reservoir of eddy kinetic energy impacts the general circulation through the lens of this associated structure. The examination of the eddy heat flux has shown that is quite robust in structure at varying pressure levels, especially those within a few hundred millibars of the surface. This leads one to believe that the structure that is therefore associated with this eddy heat flux is substantial and quite evident in the observations of the general circulation.

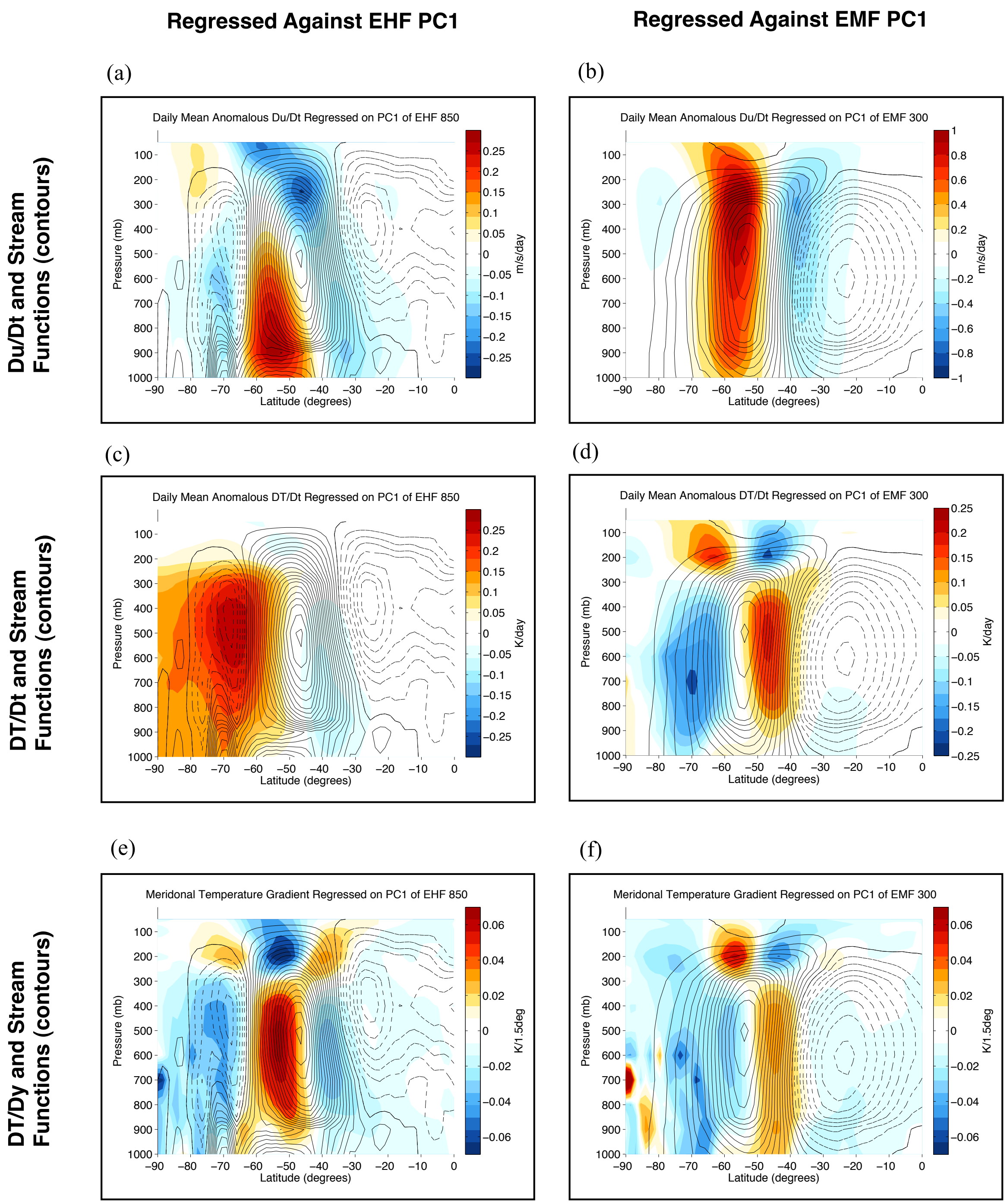

Figure 5.1 Various dynamical fields and mass flow stream functions regressed upon the leading indexes of the eddy heat flux (left column) and the eddy momentum flux (right column). Contours for the mass flow stream function are spaced by 2e8 (kg/s) when regressed upon EHF and 8e8 (kg/s) when regressed upon EMF. Solid contours denote clockwise motion and dashed denote counterclockwise motion.

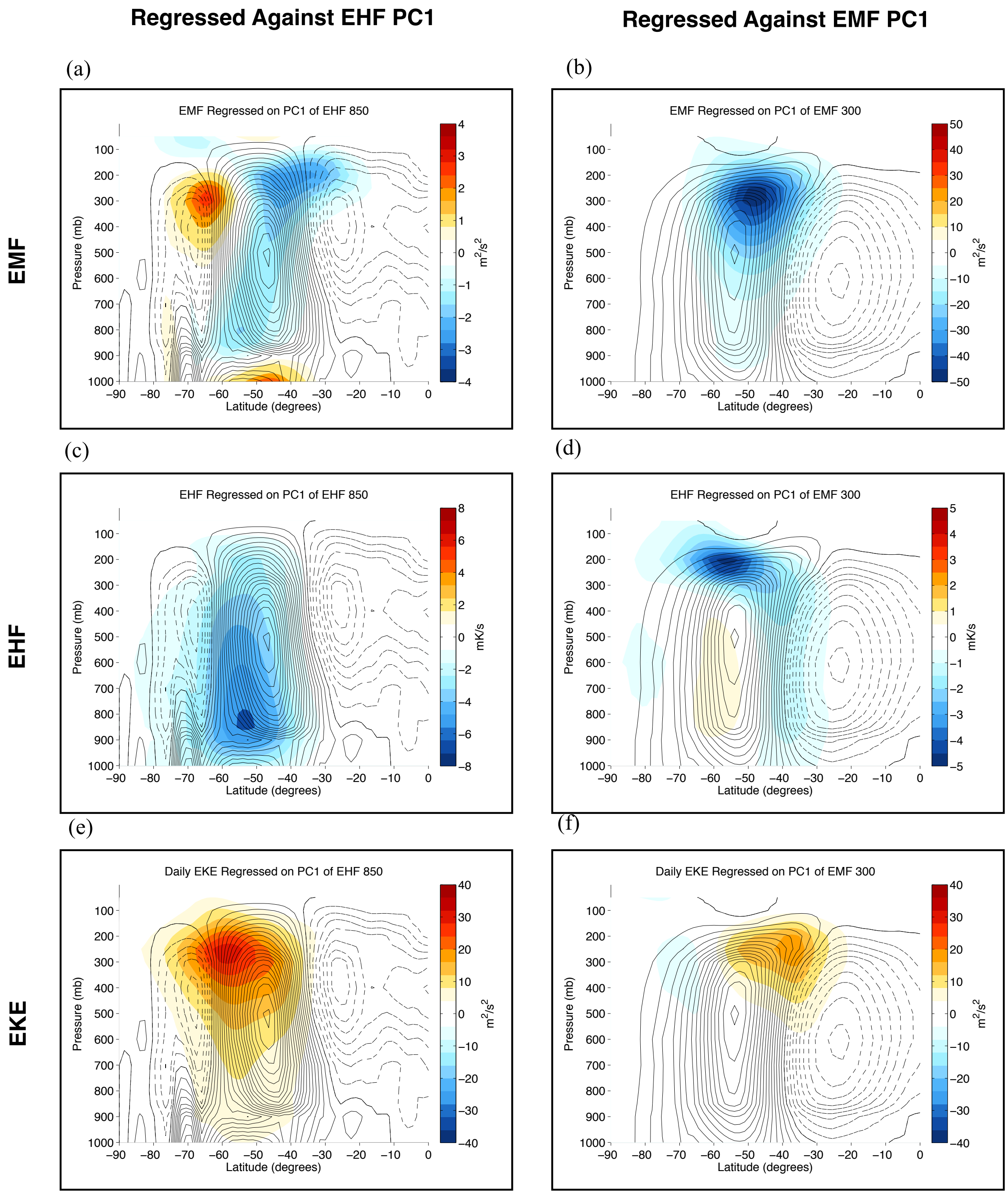

Figure 5.2 Various dynamical fields and mass flow stream functions regressed upon the leading indexes of the eddy heat flux (left column) and the eddy momentum flux (right column). Contours for the mass flow stream function are spaced by 2e8 (kg/s) when regressed upon EHF and 8e8 (kg/s) when regressed upon EMF. Solid contours denote clockwise motion and dashed denote counterclockwise motion.

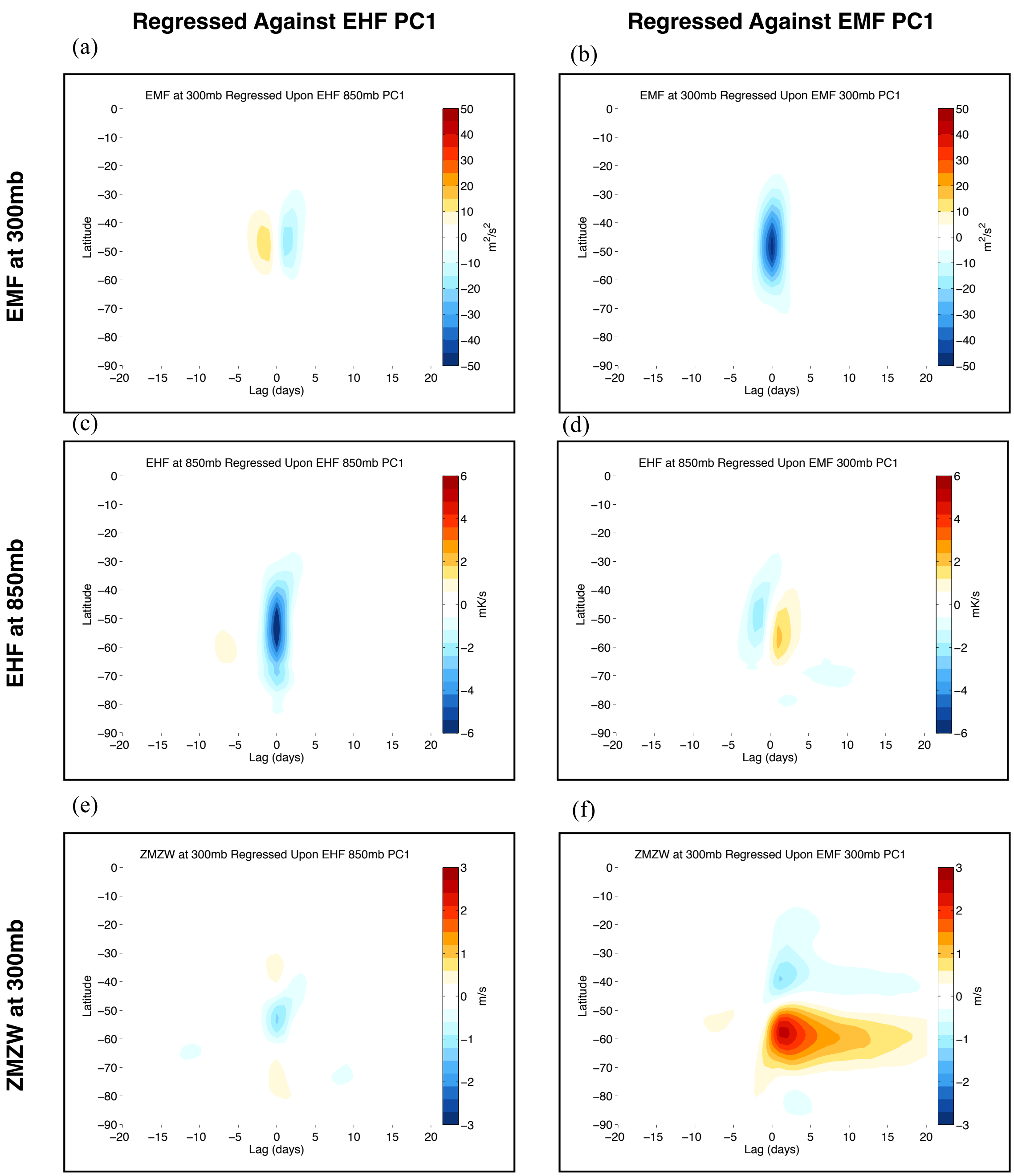

Figure 5.3 EMF, EHF, and ZMZW lag regression plots when regressed on EHF (left column) and EMF (right column).

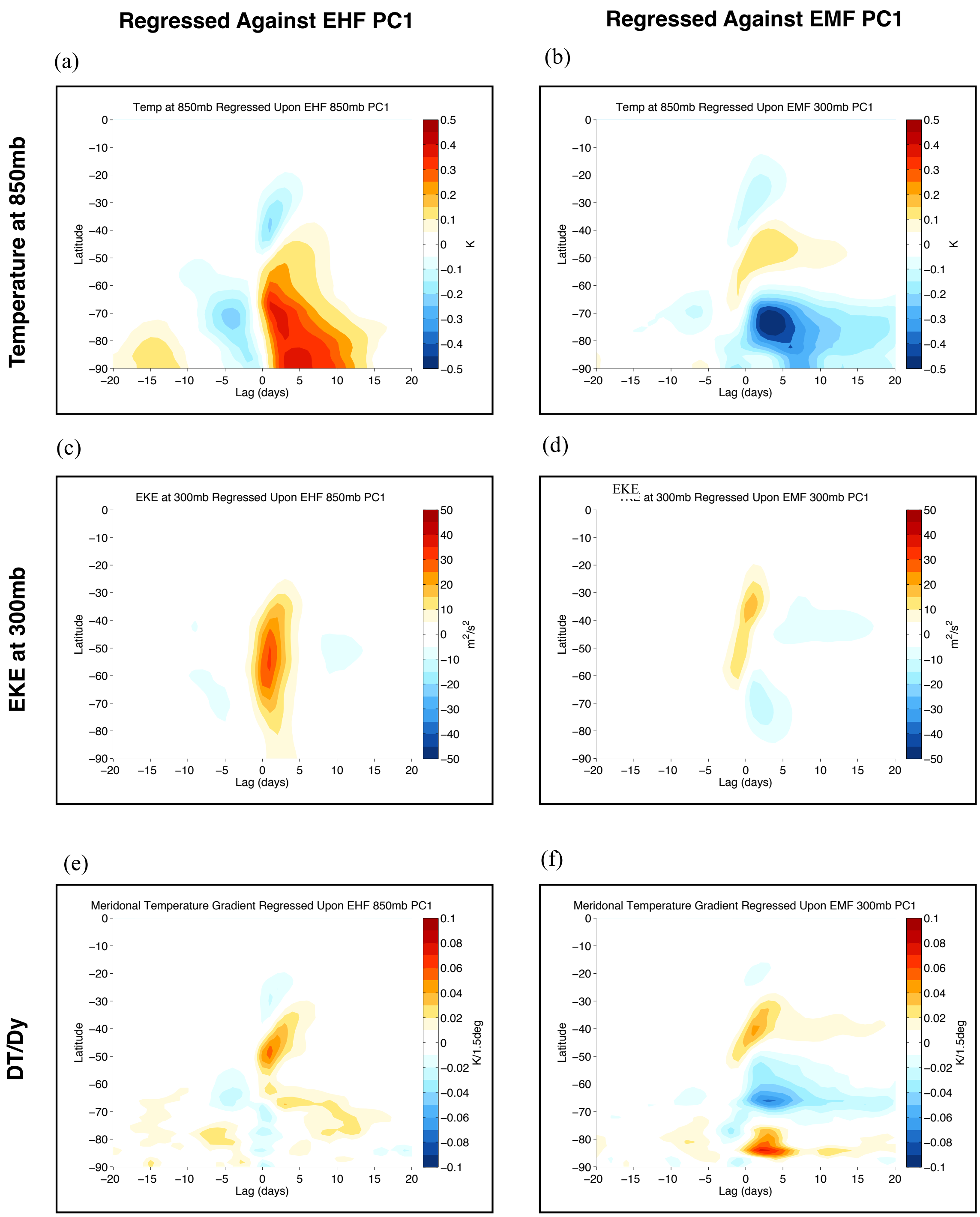

Figure 5.4 Temperature, EKE, and the meridional temperature gradient, DT/Dy lag regression plots when regressed on EHF (left column) and EMF (right column).

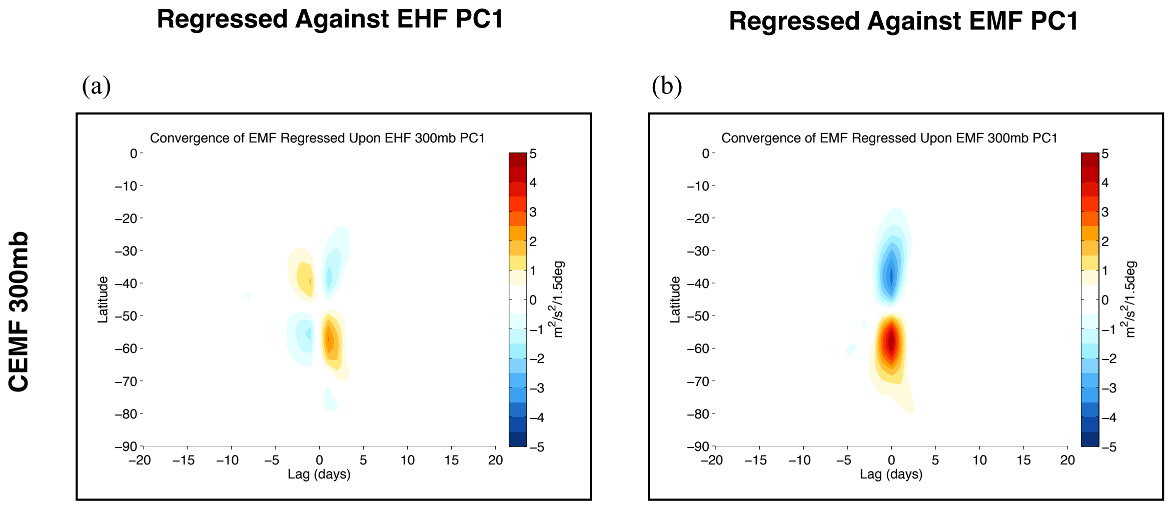

Figure 5.5 Convergence of eddy momentum flux lag regression plots when regressed on EHF (left column) and EMF (right column).

Table 5.1 Cross correlations between various dynamical fields for daily (top) and monthly (bottom) means.

Daily Cross-Correlations

	ZMZW PC1	ZMZW PC2	EMF PC1	EMF PC2	EHF PC1	EHF PC2	EKE PC1	EKE PC2
ZMZW PC1	1	0	0.2681	0.1951	-0.0822	-0.101	0.1031	0.0137
ZMZW PC2	0	1	0.1291	-0.1738	-0.2661	0.0769	-0.2098	-0.3282
EMF PC1	0.2681	0.1291	1	0	0.0276	-0.18	0.2777	-0.2365
EMF PC2	0.1951	-0.1738	0	1	-0.0532	-0.0044	-0.1296	0.2703
EHF PC1	-0.0822	-0.2661	0.0276	-0.0532	1	0	0.4683	0.2801
EHF PC2	-0.101	0.0769	-0.18	-0.0044	0	1	-0.23	0.26
EKE PC1	0.1031	-0.2098	0.2777	-0.1296	0.4683	-0.23	1	0
EKE PC2	0.0137	-0.3282	-0.2365	0.2703	0.2801	0.26	0	1

Monthly Cross-Correlations

	ZMZW PC1	ZMZW PC2	EMF PC1	EMF PC2	EHF PC1	EHF PC2	EKE PC1	EKE PC2
ZMZW PC1	1	0	0.569	0.5315	-0.2676	-0.0646	0.348	-0.6326
ZMZW PC2	0	1	-0.4388	0.3703	0.111	-0.141	-0.1416	-0.312
EMF PC1	0.569	-0.4388	1	0	-0.276	-0.121	0.1972	-0.1417
EMF PC2	0.5315	0.3703	0	1	-0.1873	-0.0867	0.0435	-0.478
EHF PC1	-0.2676	0.111	-0.276	-0.1873	1	0	-0.3404	0.0269
EHF PC2	-0.0646	-0.141	-0.121	-0.0867	0	1	0.4459	0.292
EKE PC1	0.348	-0.1416	0.1972	0.0435	-0.3404	0.4459	1	0
EKE PC2	-0.6326	-0.312	-0.1417	-0.478	0.0269	0.292	0	1

Autocorrelations

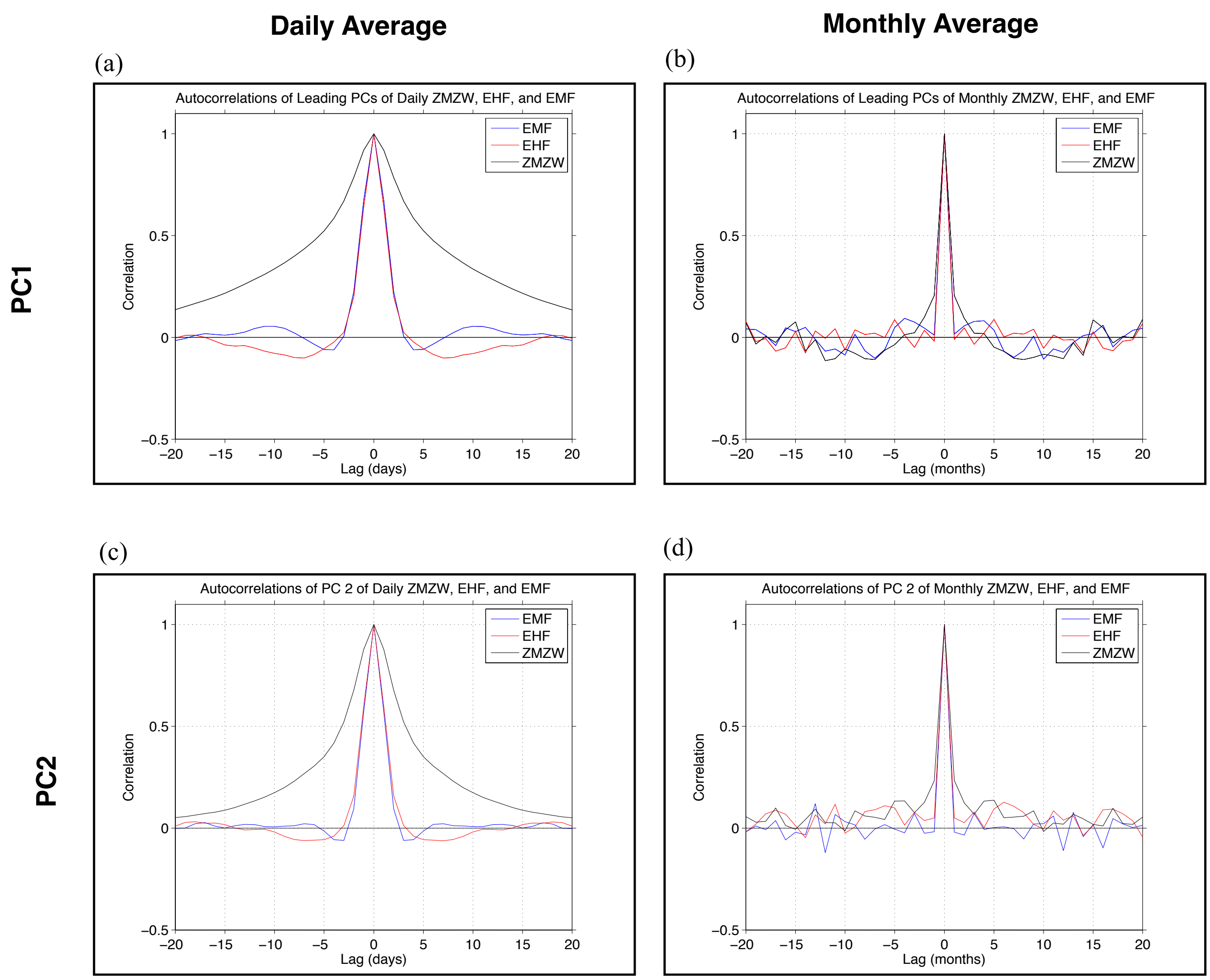

Figure 5.6 Daily and Monthly mean auto-correlations as a function of lag for the fields of EMF 300mb, EHF 850mb, and ZMZW 300mb for the two leading PCs.

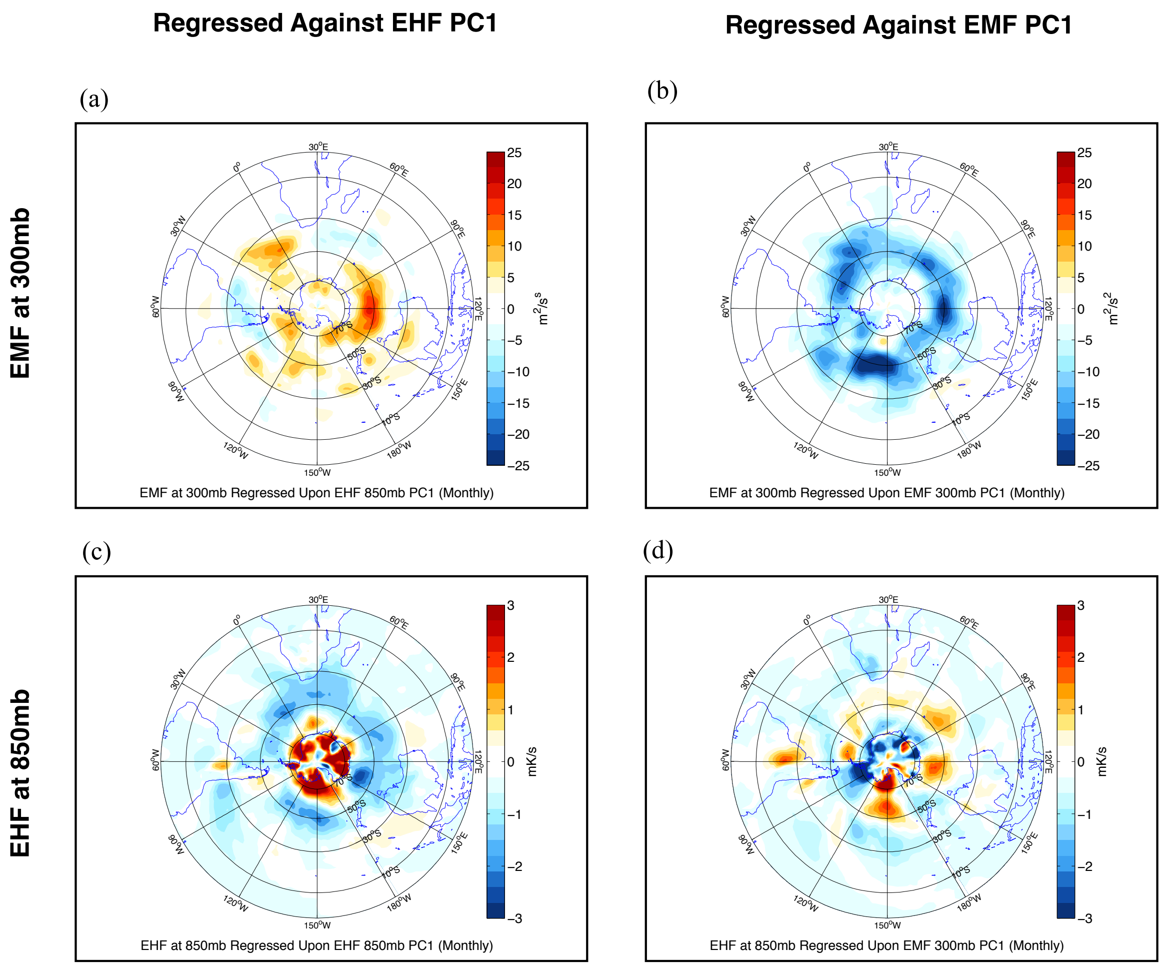

Figure 5.7 Zonally varying regression maps between the leading indexes of eddy momentum flux at 300mb and eddy heat flux at 850mb.

EHF 850mb (0-70S) Regressed on various levels of EHF (20-70S)

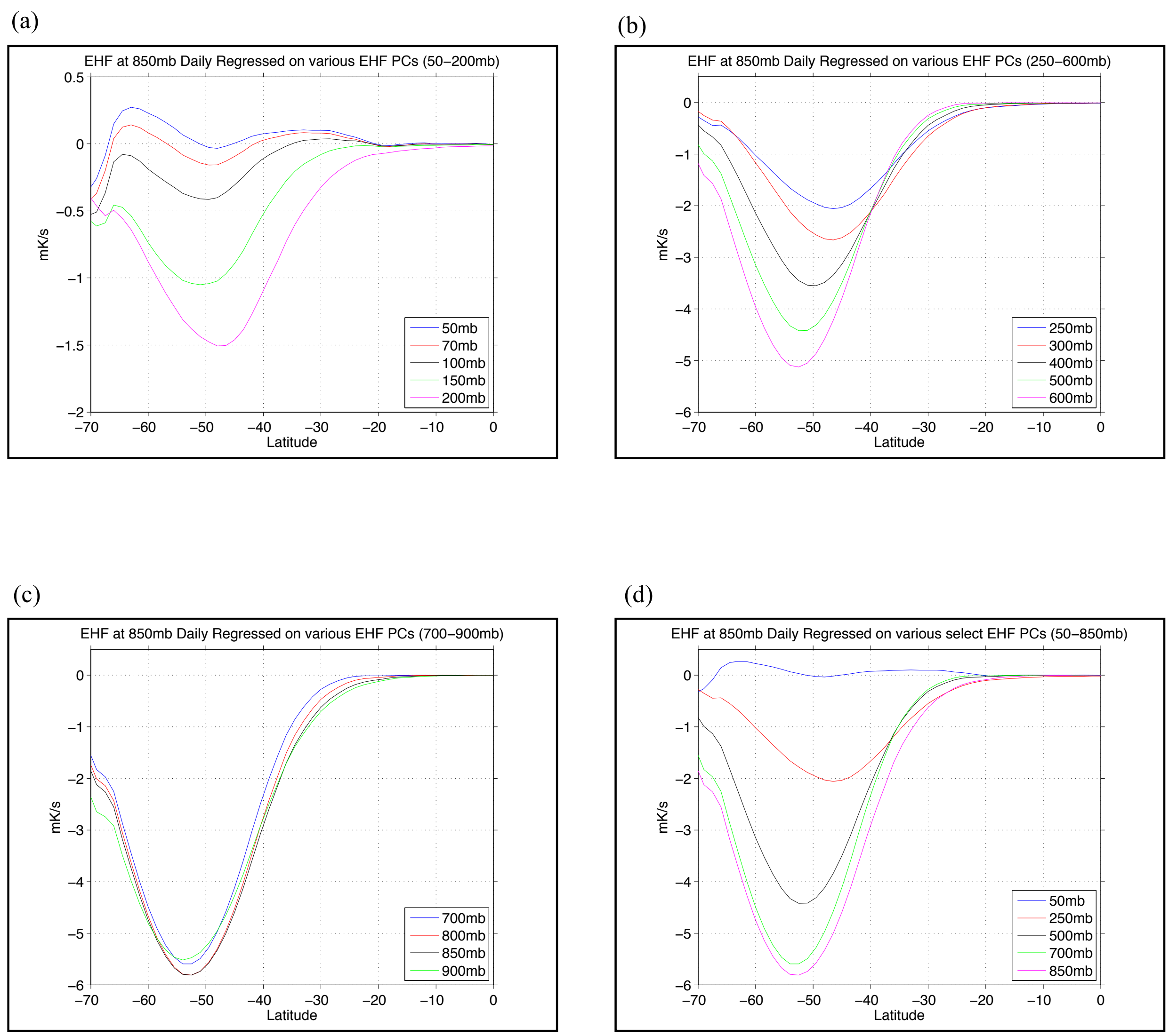

Figure 5.8 The eddy heat flux field regressed upon the leading PCs of various pressure levels of eddy heat flux. Each panel is a different range of pressures as indicated by the associated legends.

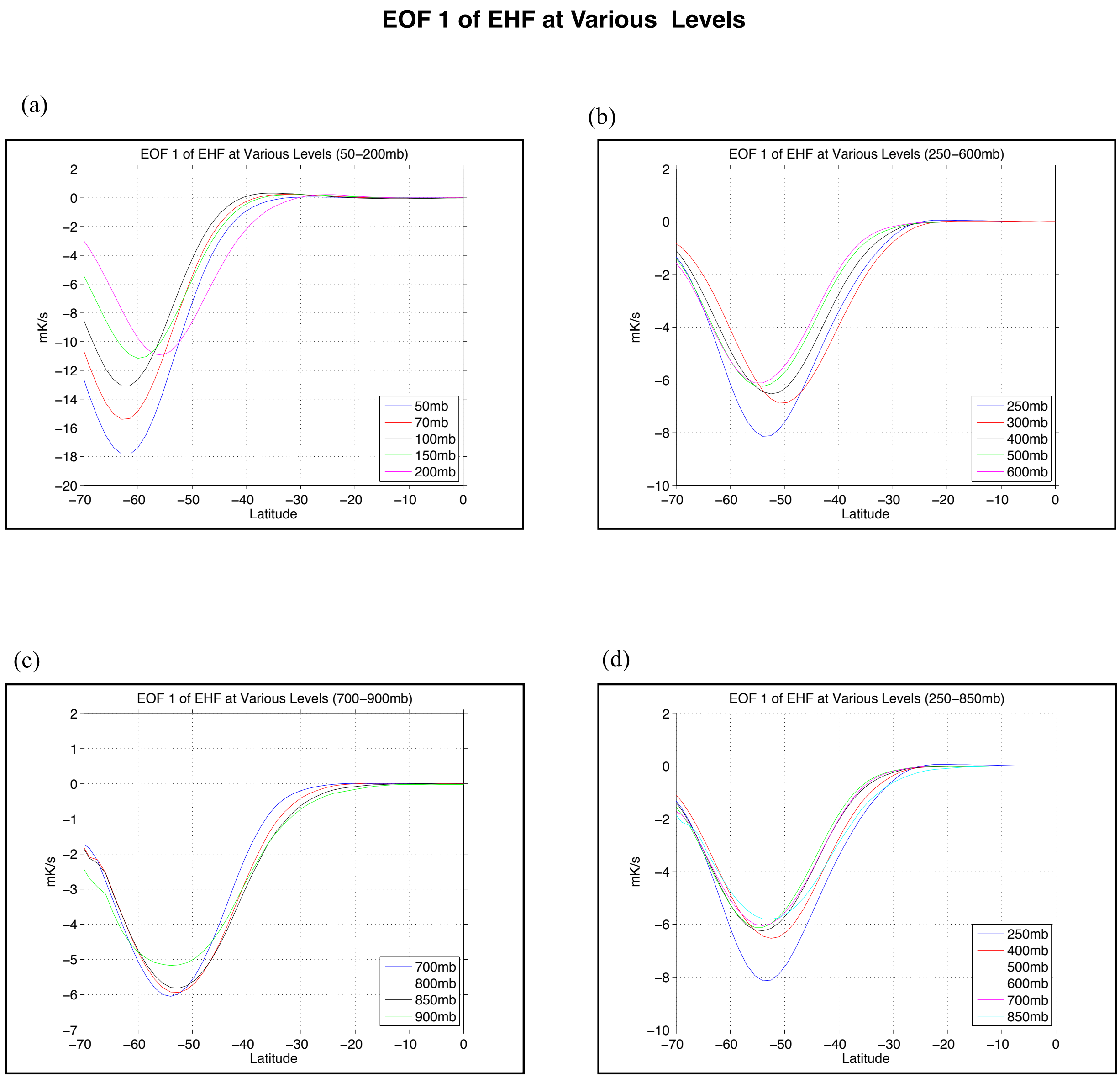

Figure 5.9 EOF 1 of the eddy heat flux at various pressure levels. Each panel is a different range of pressures as indicated by the associated legends.

CHAPTER 6 – CONCLUSIONS

In this chapter, a summary of the findings of this thesis will be presented, as will suggestions for future work.

Understanding the dynamics that are associated with the global mean circulation is crucial for predicting future climate patterns. Much of this change in climate, especially in the midlatitudes, is due to the behavior of the zonal mean zonal winds and its inherent variability. As has been mentioned in the study, this variability is known as the SAM in the Southern Hemisphere and represents the north-south fluctuation of the jet. In attempts to analyze this fluctuation, many studies have been undertaken.

As mentioned early on in this thesis, past studies have looked at a variety of ways to further understand the dynamics associated with the variability. These studies have looked at varying aspects including that of understanding how anthropogenic forcing influences the jet. Studies focusing on the rise in greenhouse gas emissions, the effects of a cooling stratosphere, ozone recovery, and other aspects have been of great interest. Other studies have focused on simple dynamical models to attempt to understand the existence of the annular modes of variability. These efforts have including changing prescribed parameters in the model and seeing how the dynamics react to these set parameters. These parameters may consist of heating profiles, initial jet location, jet speed, and other components of interest. Efforts concurrent to these is the emphasis to the initial part of this study.

6.1 - Part 1 Summary

Concurrent with these efforts, there has been studies that suggest that the jet, once in a location tends to persist. This has lead to efforts to understand how the dynamics would support this behavior via a variety of mechanisms. One such mechanism, which provides the foundation for the first component of this study, is that of a baroclinic mechanism put forth by Robinson (2000). This mechanism suggests that following the fluxes of eddy momentum aloft, there is a chain of events where the corresponding poleward flux of heat would feedback onto this initial flux of eddy momentum, thereby allowing the jet to persist in a location. The aim of the first part of this study was to utilize statistical methods to diagnose whether this proposed mechanism manifested itself in the observational data.

To do this, the study of this thesis took the standardized leading PC of the zonal mean zonal wind at 300mb in the latitude band of 20°S to 90°S formulated from daily mean values. This PC is known as the SAM. To see if the dynamical fields present in the Robinson (2000) mechanism were related to the SAM, a series of lag-lead regression plots were created. The key findings of this initial part of the study are discussed below:

1) The Robinson (2000) mechanism seems to present itself in the observational data.
    a. When the appropriate dynamical fields are regressed upon the SAM, the sequence of events beginning with the initial flux of eddy momentum, to a change in the zonal mean zonal winds aloft, to a change in the meridional

temperature gradient and surface zonal winds, to a poleward flux of heat is present, as seen in Figure 4.7.

b. The key aspect is that there is evidence that the poleward flux of heat being re-projected onto the initial flux of eddy momentum that had initially started the process.

2) There is evidence that there is a frequency component associated with this poleward flux of heat that is responsible for this positive feedback. As seen via Figure 4.8, much of the poleward flux of heat is dominated in the high frequency domain, being defined in this study as time periods consisting of less than 10 days.

These findings warranted the motivation to further diagnose the two forcings that drive the general circulation. This examination was the point of emphasis in the second part of this study.

6.2 – Part 2 Summary

As the first part of this study seems to suggest that the poleward flux of heat feeds back onto that of the initial eddy momentum flux, it was of interest to further examine these two separate forcings independently and attempt to gain any insight to how they affect the dynamics that drive the variability.

When observing the energy cycle associated with the atmosphere, there are many conversion terms and energy reservoirs that influence the general circulation. This concept was first discussed via Lorenz (1955) and a schematic of the process may be seen via Figure 1.5.

As was discussed in Chapter 4 and seen by Figure 1.5, the general circulation responds to both forcings provided by the fluxes of eddy heat and momentum. However, much of the research to date has focused on solely the role that the eddy momentum flux has on the SAM, and not on the eddy heat flux and its corresponding energy reservoir, being EKE. Thus, it was of interest to take these two forcing terms and examine their role in driving the extratropical circulation.

To perform this analysis, similar techniques that were used in Chapter 4 were implemented. Using the standardized leading PCs of the two forcing terms, lag-regression plots were created using a variety of various dynamical fields that were discussed in Chapter 5. To validate the robustness of the findings, various pressure levels were also examined for select fields. The key findings of this part of the study are provided below:

1) In examining the two forcing terms and their corresponding energy reservoirs, it was found that the structures that are associated with each are distinct from each other. This is of note as what does this other structure mean? In the case of the eddy momentum fluxes, they can be interpreted as driving the structure that is associated with the SAM. However, what does the structure that is seen with the EKE and its forcing term of the eddy heat flux represent?
2) With these structures, it is found that the zonal mean zonal wind projects strongly onto the leading PC of the eddy momentum flux but quite weakly onto the leading PC of the eddy heat flux. Similarly, the EKE projects strongly onto the leading PC of the eddy heat flux but quite weakly onto the leading PC of the eddy flux of momentum. This is seen via Figure 5.3 and 5.4.

3) The structures associated with the leading PC of the eddy flux of heat seem to be robust in structure lending support that it is not isolated to a certain pressure level.

These findings seem to be novel. However, to further understand the dynamics and what these structures mean, further work remains to be done.

6.3 – Suggestions for Future Work

With the results presented in this study, there are natural extensions that could be done. It would be of benefit to confirm the finding that the Robinson (2000) mechanism presented in the data would present itself in the Northern Hemisphere. This would be of interest, as the Northern Hemisphere does not contain the same degree of zonal symmetry that the Southern Hemisphere possesses. Additionally, more analysis looking at the frequency component of the eddy heat fluxes should be examined. It would be interesting to see if the Robinson (2000) mechanism were to project in a more convincing fashion if isolated to a certain frequency. Further work concerning the role of tropospheric warming/stratospheric cooling on this mechanism would be of interest. These suggestions have the goal of establishing the robustness of the Robinson (2000) mechanism in the observational data.

Concerning the second part of the study, it would be of importance to diagnose what the structure that is associated with the EKE means. It is known that the SAM represents the north-south fluctuation of the midlatitude jet, but what does the variability seen with the EKE represent? Steps taken to explain this would be a logical next step. Additionally, it would be of interest to examine if this structure is present in the Northern Hemisphere as well, for the same reasons as listed above. As with the examinations in the literature concerning the SAM, the same could be done with this new structure that is associated with the EKE. Questions regarding the sensitivity of this structure to anthropogenic forcing could be examined as well as how sensitive the structure is to regions where baroclinicity is greatest at the surface. As with the SAM, can precipitation patterns be explained by this new structure in a clearer manner? These are just some ideas that would be able to be pursued with this topic. Any research done to further this examination beyond what has been presented here would lend additional support to understanding the processes that govern the circulation in the extratropics.

REFERENCES

American Meteorological Society (AMS) Glossary, cited 2012. [Available online at http://amsglossary.allenpress.com/glossary].

Andrews, D.G., J.R. Holton, C.B. Levoy, 1987: *Middle Atmosphere Dynamics.* Academic Press, 489pp.

Arblaster, J.M., and G.A. Meehl, 2006: Contributions of External Forcings to Southern Annular Mode Trends. *Journal of Climate.*, 19, 2896-2905.

Baldwin, M.P., 2001: Annular modes in daily surface pressure. *Geophysical Research Letters,* 28, 21, 4115-4118.

Barnes, E. A., & Hartmann, D. L., 2010: Dynamical Feedbacks of the Southern Annular Mode in winter and summer. *Journal of the Atmospheric Sciences*, *67*(2010), 2320–2330.

Barnes, E.A., D.L. Hartmann, D.M.W. Frierson, and J. Kidston, 2010: Effect of latitude on the persistence of eddy-driven jets. *Geophysical Research Letters,* 37, L11804(1-5).

Blanco-Fuentes, J. and P. Zurita-Gotor, 2011: The driving of baroclinic anomalies at different timescales. *Geophysical Research Letters,* 38, L23805(1-7).

Boer, G.J., 1989: On exact and approximate energy equations in pressure coordinates. *Tellus,* 41A, 97-108.

Chen, G., R.A. Plumb, and J. Lu, 2010: Sensitivities of zonal mean atmospheric circulation to SST warming in an aqua-planet model. *Geophysical Research Letters,* 37, L12701 (1-4).

Codron, F., 2007: Relations between Annular Modes and the Mean State: Southern Hemisphere Winter. *Journal of the Atmospheric Sciences,* 64, 3328-3339.

Doos, K., and J. Nilsson, 2011: Analysis of the Meridonal Energy Transport by Atmospheric Overturning Circulations. *Journal of the Atmospheric Sciences,* 68, 1806-1820.

Eady, E.T. , 1949: Long Waves and Cyclone Waves. Imperial College of Science, London.

Fyfe, J.C., G.J. Boer, G.M. Flato, 1999: The Arctic and Antarctic Oscillations and their Projected Changes Under Global Warming. *Geophysical Research Letters.,* 26,11, 1601-1604.

Gerber, E.P., and G.K. Vallis, 2007: Eddy-Zonal Flow Interactions and the Persistence of the Zonal Index. *Journal of the Atmospheric Sciences,* 64, 3296-3311.

Gillett, N.P., and D.W.J. Thompson, 2003: Simulation of Recent Southern Hemisphere Climate Change. *Science.* 302. 273-275.

Hantel, M. 1974: On the Display of the Atmospheric Circulation with Streamfunctions. *Monthly Weather Review*. September, 649-661.

Hartmann, D.L., 1994: *Global Physical Climatology*. Academic Press, 411p.

Hartmann, D.L., 2000: The Key Role of Lower Level Meridonal Shear in Baroclinic Life Cycles. *Journal of the Atmospheric Sciences,* 57, 389-401.

Hartmann, D. L., and F. Lo, 1998: Wave-driven zonal flow vacillation in the Southern Hemisphere. *Journal of the Atmospheric Sciences*., 55, 1303–1315.

Holton, J.R., 2004: *An Introduction to Dynamical Meteorology, 4th ed.* Elsevier Academic Press, 535 pp.

Hoskins, B.J., and K.I. Hodges, 2005: A New Perspective on Southern Hemisphere Storm Tracks. *Journal of Climate,* 18, 4108-4129.

Hudson, R.D., 2012: Measurements of the movement of the jet streams at mid-latitudes in the Northern and Southern Hemispheres, 1979 to 2010. *Atmospheric Chemistry and Physics,* 12, 7797-7808.

IPCC Chapter 3, 2007 :Climate Change 2007: The Physical Science Basis. Contribution of Working Group 1 to the Fourth Assessment Report of the Intergovernmental Panel on Climate Change. Cambridge Univ. Press, 2007.

Kalnay, E., M. Kanamitsu, R. Kistler, W. Collins, D. Deaven, L. Gandin, M. Iredell, S. Saha, G. White, J. Woollen, Y. Zhu, M. Chelliah, W. Ebisuzaki, W. Higgins, J. Janowiak, K. C. Mo, C. Ropelewski, J. Wang, A. Leetmaa, R. Reynolds, R. Jenne, and D. Joseph, 1996: The NCEP/NCAR 40-Year Reanalysis Project. Bull. Amer. Meteor. Soc., 77, 437-471.

Karoly, D.J. 1990: The role of transient eddies in low frequency zonal variations of the Southern Hemisphere circulation. *Tellus,* 42A, 41-50.

Kaspi, Y., and T. Schneider, 2011: Downstream Self-Destruction of Storm Tracks. *Journal of the Atmospheric Sciences,* 68,2459-2464.

Kidston, J., D.M.W. Frierson, J.A. Renwick, and G.K. Vallis, 2010: Observations, Simulations, and Dynamics of Jet Stream Variability and Annular Modes. *Journal of Climate*. 23, 6186-6199.

Kidson, J.W., 1988: Interannual Variations in the Southern Hemisphere Circulation. *Journal of Climate,* 1, 1177-1198.

Kodera, K. (2004). Solar influence on the Indian Ocean Monsoon through dynamical processes. *Geophysical Research Letters*, *31*(24), L24209. doi:10.1029/2004GL020928

Kushner, P.J., Held, I.M., and Delworth, T.L., 2001: Southern Hemisphere Atmospheric Circulation Response to Global Warming. *Journal of Climate.* 14, 2238-2249.

Limpasuvan, V. and D.L. Hartmann, 2000: Wave-Maintained Annular Modes of Climate Variability. *Journal of Climate*. 13, 4414-4429.

Lorenz, E.N., 1955: Available Potential Energy and the Maintenance of the General Circulation. *Tellus VII,* 2,157-167.

Lorenz, D. J., and D. L. Hartmann, 2001: Eddy–zonal flow feed- back in the Southern Hemisphere. *Journal of the Atmospheric Sciences*, 58, 3312– 3327.

Nakamura, H., and A. Shimpo, 2004: Seasonal Variations in the Southern Hemisphere Storm Tracks and Jet Streams as Revealed in a Reanalysis Dataset. *Journal of Climate,* 17, 1828-1844.

Pauluis, O. 2007: Sources and Sinks of Available Potential Energy in a Moist Atmosphere. *Journal of the Atmospheric Sciences,* 64, 2627-2641.

Polvani, L.M., and P.J. Kushner, 2002: Tropospheric response to stratospheric perturbations in a relatively simple general circulation model. *Geophysical Research Letters,* 29,7, 18(1)-18(4).

Randall, D., 2010: *An Introduction to the General Circulation of the Atmosphere.*

Ring, M.J., and R.A. Plumb, 2007: Forced Annular Mode Patterns in a Simple Atmospheric General Circulation Model. *Journal of the Atmospheric Sciences,* 64, 3611-3626.

Robinson, W. A., 2000: A Baroclinic Mechanism for the Eddy Feedback on the Zonal Index. *Journal of the Atmospheric Sciences*, 57(3), 415–422.

Robinson, W.A., 2006: On the Self-Maintenance of Midlatitude Jets. *Journal of the Atmospheric Sciences,* 63, 2109-2122.

Simpson, I.R., M. Blackburn, and J.D. Haigh, 2012: A Mechanism for the Effect of Tropospheric Jet Structure on the Annular Mode-Like Response to Stratospheric Forcing. *Journal of the Atmospheric Sciences,* 69, 2152-2170.

Smith, P.J., 1969: On the contribution of a limited region to the global energy budget. *Tellus XXI*, 202-207.

Straus, D. (1983). On the Role of the Seasonal Cycle, *Journal of the Atmospheric Sciences, 40*, 303-313.

Thompson, D. W. J., and J. M. Wallace, 2000: Annular modes in the extratropical circulation. Part I: Month-to-month variability. *Journal of Climate,* 13, 1000–1016.

Trenberth, K., Stepaniak, D., Hurrell, J., & Fiorino, M. 2001: Quality of reanalyses in the tropics. *Journal of Climate*, *14*(2000), 1499–1510. Retrieved from http://journals.ametsoc.org/doi/abs/10.1175/1520-0442(2001)014%3C1499:QORITT%3E2.0.CO%3B2

Uppala SM, Dee DP, Kobayashi S, Simmons AJ. 2008: Evolution of reanalysis at ECMWF. In *Proceedings of Third WCRP International Conference on Reanalysis*, 28 January–1 February 2008, Tokyo, Japan.

Vallis, G.K., E.P. Gerber, P.J. Kushner, and B.A. Cash, 2004: A Mechanism and Simple Dynamical Model of the North Atlantic Oscillation and Annular Modes. *Journal of the Atmospheric Sciences,* 61, 264-280.

Vallis, G.K., 2006: *Atmospheric and Oceanic Fluid Dynamics*. Cambridge University Press, 745p.

Wang, B., Zou, X., & Zhu, J. 2000: Data assimilation and its applications. *Proceedings of the National Academy of Sciences of the United States of America*, *97*(21), 11143–11144. Retrieved from http://www.pnas.org/content/97/21/11143.short

Winters, K.B., and W.R. Young 2009: Available potential energy and buoyancy variance in horizontal convection. *Journal of Fluid Mechanics,* 629, 221-230.

Yin, J.H., 2005: A consistent poleward shift of the storm tracks in the simulations of 21st century climate. *Geophysical Research Letters,* 32, L18701 (1-4).